

NOAA Technical Report NOS CS 29

THE SECOND GENERATION CHESAPEAKE BAY OPERATIONAL FORECAST SYSTEM (CBOFS2): MODEL DEVELOPMENT AND SKILL ASSESSMENT

Silver Spring, Maryland
March 2011



noaa National Oceanic and Atmospheric Administration

U.S. DEPARTMENT OF COMMERCE
National Ocean Service
Coast Survey Development Laboratory

**Office of Coast Survey
National Ocean Service
National Oceanic and Atmospheric Administration
U.S. Department of Commerce**

The Office of Coast Survey (OCS) is the Nation's only official chartmaker. As the oldest United States scientific organization, dating from 1807, this office has a long history. Today it promotes safe navigation by managing the National Oceanic and Atmospheric Administration's (NOAA) nautical chart and oceanographic data collection and information programs.

There are four components of OCS:

The Coast Survey Development Laboratory develops new and efficient techniques to accomplish Coast Survey missions and to produce new and improved products and services for the maritime community and other coastal users.

The Marine Chart Division acquires marine navigational data to construct and maintain nautical charts, Coast Pilots, and related marine products for the United States.

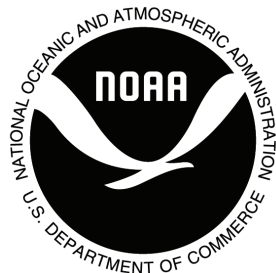
The Hydrographic Surveys Division directs programs for ship and shore-based hydrographic survey units and conducts general hydrographic survey operations.

The Navigational Services Division is the focal point for Coast Survey customer service activities, concentrating predominately on charting issues, fast-response hydrographic surveys, and Coast Pilot updates.

THE SECOND GENERATION CHESAPEAKE BAY OPERATIONAL FORECAST SYSTEM (CBOFS2): MODEL DEVELOPMENT AND SKILL ASSESSMENT

Lyon W. J. Lanerolle, Richard C. Patchen and Frank Aikman III
Office of Coast Survey, Coast Survey Development Laboratory,
Silver Spring, MD

March 2011



noaa National Oceanic and Atmospheric Administration

U. S. DEPARTMENT
OF COMMERCE
Gary Locke,
Under Secretary

National Oceanic and
Atmospheric Administration
Dr. Jane Lubchenco
Administrator

National Ocean Service
David Kennedy
Assistant Secretary

Office of Coast Survey
Captain John Lowell, NOAA

Coast Survey Development Laboratory
Mary Erickson

NOTICE

Mention of a commercial company or product does not constitute an endorsement by NOAA. Use for publicity or advertising purposes of information from this publication concerning proprietary products or the tests of such products is not authorized.

TABLE OF CONTENTS

LIST OF FIGURES	iv
LIST OF TABLES	viii
EXECUTIVE SUMMARY	xi
1. INTRODUCTION	1
2. CBOFS2 MODEL DOMAIN, GRID AND BATHYMETRY	3
3. CONSTANT DENSITY TIDAL SIMUALTION	7
3.1 Water Level Comparisons and Skill Assessments	9
3.2 Currents Comparisons and Skill Assessments	15
4. SYNOPTIC HINDCAST SIMULATION	23
4.1 Initial Conditions and Model Forcings	24
4.2 Water Level Comparisons	27
4.3 Currents Comparisons	31
4.4 Temperature and Salinity Comparisons	36
5. SEMI-OPERATIONAL NOWCAST/FORECAST SIMULATION	43
5.1 Water Level Comparisons	43
5.2 Currents Comparisons	45
5.3 Temperature Comparisons	45
5.4 Salinity Comparisons	45
6. SUMMARY AND CONCLUSIONS	47
ACKNOWLEDGMENTS	49
REFERENCES	51
APPENDIX A: CBOFS2 CONSTANT DENSITY WATER LEVEL HARMONIC CONSTITUENTS AND SKILL ASSESSMENTS	55
APPENDIX B: CBOFS2 CONSTANT DENSITY CURRENTS HARMONIC CONSTITUENTS AND SKILL ASSESSMENTS	57
APPENDIX C: CBOFS2 SYNOPTIC HINDCAST TEMPERATURE AND SALINITY SKILL ASSESSMENTS	61
APPENDIX D: CBOFS2 SEMI-OPERATIONAL NOWCAST/FORECAST SKILL ASSESSMENTS	75

LIST OF FIGURES

Figure 1. CBOFS2 model domain and orthogonal, curvilinear grid (left) and model Bathymetry (right)	3
Figure 2. CBOFS2 water level stations archive locations (and the NOS/CO-OPS identification numbers) for comparison with tidal predictions in the constant density simulation	9
Figure 3. Amplitude differences (CBOFS2-observations in cm) for M2, N2, K1, O1, P1 and L2 harmonic constituents in the constant density CBOFS2 simulation.....	10
Figure 4. Phase differences (CBOFS2-observations in hours) for M2, N2, K1, O1, P1 and L2 harmonic constituents in the constant density CBOFS2 simulation	11
Figure 5. RMS water level errors (in cm) for the constant density CBOFS2 simulation	12
Figure 6. Splitting methodology of the RMS error into an amplitude component and a phase component. Here, x-axis annotation of phase variation or difference is equivalent to the amount by which the who water level time-series have been translated relative to each other	13
Figure 7. CBOFS2 RMSE translation curves for the comparison stations given in Figure 2	14
Figure 8. The amplitude error (in cm) and phase error (in hours) components of the RMS errors associated with the water levels for the constant density CBOFS2 simulation.....	15
Figure 9. CBOFS2 currents stations archive locations for comparison with tidal predictions in the constant density simulation.....	16
Figure 10. CBOFS2 currents stations archive locations for comparison with tidal predictions in the constant density simulation	17
Figure 11. M2, N2 and K1 constituent CBOFS2 amplitude (in cm/s) and phase (in hours) errors (CBOFS2 minus prediction) for the true northward current component in the constant density simulation.....	18
Figure 12. RMS current speed (left, cm/s) and current direction (right, degrees) errors (from the CSDL skill-assessment software package) at a depth of 15 feet (4.6m) for the CBOFS2 constant density simulation at the NOS/CO-OPS/CMIST observational stations.....	19

Figure 13. RMSE translation curves for the CBOFS2 major current component for the comparison stations	20
Figure 14. The amplitude (left, cm/s) and phase error (right, hours) components of the RMS errors associated with the major current in the constant density CBOFS2 simulation	21
Figure 15. Vertical structure of major-direction currents for the constant density CBOFS2 simulation (black – NOS/CO-OPS/CMIST prediction, blue – CBOFS2, red – CBOFS2 with 1 hr. phase lead, green – CBOFS2 with 1 hr. phase lag)	22
Figure 16. Total river volume discharge for the CBOFS2 model domain spanning 2003-2005	23
Figure 17. Wind speed plot for August-October, 2003 at Chesapeake Light, VA NOAA/ National Data Buoy Center (NDBC) station showing hurricane Isabel	23
Figure 18. NARR (blue circles) and NDBC (red squares) data points used in the creation of the wind, air temperature, relative humidity/dew point and net shortwave radiation fields; the thick black line is the southern open boundary of the CBOFS2 computational domain	25
Figure 19. CFL number time-history for the synoptic hindcast simulation	26
Figure 20. Water level and currents stations archive locations for the synoptic hindcast CBOFS2 simulation for comparison with observations	27
Figure 21. RMS water level errors (in cm) for the synoptic hindcast CBOFS2 simulation	28
Figure 22. CBOFS2 synoptic hindcast RMSE translation curves for the comparison stations	29
Figure 23. The amplitude error (cm) and phase error (hours) components of the RMS errors associated with the water levels for the synoptic hindcast CBOFS2 simulation	30
Figure 24. RMS current speed (left, cm/s) and current direction (right, degrees) errors at a depth of 5m for the CBOFS2 synoptic hindcast simulation at the NOS/CMIST observational stations (from the CSDL skill-assessment software package)	32
Figure 25. CBOFS2 synoptic hindcast RMSE translation curves for the major-current component at the comparison stations	33
Figure 26. The amplitude (left, cm/s) and phase error (right, hours) components of the RMS errors associated with the major current in the synoptic hindcast CBOFS2 simulation	34

Figure 27. Vertical structure of the major-direction currents for the synoptic hindcast CBOFS2 simulation (black – NOS/CO-OPS/CMIST obs., blue – CBOFS2, red – CBOFS2 with 1 hr. phase lead, green – CBOFS2 with 1 hr. phase lag)	35
Figure 28. Temperature and salinity stations archive locations for the CBOFS2 synoptic hindcast simulation. Locations in red are stations at which local and global error analyses were performed (Figures C1-C10 in Appendix C).....	36
Figure 29. Plot of the RMS and mean errors for T and S as listed in Tables C1 and C1 in Appendix C	39
Figure 30. Plot of the RMS and mean errors for T at the surface, at 15-feet and at the bottom	40
Figure 31. Plot of the RMS and mean errors for S at the surface, at 15-feet and at the bottom	41
Figure 32. Locations of the stations where water level (blue circles) and currents (red squares) skill assessments were performed. The temperature and salinity comparison stations are demarcated with a box next them.....	44
Figure 33. Salinity time-series at station 8638863 (CBBT).....	46
Figure C1. Observed Bay Program T/S, CBOFS2 predicted T/S and their differences at station CB7.4.....	61
Figure C2. Observed Bay Program T/S, CBOFS2 predicted T/S and their differences at station CB5.4.....	62
Figure C3. Observed Bay Program T/S, CBOFS2 predicted T/S and their differences at station CB4.2C.....	63
Figure C4. Observed Bay Program T/S, CBOFS2 predicted T/S and their differences at station CB2.1.....	64
Figure C5. Observed Bay Program T/S, CBOFS2 predicted T/S and their differences at station RET5.2	65
Figure C6. Observed Bay Program T/S, CBOFS2 predicted T/S and their differences at station LE3.1	66
Figure C7. Observed Bay Program T/S, CBOFS2 predicted T/S and their differences at station RET2.4	67
Figure C8. Observed Bay Program T/S, CBOFS2 predicted T/S and their differences at station LE1.3	68

Figure C9. Observed Bay Program T/S, CBOFS2 predicted T/S and their differences at station EE3.4	69
Figure C10. Observed Bay Program T/S, CBOFS2 predicted T/S and their differences at station ET5.2.....	70
Figure C11. Histograms of local errors (in time and depth) for T and S corresponding to Figures C1-C10. The T and S histogram bin widths are 0.5 °C and 0.5 PSU respectively	71

LIST OF TABLES

Table 1. Water level error summary for the synoptic hindcast CBOFS2 : Tidal range (cm), RMS error (cm) and its Central Frequency (CF), high water amplitude error (AHW_err, cm) and its CF, low water amplitude error (ALW_err, cm) and its CF (all from the CSDL skill-assessment software package), amplitude component of the RMSE (cm) and the phase component of the RMSE(hours).....	31
Table 2. Current speed error summary for CBOFS2 synoptic hindcast simulation: RMS of current speed error (cm/s) and its Central Frequency (CF), maximum flood current amplitude error (AFC_err, cm) and its CF, maximum ebb current amplitude error (AEC_err, cm) and its CF (all from the CSDL skill-assessment software package)....	32
Table 3. Current direction error summary for CBOFS2 synoptic hindcast simulation: RMS of current direction error (degrees) and its Central Frequency (CF), maximum flood current direction error (DFC_err, degrees) and its CF, maximum ebb current direction error (DEC_err, degrees) and its CF (all from the CSDL skill-assessment software package)	33
Table 4. Major current error summary for the synoptic hindcast simulation: raw RMS error (cm/s), the amplitude component of the RMSE (cm/s) and the phase component of the RMSE (hours).....	34
Table A1. Water level harmonic constituents summary for CBOFS2; amplitudes are in meters and phases are in hours.....	55
Table A2. Water level harmonic constituents summary from observations (NOS/CO-OPS Database); amplitudes are in meters and phases in hours.....	55
Table A3. Water level error summary: Tidal range (cm), RMS error (cm) and its Central Frequency (CF), high water amplitude error (AHW_err, cm) and its CF, low water amplitude error (ALW_err, cm) and its CF (all from the CSDL skill-assessment software package), amplitude component of the RMSE (cm) and the phase component of the RMSE (hours)	56
Table B1. True eastward current harmonic constituents summary for CBOFS2; amplitudes are in m/s and phases are in hours	57
Table B2. True northward current harmonic constituents summary for CBOFS2; amplitudes are in m/s and phases are in hours	57
Table B3. True eastward current harmonic constituents summary from observations (NOS/CO-OPS/CMIST database and NOS survey); amplitudes are in m/s and phases are in hours	58

Table B4. True northward current harmonic constituents summary from observations (NOS/CO-OPS/CMIST database and NOS survey); amplitudes are in m/s and phases are in hours	58
Table B5. Current speed error summary: RMS of current speed error (cm/s) and its Central Frequency (CF), maximum flood current amplitude error (AFC_err, cm) and its CF, maximum ebb current amplitude error (AEC_err, cm) and its CF (all from the CSDL skill-assessment software package)	58
Table B6. Current direction error summary: RMS of current direction error (degrees) and its Central Frequency (CF), maximum flood current direction error (DFC_err, degrees) and its CF, maximum ebb current direction error (DEC_err, degrees) and its CF (all from the CSDL skill-assessment software package)	59
Table B7. Major current error summary: raw RMS error (cm/s), the amplitude component of the RMSE (cm/s) and the phase component of the RMSE (hours)	59
Table C1. The RMS and mean errors (calculated in time) for temperature at the surface, at 15-feet below the surface and at the bottom	72
Table C2. The RMS and mean errors (calculated in time) for salinity at the surface, at 15-feet below the surface and at the bottom	73
Table D1. RMSE (m) values for the water levels for the semi-operational nowcast/forecast CBOFS2 (from the CSDL skill assessment software package).....	75
Table D2. CF(15cm) values for the water levels for the semi-operational nowcast/forecast CBOFS2 (from the CSDL skill assessment software package).....	75
Table D3. RMSE (m/s) values for the current speed at 15 feet for the semi-operational nowcast/forecast CBOFS2 (from the CSDL skill assessment software package).....	76
Table D4. CF(26cm/s) values for the current speed at 15 feet for the semi-operational nowcast/forecast CBOFS2 (from the CSDL skill assessment software package).....	76
Table D5. RMSE (degrees) values for the current direction at 15 feet for the semi-operational nowcast/forecast CBOFS2 (from the CSDL skill assessment software package).....	76
Table D6. CF(22.5°) values for the current direction at 15 feet for the semi-operational nowcast/forecast CBOFS2 (from the CSDL skill assessment software package).....	76
Table D7. RMSE (°C) values for temperature at a 1m depth for the semi-operational nowcast/forecast CBOFS2 (from the CSDL skill assessment software package).....	77
Table D8. CF(3°C) values for temperature at a 1m depth for the semi-operational nowcast/forecast CBOFS2 (from the CSDL skill assessment software package).....	77

Table D9. RMSE (PSU) values for salinity at a 1m depth for the semi-operational
nowcast/forecast CBOFS2 (from the CSDL skill assessment software package).....77

Table D10. CF(3.5 PSU) values for salinity at a 1m depth for the semi-operational
nowcast/forecast CBOFS2 (from the CSDL skill assessment software package).....77

EXECUTIVE SUMMARY

The National Ocean Service presently has an Operational Forecast System for the Chesapeake Bay (CBOFS) which generates only water levels and depth-integrated currents. As a next generation system, a fully three-dimensional, baroclinic forecast system (CBOFS2) was developed, calibrated and validated; this system will produce water levels, currents, temperature and salinity predictions. CBOFS2 covers the whole of the Chesapeake Bay up to and including Reedy Point, DE along the Chesapeake & Delaware canal and also includes Ocean City, MD and Duck, NC along its southern boundary which extends as far as the 100m isobath on the shelf.

First, a two-month tides-only simulation was conducted to validate the tidal water levels and currents and thereafter, a synoptic hindcast simulation from June 01, 2003 – September 01, 2005 was performed to validate water levels, currents, temperature and salinity. The synoptic hindcast simulation included a diverse range environmental conditions in the Bay including very high and very low river volume discharges and a hurricane (Isabel, in September of 2003). Finally, CBOFS2 was run in a semi-operational, nowcast/forecast mode to validate these model outputs.

The simulations showed that both the constant density and synoptic hindcast CBOFS2 configurations were numerically stable and highly efficient under a MPI parallelization environment. A computational effort ratio of 1:144 resulted when employing 96 parallel processors. The numerical stability of the computations was accounted for by monitoring the Courant-Friedrichs-Lewy (CFL) stability parameter during model simulations.

As for the quality of the CBOFS2 predictions, when compared with observations, it was found that: (i) the water level amplitude errors were less than 22 cm and phase errors generally less than 0.5 hours and, both the amplitude and phase errors increase in magnitude when moving up the Bay and for the latter, this is also true when moving up tributaries, (ii) currents speed errors were less than 26 cm/s and the direction errors less than 22.5° which are the NOS skill criteria and for the major-direction components, the phase errors were also less than 0.5 hours, (iii) the temperature Root Mean Square (RMS) errors were generally less than 2°C and the mean errors were in the range $[-1^\circ\text{C}, 1^\circ\text{C}]$ and near the ocean surface CBOFS2 was cooler and near the bottom warmer relative to observations and (iv) the salinity RMS errors were generally less than 4 PSU and the mean errors were in the range $[-2\text{ PSU}, 3\text{ PSU}]$ and CBOFS2 was saltier near the surface and fresher near the bottom when compared with observations. The accuracy of the semi-operational, nowcast/forecast predictions are as good as and if not better than those from the synoptic hindcast and in general meet the NOS skill criteria; furthermore, the forecasts are valid for up to a 24-hour period without deterioration of their accuracy.

This report also describes a RMS error splitting (into an amplitude and phase component) procedure which was found to be very reliable for both water level and current comparisons (with observations) and for both the constant density and synoptic hindcast simulations.

Therefore, the predictive accuracy for water level, currents, temperature and salinity associated with CBOFS2 warrants it being accepted as a NOS Operational Forecast System (OFS) upgrade to the presently available CBOFS set-up. It is expected that the predictions from this modeling set-up may be further enhanced in the future by experimenting with: (a) spatially variable bottom friction formulations, (b) various shapes and extents of the shelf open ocean boundaries, (c) other model constants in the General Length Scale (GLS) vertical eddy-viscosity scheme and (d) the possibility of coupling the open ocean boundaries to a basin-scale model to better account for the shelf dynamics and its influence on the Chesapeake Bay.

1. INTRODUCTION

Presently, there exists an operational model for the Chesapeake Bay named the Chesapeake Bay Operational Forecast System (CBOFS), which runs routinely at the Center for Operational Oceanographic Products and Services (CO-OPS) of the National Ocean Service (NOS) of NOAA (Gross et al., 2000). This model set-up, since being two-dimensional and barotropic in nature, only generates water levels (elevations) and barotropic (depth-integrated) currents for Chesapeake Bay. The navigational and ecological communities in particular are increasingly demanding not only water levels and depth-integrated currents but also the full three-dimensional currents, salinity and temperature fields. Therefore, a second generation three-dimensional Chesapeake Bay Operational Forecast System (CBOFS2) has been developed, calibrated, implemented and vetted which will provide these additional physical fields. This model is based on the Rutgers University's Regional Ocean Modeling System (ROMS).

ROMS is a split-explicit, finite difference based orthogonal, curvilinear grid numerical ocean model (Shchepetkin and McWilliams, 2004). The vertical grid is of a stretched, terrain-following, sigma coordinate (Song and Haidvogel, 1994) type. The momentum and tracer advection terms are discretized using high resolution, third order upstream-biased advection schemes which alleviate the need to add explicit horizontal viscosity/diffusivity in the numerical computations (Shchepetkin and McWilliams, 1998). The hydrostatic pressure gradient terms are also discretized using an extremely robust and accurate piecewise cubic spline construction (Shchepetkin and McWilliams, 2003). The vertical turbulence/eddy mixing is carried out using a standard Mellor-Yamada 2.5 scheme (Mellor and Yamada, 1982), a non-local K-Profile Parameterization (KPP) scheme or a family of General Length Scale (GLS) schemes consisting of k - ϵ , k - τ and k - ω schemes (Warner et al., 2005). Along the ocean bottom bathymetry, friction can be prescribed with a logarithmic, linear, quadratic law or a Bottom Boundary Layer (BBL) formulation (Styles and Glenn, 2000). At the ocean surface, the surface meteorological forcing can be imposed in two ways in ROMS – (a) if the wind stresses and net heat fluxes are available then, they can be prescribed directly but otherwise, (b) the wind speeds, air pressure, air temperature, relative humidity, net shortwave radiation flux and downward longwave radiation flux observations when available are specified and then the wind stresses and the net heat flux are estimated internally using a Bulk Flux formulation (Liu et al., 1979; Fairall et al., 1996a,b). If downward longwave radiation data is unavailable, the net longwave radiation can be computed internally using the Berliand formulation (Berliand and Berliand, 1952). The perfect restart mechanism contained in the ROMS allows lengthy computations to be carried out in reasonably sized run segments.

The CBOFS2 model domain was designed to include the whole of the Chesapeake Bay and a piece of the shelf to allow a realistic interaction between the shelf and the entrance to the Bay. The domain therefore included Washington, DC to the west, Reedy Point, DE (along the Chesapeake & Delaware (C & D) canal) to the east, the Susquehanna River (near the river reservoir) to the north and in the south out to the 100m isobath with Ocean City, MD and Duck, NC as the end points. The inclusion of the C & D canal is necessary in order to account for the interaction with the Delaware Bay, but it forces the use of a particular set of open ocean boundary conditions which required a smaller model time step in order to maintain numerical

stability. The model grid is curvilinear and orthogonal in nature in the horizontal and in the vertical, it was of a terrain-following, sigma-coordinate nature.

The calibration and validation of the CBOFS2 set-up was performed in three stages. First, a constant density, three-dimensional baroclinic simulation was run to validate the accuracy of the tides (water levels and currents). Once this simulation was validated, a synoptic hindcast simulation spanning June, 2003 to September, 2005 was carried out where the initialization fields and the model forcings (rivers, meteorology, etc.) were based on both synoptic observations and climatological fields; this period included very high and very low river discharges and a hurricane (Isabel). This second set-up was employed to validate the accuracy of the full suite of model outputs – water levels, currents, temperature and salinity against observations. Finally, CBOFS2 was run in a semi-operational, nowcast/forecast model and the model outputs (same as those for the hindcast) were validated to ensure its suitability for being an Operational Forecast System (OFS); the model forcing were from model-generated forecast products. All of these scenarios also served to examine the numerical stability properties associated with the CBOFS2 set-up.

This report is arranged as follows: In section 2, the model domain, grid and bathymetry are described and in section 3, the constant density simulation and its results are described. In section 4 the synoptic hindcast simulation is discussed together with the validation efforts of the model output fields. Section 5 describes the semi-operational, nowcast/forecast CBOFS2 system and the validation of its outputs. Finally, in section 6, a summary of the findings in this paper and the conclusions pertaining to its research are provided.

2. CBOFS2 MODEL DOMAIN, GRID AND BATHYMETRY

The CBOFS2 model domain and the model grid are given in Figure 1. The domain extends from the 100m isobath in the south to the Susquehanna River (at the river reservoir) in the north and from Washington, DC in the west to Reedy Point, DE in the east. There are two open ocean (lateral) boundaries in this domain with the first situated on the shelf between Duck, NC and Ocean City, MD and the second at Reedy Point, DE where the C & D canal exits to Delaware Bay. The C & D canal was included to ensure a realistic interaction between the two Bays and its termination at Reedy Point, DE was selected since water level observations are available at this location and a nearby US Geological Survey (USGS) gauge in Delaware Bay can be used to provide the temperature and salinity values. Along the southern open boundary, the end points

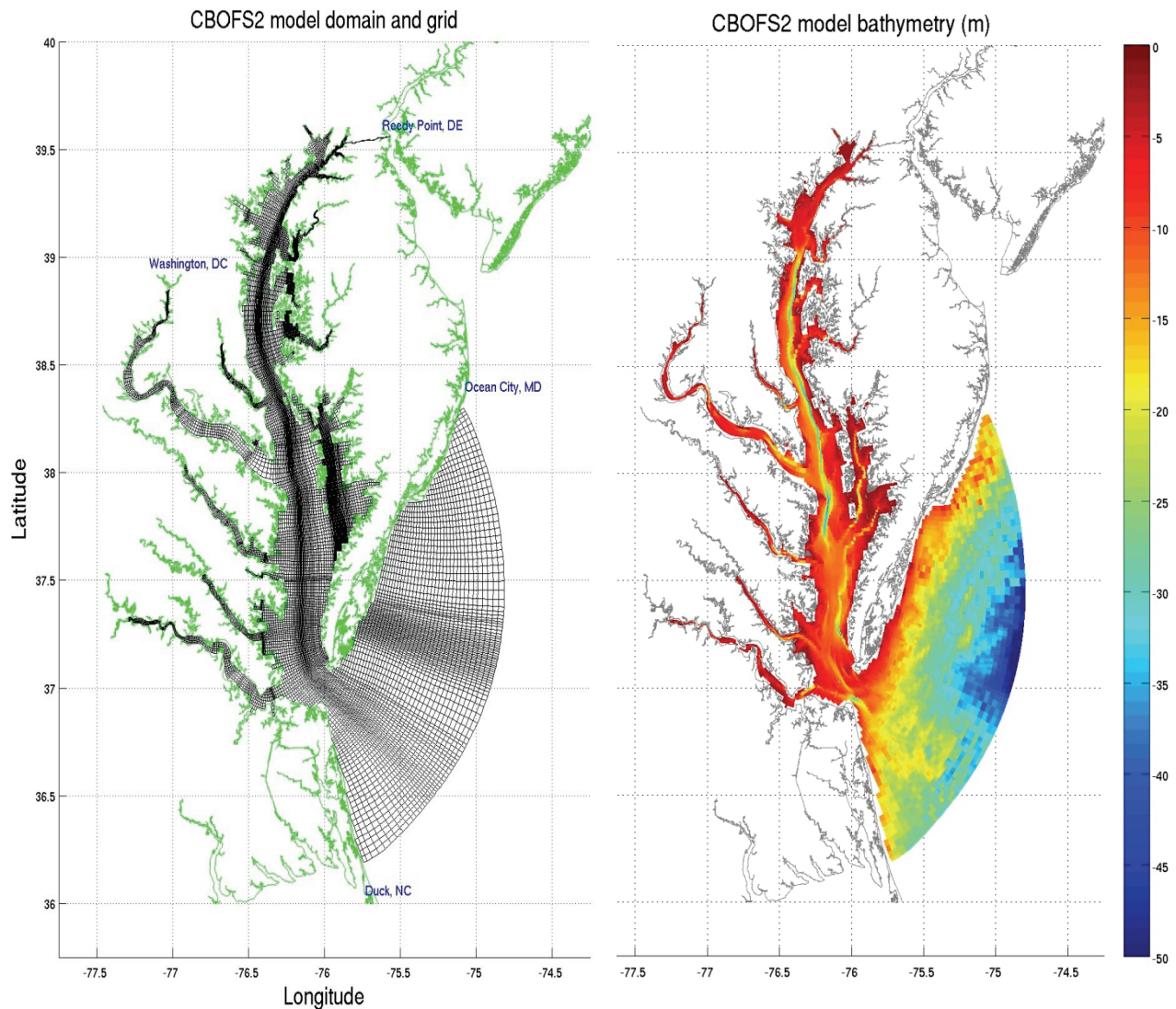


Figure 1. CBOFS2 model domain and orthogonal, curvilinear grid (left) and model bathymetry (right).

of Duck, NC and Ocean City, MD were selected because water level observations are available at these locations (temperature and salinity boundary values are from climatological fields). The above mentioned observations for water levels, temperature and salinity are required for model open boundary conditions/forcings in the synoptic hindcast simulation.

The CBOFS2 model grid was generated using the DELFT3D grid generator (Delft3D, 2008) and is curvilinear and orthogonal in nature. It was produced within the generator as multiple smaller curvilinear, orthogonal grid segments (so as to fit the local coastline segments as accurately as possible) and thereafter pasted together seamlessly within the grid generator but still maintaining continuity and global orthogonality. This grid generator only outputs the grid point locations of the wet-points and its output was converted to a ROMS-compatible grid file (in Matlab) by generating a pseudo land-mask and yet preserving a matrix structure for the grid file variables (eg. land-sea mask, bathymetry, etc.) with fixed dimensional limits. The grid has 332 x 291 points in the horizontal. The finest grid resolutions in the x- and y- directions are 34m and 29m, respectively, and the coarsest resolutions are 4895m and 3380m, respectively. For this CBOFS2 grid, unfortunately, due to the presence of many near-radial (as opposed to near-axial) tributaries, only 20.5% of the grid points are wet, implying that the vast majority of the points are land points and ROMS computes solutions on both sets of points without any discrimination.

The vertical grid is a terrain following, sigma coordinate system (Song and Haidvogel, 1994) consisting of 20 model levels. The true vertical depth z (in meter) is related to the sigma level, σ for a given bathymetric water depth, h (relative to model datum) through the following formulation:

$$z = z_0 + \eta(t) \cdot [1 + z_0/h] \text{ with } z_0 = \sigma h_C + (h - h_C) C_\sigma,$$

where σ lies within the interval $[-1,0]$ and is equally spaced. In the above formula, $h_C = \min(h_{\min}, T_{\text{cline}})$ with h_{\min} , T_{cline} being the globally minimum bathymetric depth and a guessed depth of the thermocline, respectively and, $\eta(t)$ is the time-dependent water level/free-surface elevation (at the horizontal geographical location associated with the depth, h). The stretching function C_σ is given by

$$C_\sigma = (1 - \theta_b) P(\sigma) + \theta_b R(\sigma)$$

where $P(\sigma) = \sinh(\theta_s \sigma) / \sinh(\theta_s)$ and $R(\sigma) = \tanh(\theta_s(\frac{1}{2} + \sigma)) / 2 \tanh(\theta_s/2) - \frac{1}{2}$ with θ_b , θ_s being grid stretching parameters associated with the ocean bottom and ocean surface vicinities respectively. Numerical experiments showed that for the constant density (Section 3), synoptic hindcast (Section 4) and semi-operational (Section 5) CBOFS2 set-ups, the optimal values for the parameters θ_b , θ_s and T_{cline} were 0.95, 4.5 and 10m respectively.

The CBOFS2 bathymetry was formed by numerically interpolating National Ocean Service (NOS) bathymetric soundings on to the model grid nodes via an inverse square distance weighted interpolation. When unsmooth bathymetry related numerical instabilities occurred in the CBOFS2 simulations, the bathymetry was smoothed locally (as opposed to globally). This approach was adopted to maintain the true bathymetry of the Chesapeake Bay whenever possible. A plot of the model bathymetry is shown in Figure 1.

A comparison of the water levels with and without the ROMS wetting/drying algorithms showed that they were quite similar to each other. However, in order to generate the former, it was required to use significantly smaller time steps to maintain numerical stability. Hence, the CBOFS2 was run without the use of wetting/drying and the model bathymetry was truncated at a minimum depth of 2m globally which also improved computational efficiency.

3. CONSTANT DENSITY TIDAL SIMULATION

As the primary use of CBOFS2 will be to support the marine navigational community, tidal water levels and currents must be accurately modeled. Therefore, in order to validate these fields, a constant density tidal simulation from January 01, 2000 – February 29, 2000 was performed. This simulation was run without specifying river forcing, meteorological/atmospheric forcing or any non-tidal open ocean boundary forcing (for temperature, salinity and non-tidal water levels). The initial fields of temperature and salinity were defined to be 15 °C and 35 PSU, respectively, and these values were maintained throughout the simulation. The only model forcing employed was the tidal forcing at the open ocean boundaries.

The tidal forcing at the southern open boundary was enforced via the use of water level and barotropic current harmonic constituents from an ADCIRC model (Luetlich et al., 1992) database generated at NOAA/NOS/Office of Coast Survey (OCS)/ Coast Survey Development Laboratory (CSDL) (Feyen, 2008) using the EC2001 grid, (EC2001, 2009). This database consisted of 37 harmonics including the long-term SA and SSA constituents which were not employed in the simulations as these include the effects of meteorology. The harmonic constituents were bilinearly interpolated (using Matlab) from the EC 2001 grid on to the CBOFS2 grid. For the C & D canal, the water level harmonic constituents were prescribed using those at Reedy Point, DE from the NOS/CO-OPS database (NOAA Tides & Currents, 2009a); the currents harmonic constituents were from a harmonic analysis of observed currents associated with NOS station 154 located at the Delaware Bay entrance to the C & D canal (Browne and Fisher, 1988). The currents were first rotated to be in alignment with the axis of the C & D canal and the major component was harmonically analyzed using the T_Tide Matlab software package (T_Tide, 2007). The cross-axis component of the barotropic current was assumed to be zero. The observed data was at an approximately 6m depth which is midway down the water column in the C & D canal the averaged depth of which is approximately 12m.

It was attempted to examine the sensitivity of the CBOFS2 tide predictions for water levels to two factors:

- (1) any mismatch in the harmonic constituents between those from the ADCIRC database and observations for water levels (corresponding observed harmonics for barotropic currents are not available) and,
- (2) the various open ocean boundary condition options available in ROMS for the inclusion of tides.

To examine the effects of (1), the ADCIRC database water level harmonics were forced to match those from NOS/CO-OPS observations at Duck, NC and Ocean City, MD via a linear and an exponentially damped matching function on the southern open boundary. The independent variables in these functions were the two arc distances (of a particular CBOFS2 grid point along the open boundary) from Duck, NC and Ocean City, MD. Hence, if L is the total arc distance along the CBOFS2 southern open boundary (for wet-points only) and x is the distance of a particular grid point from Duck, NC, then the matching functions for the linear formulation respectively are $1-x/L$ and x/L and, the corresponding ones for the exponential formulation are $e^{-x/L}$

Ax and $e^{-A(L-x)}$ where A is a user-defined exponent. Therefore, at these extreme locations, the water level harmonics exactly matched the observed values and thereafter they gradually asymptoted towards the (interpolated) values from the ADCIRC database.

ROMS has a suite of open boundary conditions for tidal applications and here, three of the most common options have been examined; they are (i) Chapman-Flather (traditional, Chapman, 1985 and Flather, 1976), (ii) Clamped-Reduced Flather and (iii) Clamped-Reduced for water levels and the barotropic currents respectively. For choices (ii) and (ii) it is not necessary to supply any barotropic currents.

The tides in ROMS are ramped-up using a hyperbolic tangent function so that they reach 99.0% of their full strength after 2.65 days. The bottom drag was prescribed via a quadratic formulation and its coefficient was taken to be 0.005 (although several values in the range 0.001-0.010 were examined), which gave the best overall water level predictions. Spatially variable bottom friction coefficients/formulations were not examined. The momentum and tracer advection terms were numerically discretized using the ROMS upstream-biased advection schemes which alleviated the need for artificial/numerical horizontal viscosity and diffusivity to eliminate spurious spatial numerical oscillations. The vertical eddy-viscosity was prescribed by the Mellor-Yamada 2.5 closure scheme and its background value was set to $1.0 \times 10^{-8} \text{ m}^2/\text{s}$. For the baroclinic currents, temperature and salinity, the standard radiation open ocean boundary conditions were applied both along the southern and C & D canal boundaries. The model was run with a 30 second baroclinic time step and a 1.5 second barotropic time step in a Message Passing Interface (MPI parallelization environment using 96 processors).

The outcome of the above numerical experiments was measured by examining the Root-Mean-Square (RMS) differences in the water levels at one grid point into the domain from the southern open boundary grid nodes corresponding to Duck, NC and Ocean City, MD on the southern boundary. The differences taken were between the ROMS-generated water levels and those predicted from the harmonic constituents associated with the open boundary grid nodes. The eastern open boundary at Reedy Point, DE was treated with Flather-Chapman boundary conditions and no matching of tidal harmonic constituents was necessary. The use of other boundary condition options available within ROMS for the C & D canal open boundary did not yield numerically stable computations and even with the present choice, a reduced global time step needed to be adopted in order to maintain stability. The RMSE differences clearly showed that the Flather-Chapman option generated the largest differences and the Clamped-Reduced option generated the least differences; furthermore, for each choice of boundary condition, the exponentially damped matching of harmonic constituents produced smaller errors than those with either no matching or with linear matching. The optimal exponent, A for the exponential matching function was found to be -5.0. Therefore, it was decided to adopt the Clamped-Reduced option for the southern open boundary together with the exponentially damped harmonic constituent matching. These reduced boundary conditions however were developed ideally for two-dimensional, barotropic ROMS applications (Ocean Modeling Discussion, 2008) and their validity for and effects on three-dimensional baroclinic ROMS applications are not yet fully known.

3.1. Water Level Comparisons and Skill Assessments

The water level predictions from CBOFS2 were compared with tidal predictions (from the NOS/CO-OPS harmonic constituents (NOAA Tides & Currents, 2009a)) at the station locations (corresponding to those maintained by NOS/CO-OPS) shown in Figure 2. The differences/discrepancies between the CBOFS2 predictions and the tidal predictions will hereafter be referred to as errors.

First however, the CBOFS2 water level time-series at each of the stations in Figure 2 was harmonically analyzed using the NOS harmonic analysis software (Zervas, 1999) and compared with those from NOS/CO-OPS for the M2, N2, K1, O1,P1 and L2 constituents (as they are the most dominant). The outcome of the harmonic analysis is provided in Tables A1 and A2 in Appendix A where the constituent amplitudes are in meters and the phases in hours. The errors in constituent amplitudes and phases are plotted in Figures 3 and 4. The amplitude errors show that (i) as expected, the largest errors are for the M2 constituent, (ii) the largest errors are at the extremities of the wet-point computational domain (in the C & D canal, entrance to the Bay and

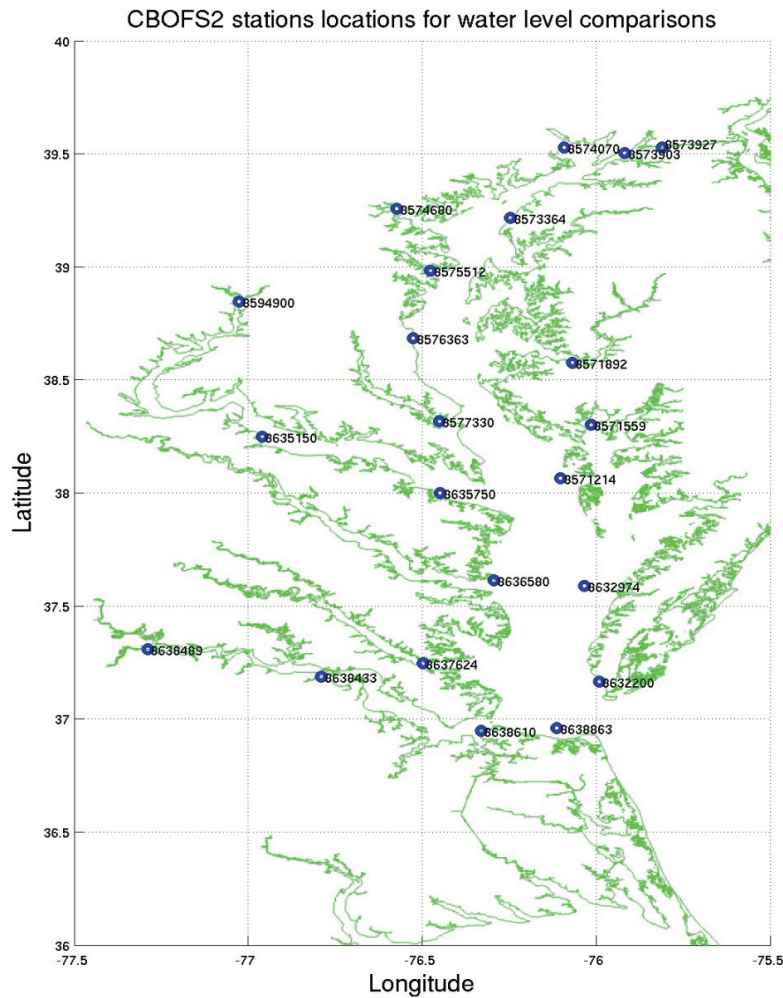


Figure 2. CBOFS2 water level stations archive locations (and the NOS/CO-OPS identification numbers) for comparison with tidal predictions in the constant density simulation.

at the beginnings of the tributaries) and (iii) there is no strong pattern to the spatial distribution of the errors and they assumed both positive and negative values. The phase errors too show both positive and negative values but their magnitudes are not clearly correlated with any particular constituent(s) and the largest errors tend to be at the extremities of the Potomac and York River tributaries where they show that CBOFS2 lags the predicted phase values. As with the amplitudes, the phase errors do not show a strong pattern to their spatial distribution within the Bay.

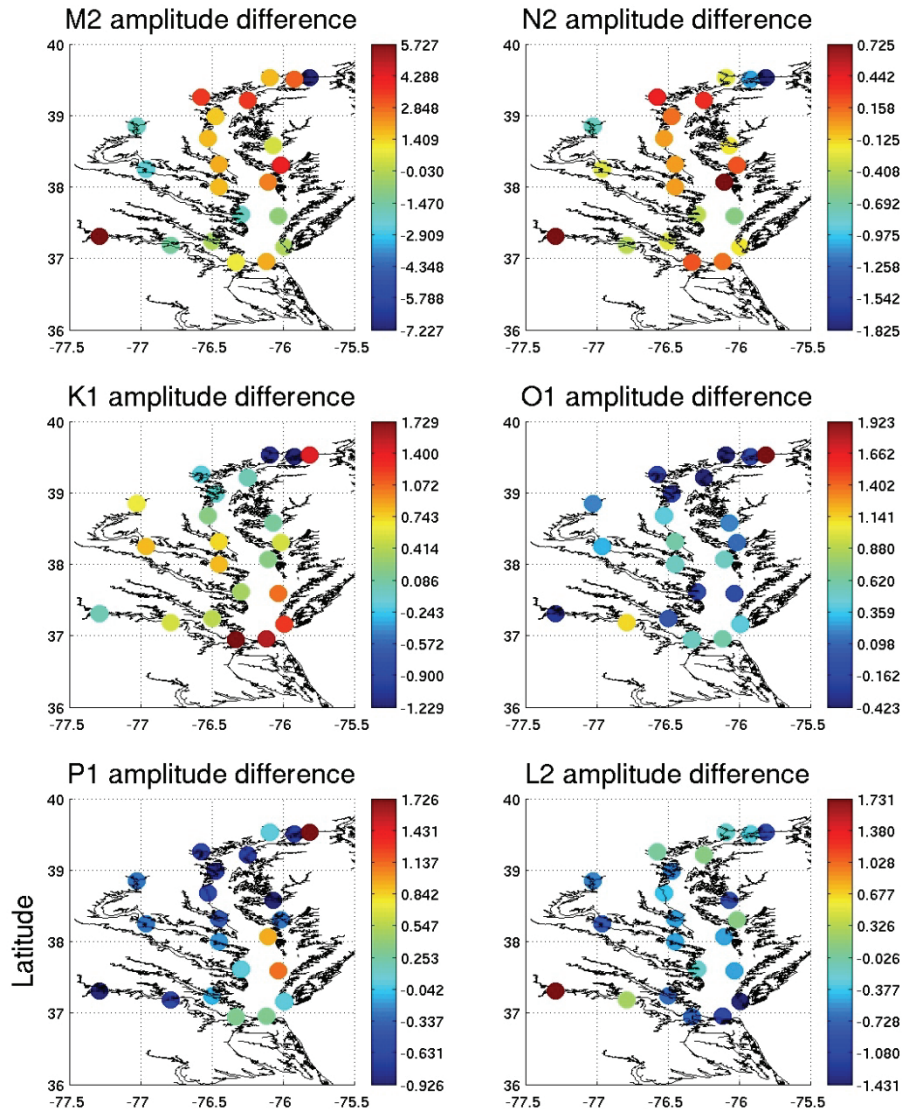


Figure 3. Amplitude differences (CBOFS2-observations in cm) for M2, N2, K1, O1, P1 and L2 harmonic constituents in the constant density CBOFS2 simulation.

The Root Mean Square Errors (RMSE) for the water levels are given in Table A3 of Appendix A and they have also been plotted in Figure 5. Table A3 also provides the high and low water amplitude errors and the Central Frequency (CF) associated with each of these three errors.

These metrics were computed using the NOS/OCS/CSDL ocean model skill-assessment software package (Zhang, et al., 2009). The NOS skill-assessment criteria for water level error is that (a) their RMSE be less than 15cm at least for 90% of the time (that is, with $CF(15cm) > 90\%$) and (b) their phase difference be less than 15 minutes also for at least 90% of the time.

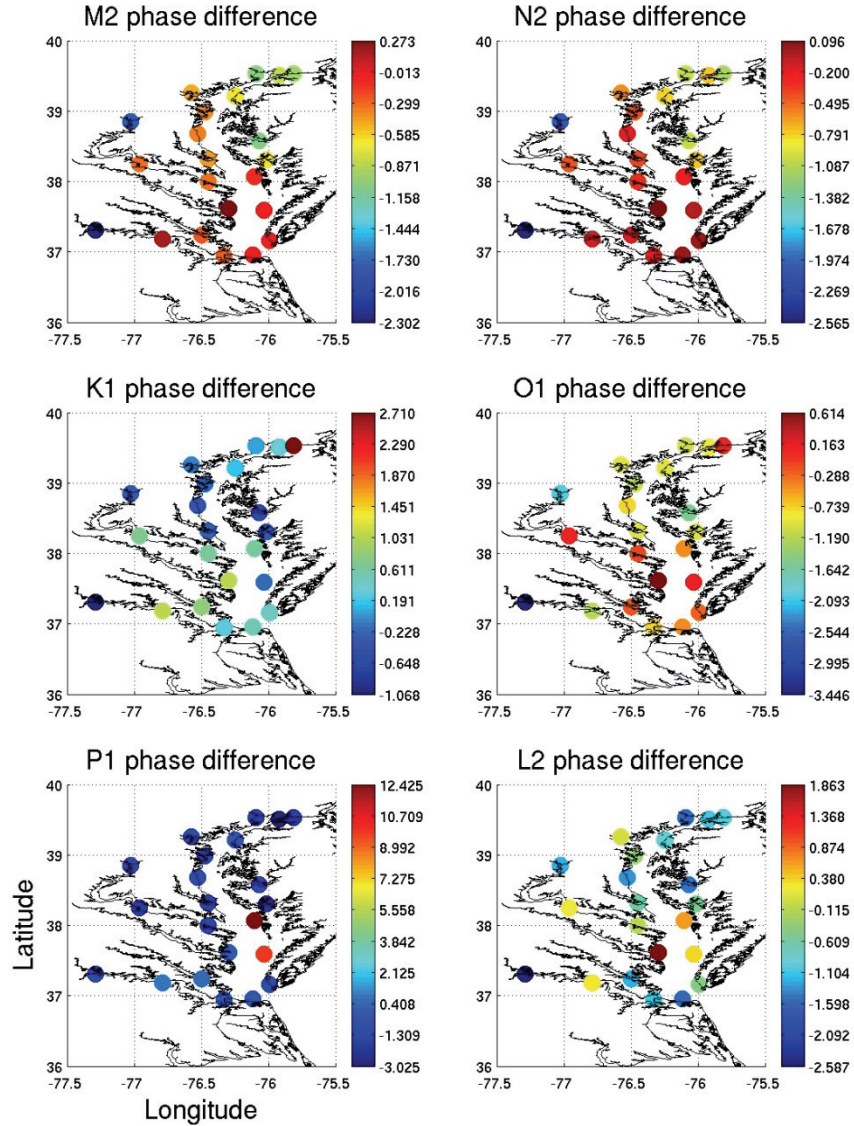


Figure 4. Phase differences (CBOFS2-observations in hours) for M2, N2, K1, O1, P1 and L2 harmonic constituents in the constant density CBOFS2 simulation.

Table A3 shows that only about half of the stations satisfy the RMSE error criterion although eleven out of fifteen stations satisfy the criterion for the high and low water amplitude errors. It is also seen that whenever the RMSE and the high and low water amplitude errors are well below the 15 cm limit, the CF parameter assumes values above 90%.

For oscillatory/periodic signals such as tidal water level and current time-series, the use of RMSE provides only a limited picture of the error content. What would be more pertinent would be to split the RMSE into an amplitude component and a phase component. Given say two water level time-series, it is possible to split the error by translating one series relative to the other (as a pair of autocorrelation functions) and estimating a RMSE for each translation and examining its structure. If this RMSE (a) forms a smooth curve and (b) has a single, unique, global minimum then at this minimum, as shown in Figure 6, the x-abcissa is the phase component of RMSE (phase error) and the y-abcissa is the amplitude component of the RMSE

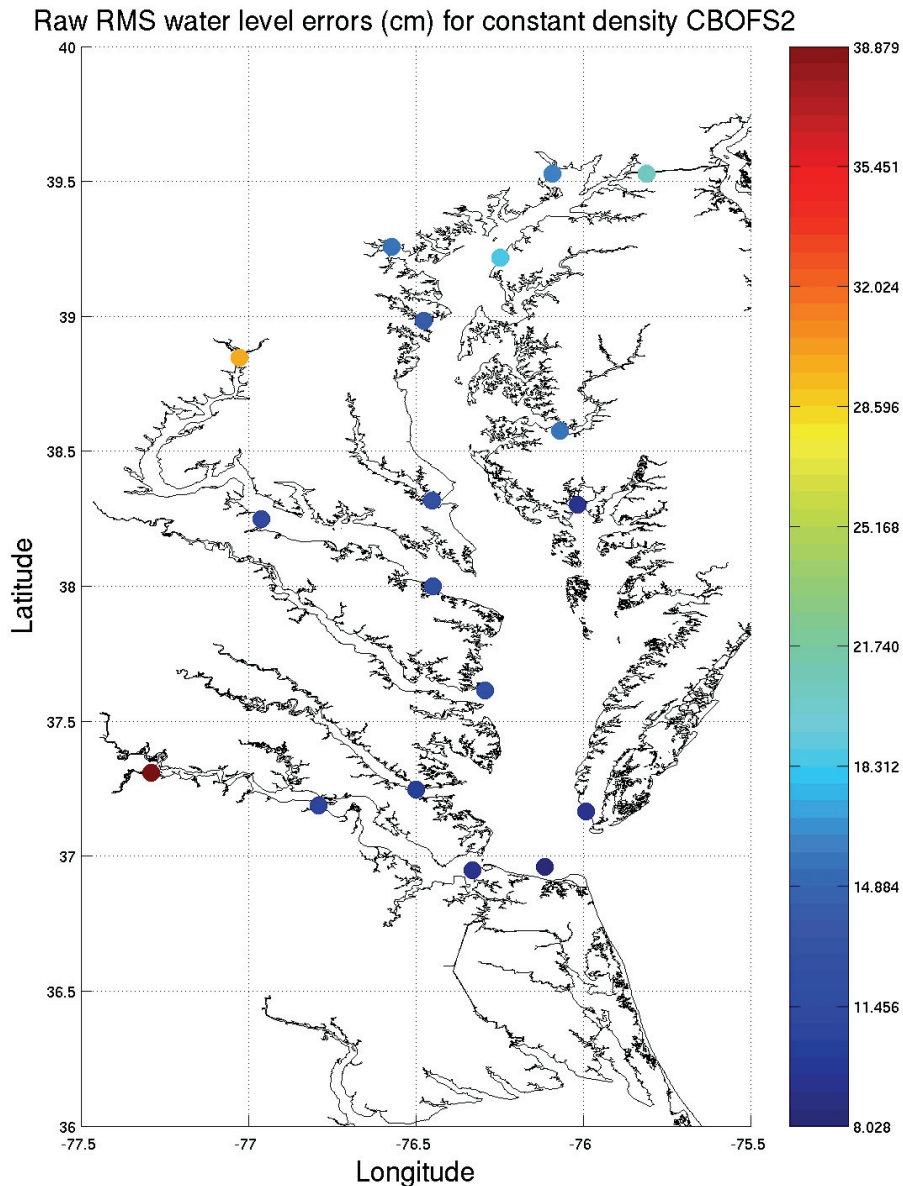


Figure 5. RMS water level errors (in cm) for the constant density CBOFS2 simulation.

(amplitude error). Conditions (a) and (b) also ensure that the two sets of time-series are composed of the same set of tidal harmonic constituents. Such RMSE translation curves were

calculated for each of the water level archive stations given in Figure 2 using a translation interval of 1-minute and the resulting curves are given in Figure 7 and each of them satisfies both conditions (a) and (b). The resulting amplitude and phase error components are also given in Table A3 of Appendix A and are plotted in Figures 8.

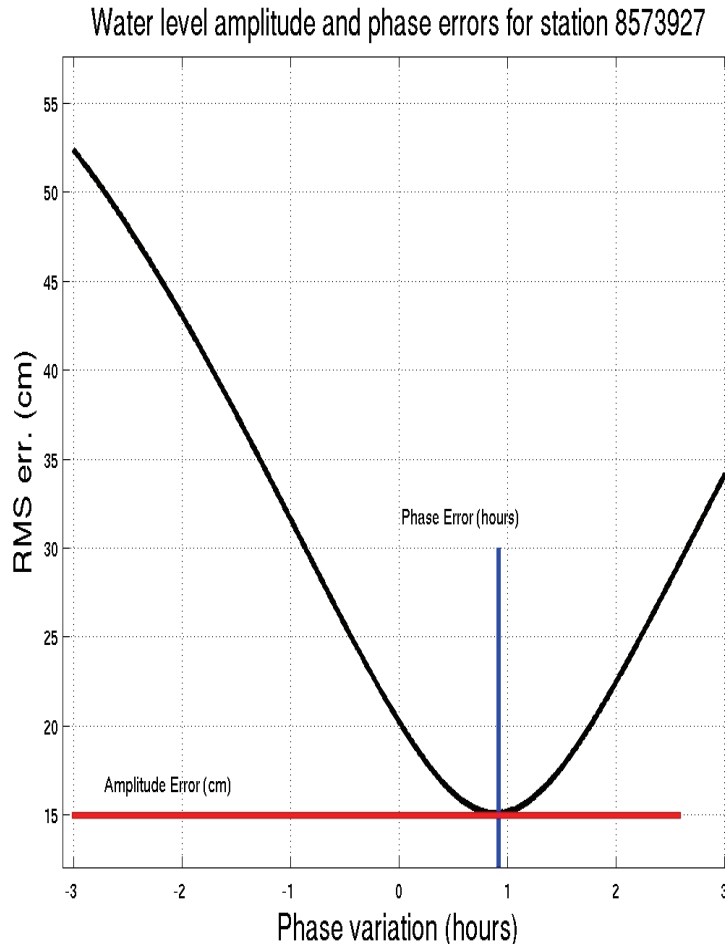


Figure 6. Splitting methodology of the RMS error into an amplitude component and a phase component. Here, x-axis annotation of phase variation or difference is equivalent to the amount by which the two water level time-series have been translated relative to each other.

Although the raw RMSE (Figure 5) shows that it is frequently above the allotted 15 cm limit, when decomposed into its amplitude and phase components, it is seen that a significant contribution to it comes from the phase error and that the amplitude component is below 15 cm. The phase error components tend to be mainly positive implying that CBOFS2 leads the tidal prediction. The raw RMSE, amplitude and phase error components are smallest in the vicinity of the mouth of the bay. It is seen that the requirement of the phase error to be less than 15 minutes/0.25 hours (for at least 90% of the time) is rarely met and perhaps this requirement is excessively stringent. Furthermore, the raw RMSE is seen to increase when moving up the bay and up the (James and Potomac) tributaries but their amplitude components only show a similar

trend for the former (up the Bay) and not for the latter (up the tributaries) ; the phase error component however, while showing a similar trend, also grows rapidly when moving up the tributaries due to an expected rapid growth in tidal phase between stations 8638433 and 8638489 and stations 8635150 and 8594900 as documented, for example, in Browne and Fisher (1988) and, which CBOFS2 is incapable of capturing. The physical reason for this rapid growth in phase could be due to the curvature of the tributaries and/or the bottom roughness (sediment type for example) and/or the local bathymetric features.

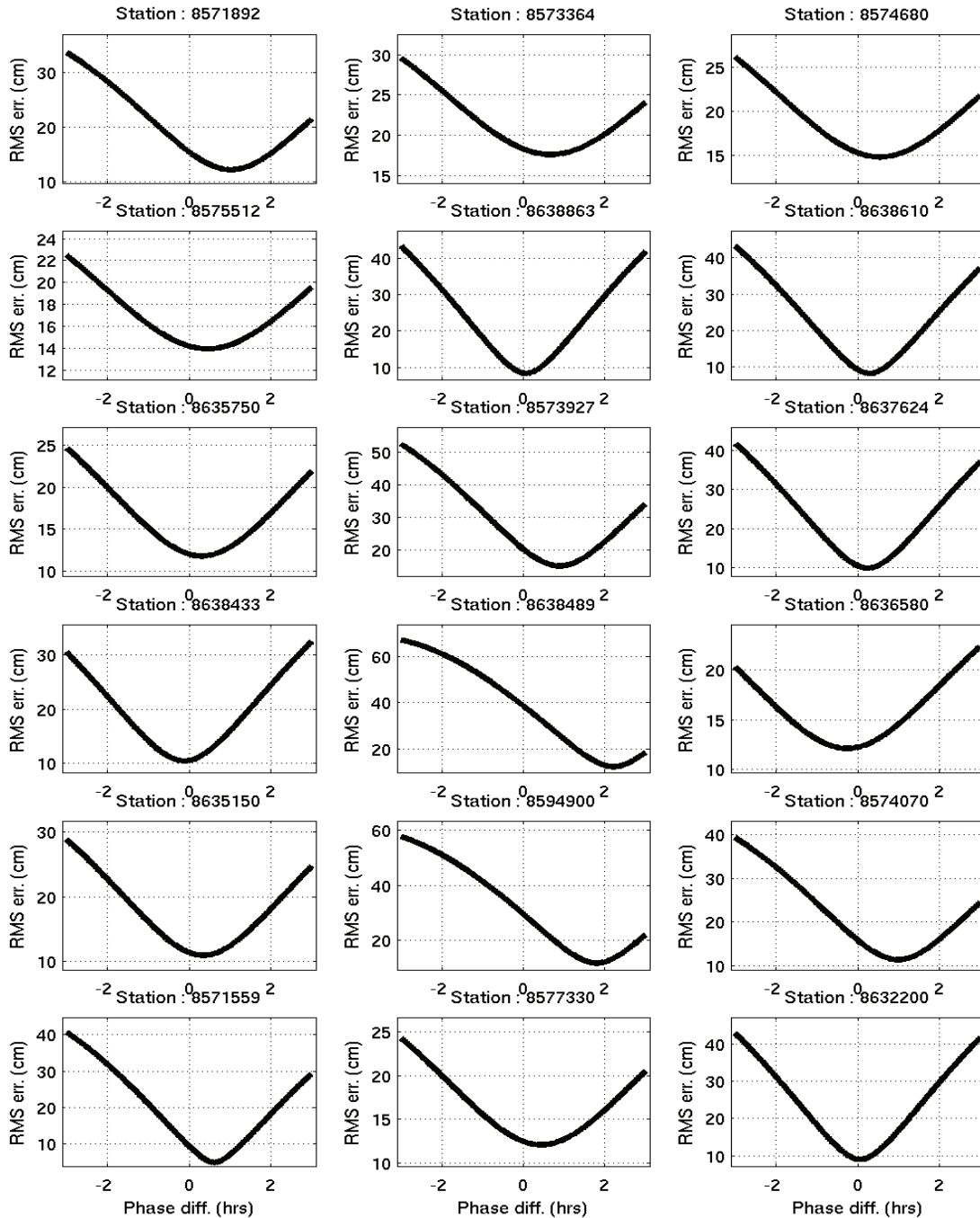


Figure 7. CBOFS2 RMSE translation curves for the comparison stations given in Figure 2.

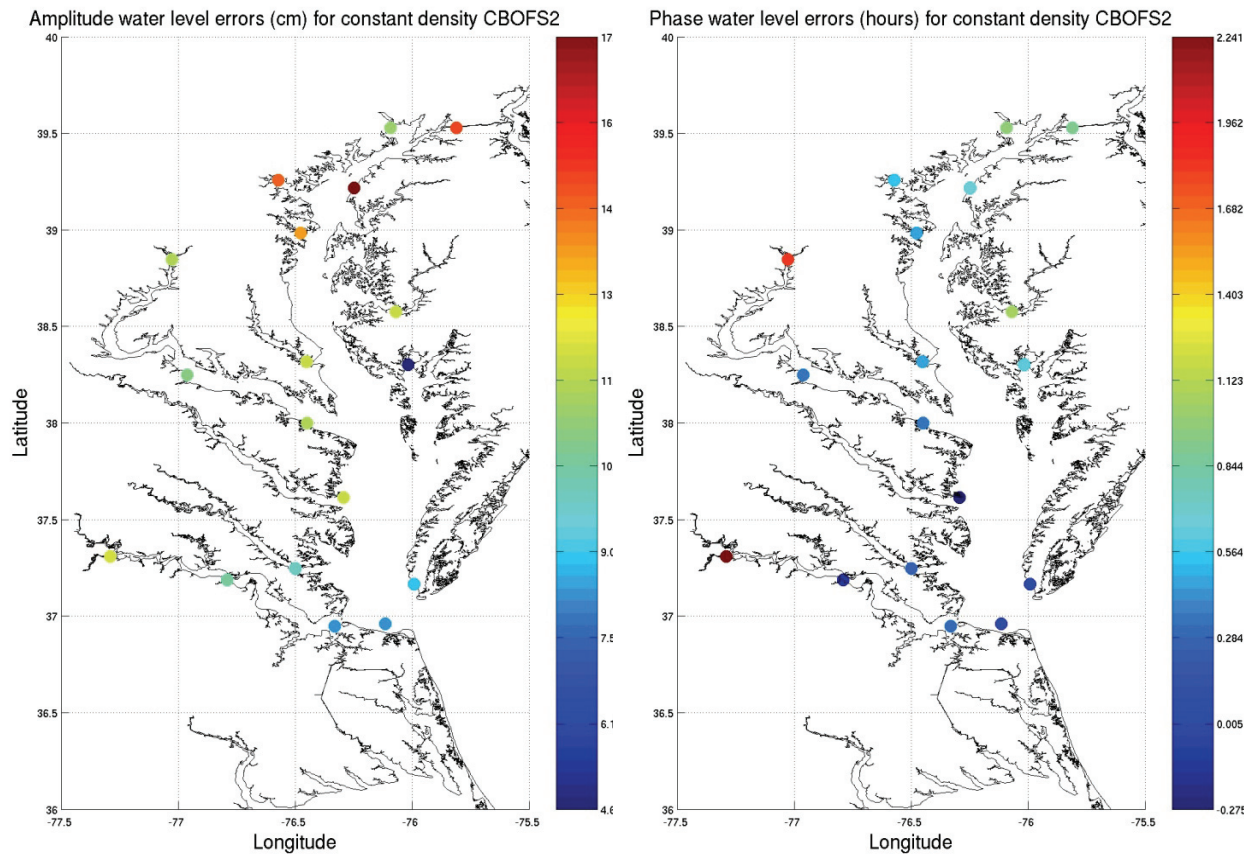


Figure 8. The amplitude error (in cm) and phase error (in hours) components of the RMS errors associated with the water levels for the constant density CBOFS2 simulation.

3.2. Currents Comparisons and Skill Assessments

The stations locations for comparison of currents are shown in Figure 9. These stations correspond to (i) those maintained by the NOS/CO-OPS/Currents Measurements Interface for the Study of Tides program (CMIST, 2009) at which currents at high vertical (< 1.0 m) and temporal (usually 6-minute) resolution are observed and archived and (ii) those from the 1981-1983 NOS Chesapeake Bay Circulation Survey (Browne and Fisher (1988)) which are usually available only at a few vertical depths. The currents comparisons were performed at 4.6m (15 ft) which is considered to be the nominal ships draft. The predicted tidal currents were obtained by using the harmonic constituents at these station locations derived by running the NOS harmonic analysis software on the CMIST and the 1981-1983 NOS observed current time-series data.

As with the water levels, the amplitude and phase errors associated with the M2, N2, K1 harmonic constituents (as they are the most dominant) for the true eastward (U) and true northward (V) currents are plotted in Figures 10 and 11 and are listed in Tables B1-B4 in Appendix B (which also contain the O1, P1 and L2 constituents).

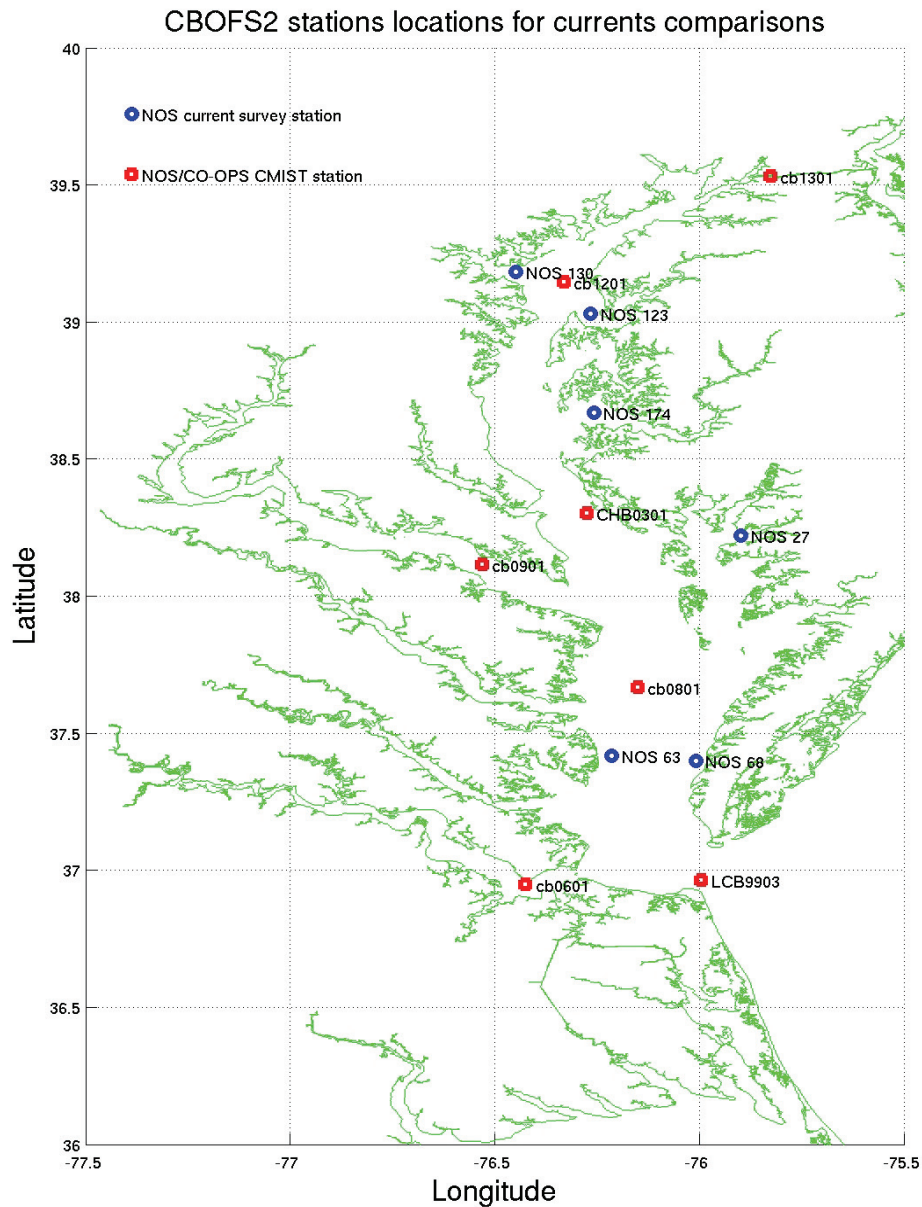


Figure 9. CBOFS2 currents stations archive locations for comparison with tidal predictions in the constant density simulation.

The greatest current amplitude errors are seen for the M2 constituent which is the most dominant and there is no strong pattern to the spatial distribution of the amplitude or phase errors. The errors however for stations cb0601 and cb1301 are excessively large because the former is in a narrow channel which the CBOFS2 grid cannot resolve and the latter is within the C & D canal the dynamics of which are modeled in a limited manner due to the use of open ocean boundary conditions and the inability to account for the full interaction with Delaware Bay.

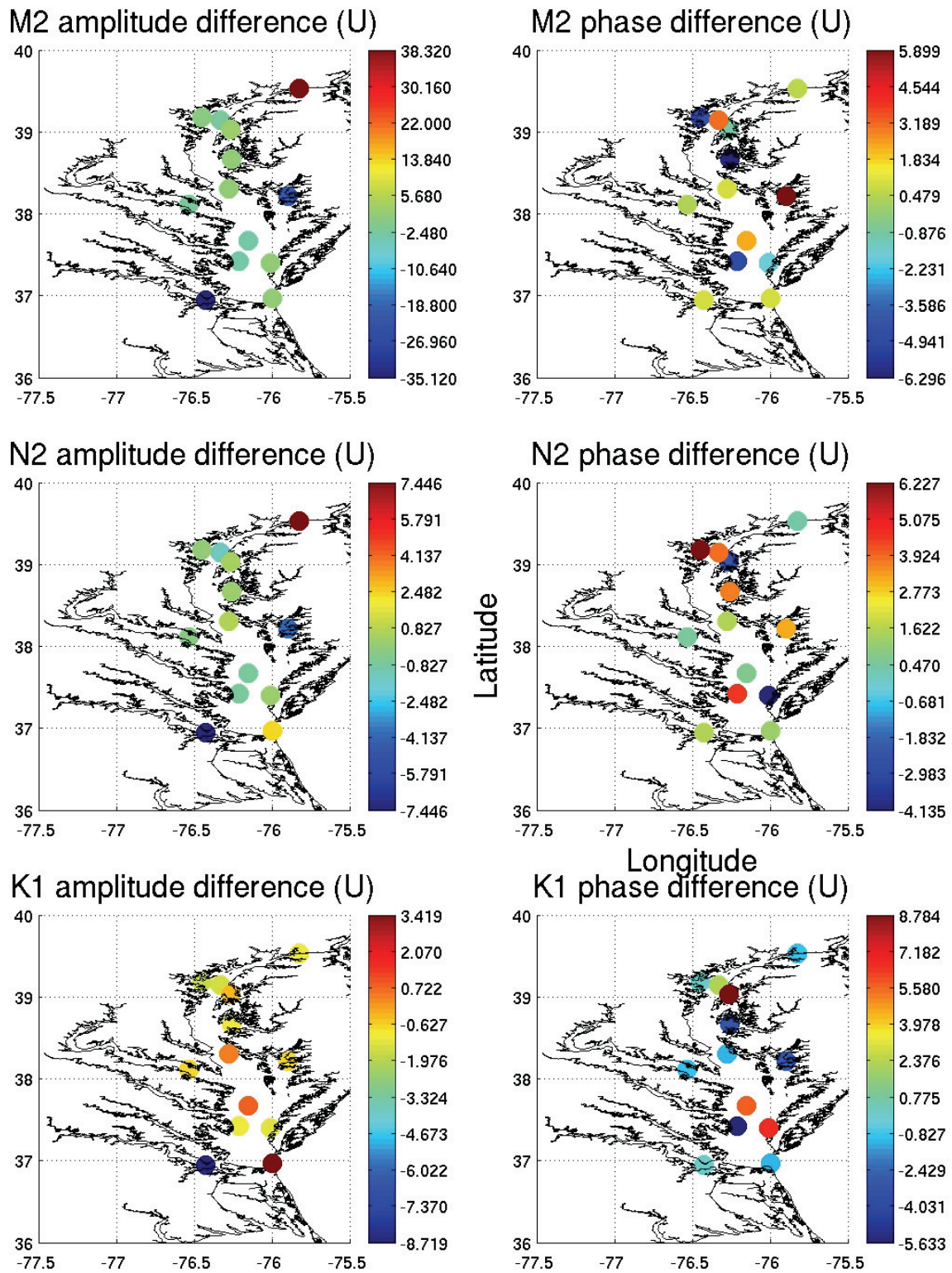


Figure 10. M2, N2 and K1 constituent CBOFS2 amplitude (in cm/s) and phase (in hours) errors (CBOFS2 minus prediction) for the true eastward current component in the constant density simulation.

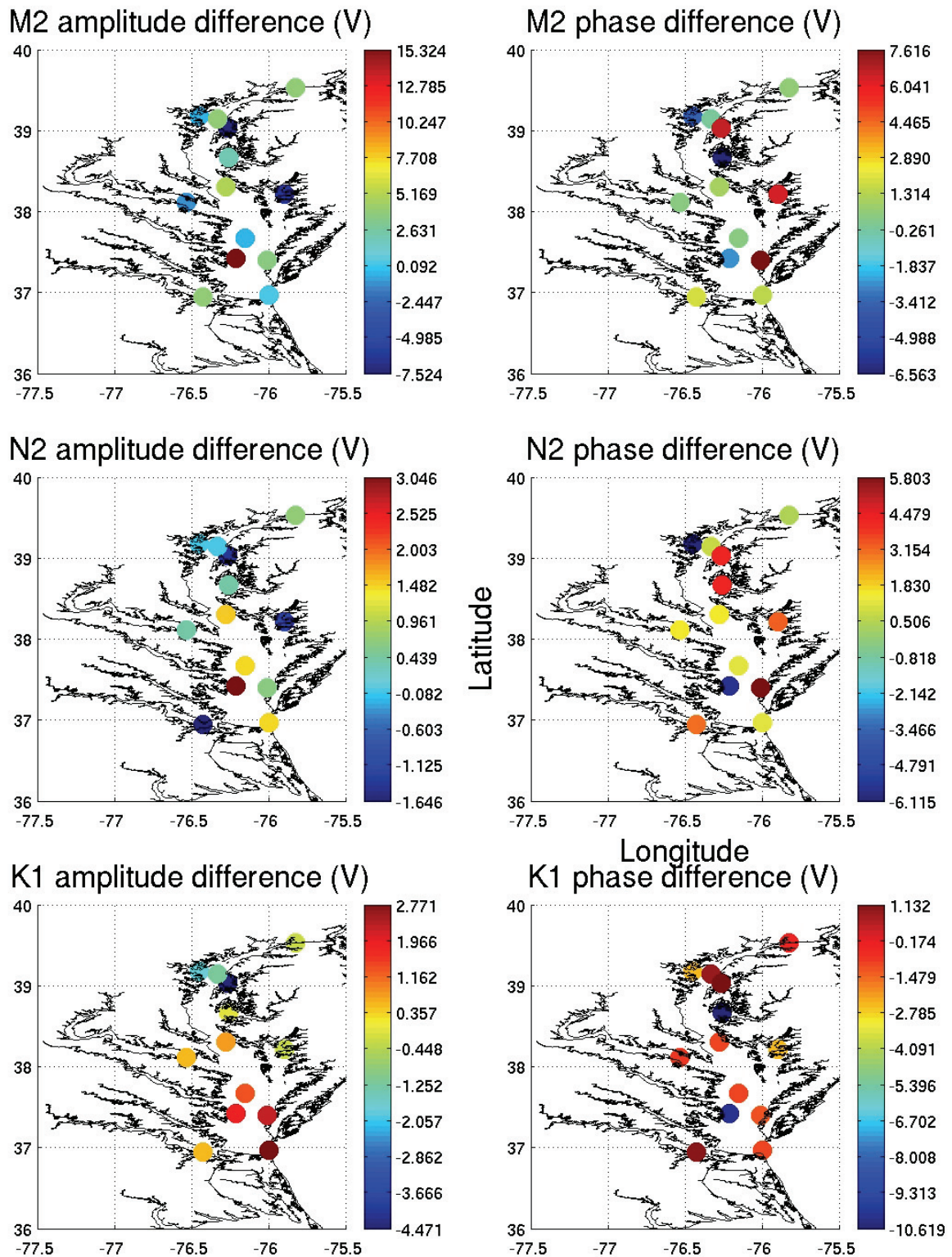


Figure 11. M2, N2 and K1 constituent CBOFS2 amplitude (in cm/s) and phase (in hours) errors (CBOFS2 minus prediction) for the true northward current component in the constant density simulation.

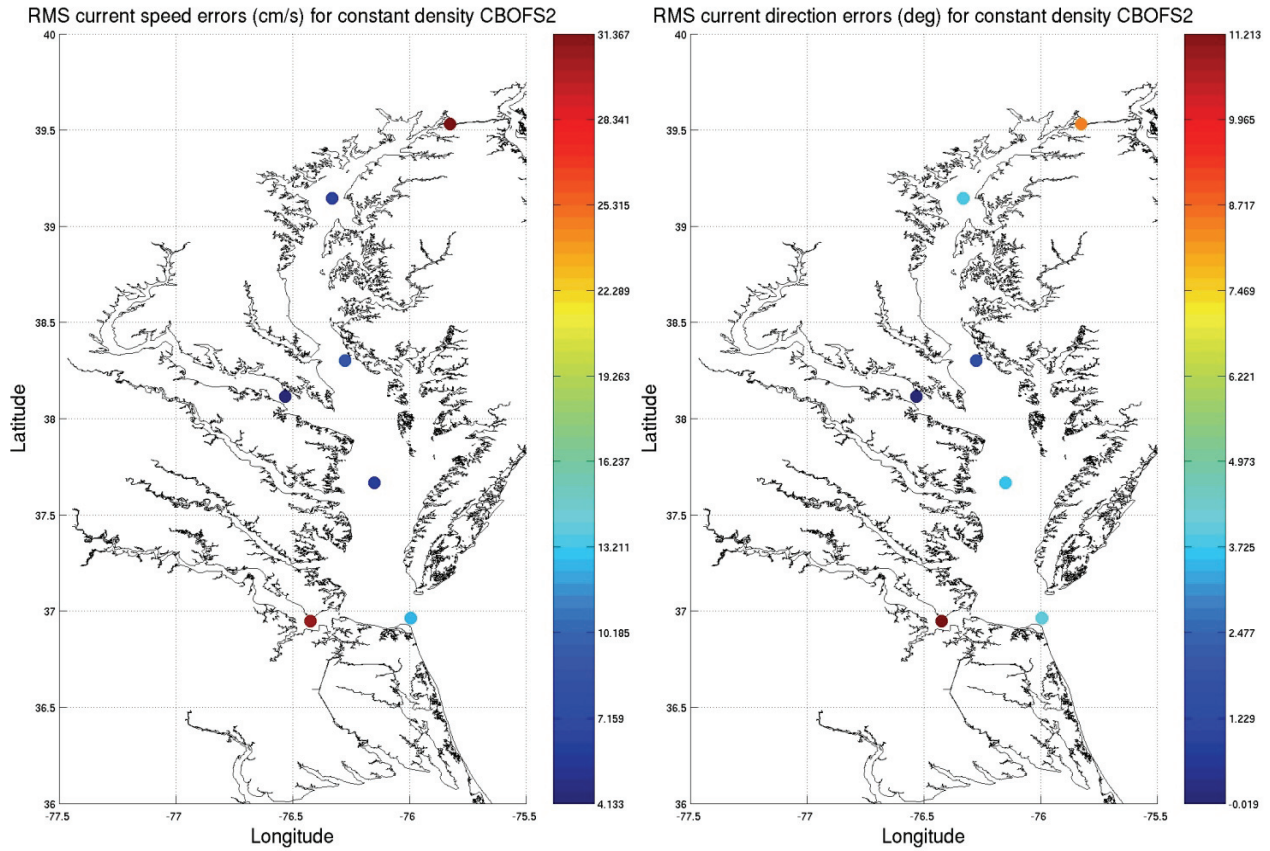


Figure 12. RMS current speed (left, cm/s) and current direction (right, degrees) errors (from the CSDL skill-assessment software package) at a depth of 15 feet (4.6m) for the CBOFS2 constant density simulation at the NOS/CO-OPS/CMIST observational stations.

The CBOFS2 versus predicted tidal currents comparisons are summarized in Tables B5-B7 in Appendix B. The NOS target skill-assessment criteria for currents comparisons is for (a) the speeds to agree to within 26 cm/s for at least 90% of the time (that is, $CF(26\text{cm/s}) > 90\%$) and (b) the directions of the major currents components to agree within 22.5° for at least 90% of the time (that is $CF(22.5^\circ) > 90\%$). The metrics in these tables too were generated using the CSDL skill-assessment package. Only the CMIST stations were employed for the comparisons as they had better quality data, for longer durations in time and which was also better resolved with depth.

Table B5 shows that the RMSE of the currents speeds satisfy the NOS criteria except for those at stations cb1301 (Chesapeake City, MD located within the C & D canal) and station cb0601, which is located within a narrow channel which the CBOFS2 model grid is unable to resolve. This also true for the maximum flood and ebb current amplitude errors.

Table B6 shows that the RMSE of the currents directions including those at maximum flood and maximum ebb and all of them meet the NOS criteria stated above.

Plotted in Figure 12 are the RMS currents speed and direction errors given in Tables B5 and B6. As explained above, the largest errors are at stations cb0601 and cb1301 and with the exception of these two stations, the errors remain well below the critical limit throughout the Bay; and, there is not a strong pattern to their spatial distribution and there is no growth in their magnitudes when moving up the Bay - although they show somewhat of a decrease in value.

The major current component (in the Principal Current/Flood Direction) RMSE, its amplitude contribution and its phase contribution comparisons are given in Table B7 and they are plotted in Figure 14. The corresponding RMSE translation curves for the comparison stations are shown in Figure 13 and they again exhibit smooth behaviors and each contain a unique, global minimum thus rendering the RMSE splitting method valid.

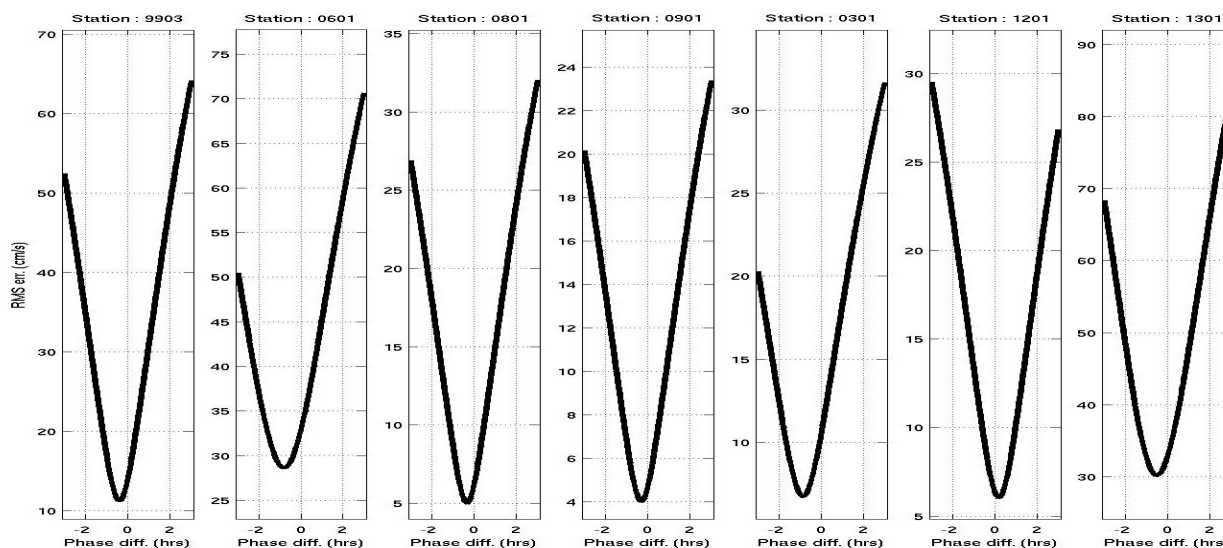


Figure 13. RMSE translation curves for the CBOFS2 major current component for the comparison stations.

The greatest amplitude error components are at the same stations mentioned above (cb1301 and cb0601), which miss the NOS criteria although not by very much whereas the other stations meet the NOS criteria quite well. The phase error component is not only largest at these two stations but also at station CHB0301 and the examination of other depths at this station showed similar trends throughout the water column. The data itself was found to be of good quality, and the CBOFS2 bottom depth was also in close agreement with the observed depth. The phase errors indicate that the CBOFS2 currents lag relative to the predicted currents. This is opposite to the phase error trend seen in the water level comparisons.

Plotted in Figure 15 are the CBOFS2 major-direction current components against depth at three separate time snapshots and their profiles ± 1 hour relative to these times (in order to account for

tidal phase errors in CBOFS2). Station cb1301 was excluded as it is based on Side Scan Sonar measurements. The predicted curve is the thick black line and it was generated using harmonic constituents extracted from observations (via the NOS software) at each of the observational stations and depths. They show in general that CBOFS2 profiles without a time shift are the ones that are best correlated with the predictions and that the predictions contain much more vertical stratification specially in the near-surface and near-bottom regions. The reason for the lack of stratification in CBOFS2 is not known but it may be due to the use of the algebraic Mellor-Yamada 2.5 vertical eddy-viscosity closure scheme.

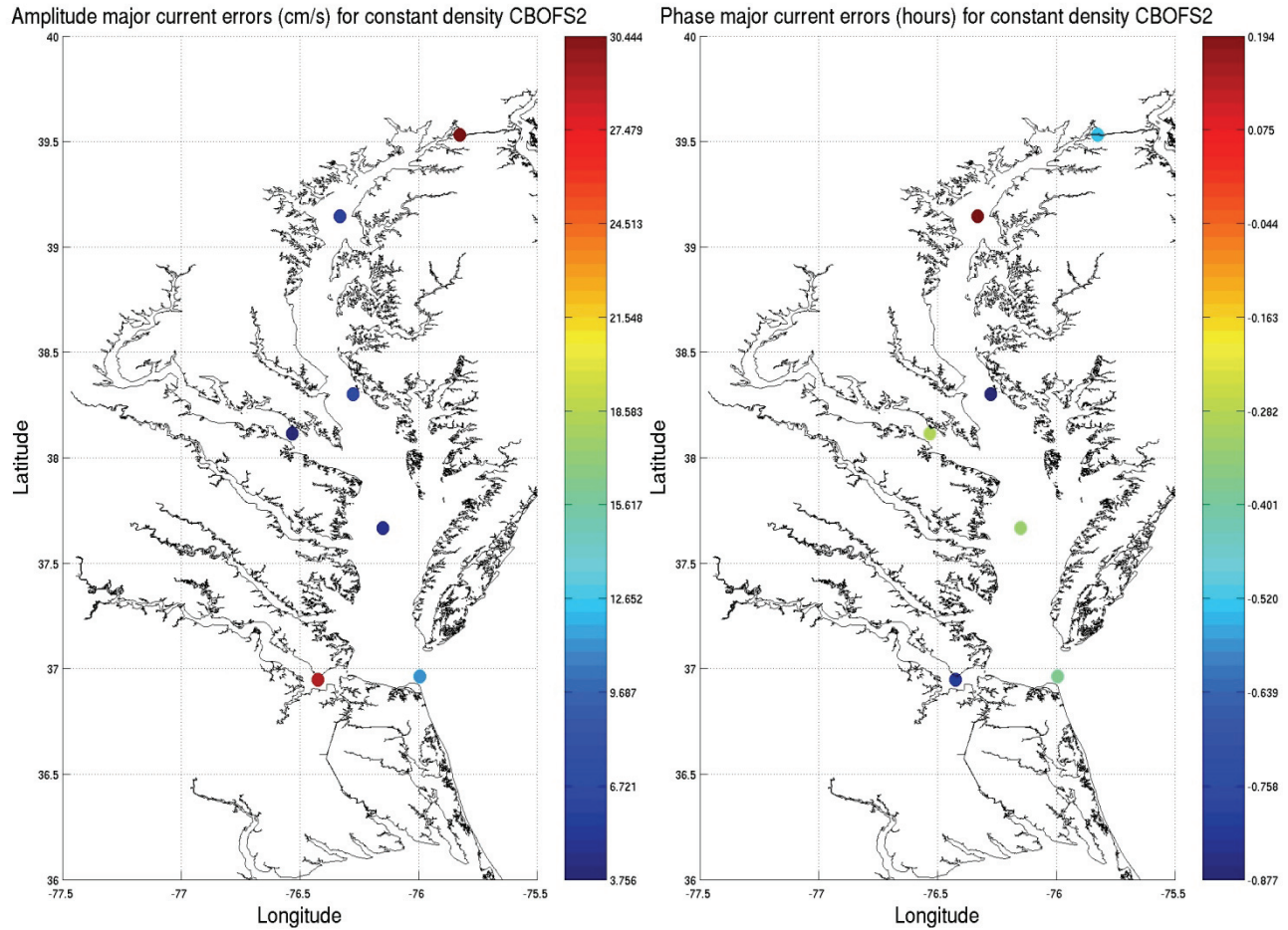


Figure 14. The amplitude (left, cm/s) and phase error (right, hours) components of the RMS errors associated with the major current in the constant density CBOFS2 simulation.

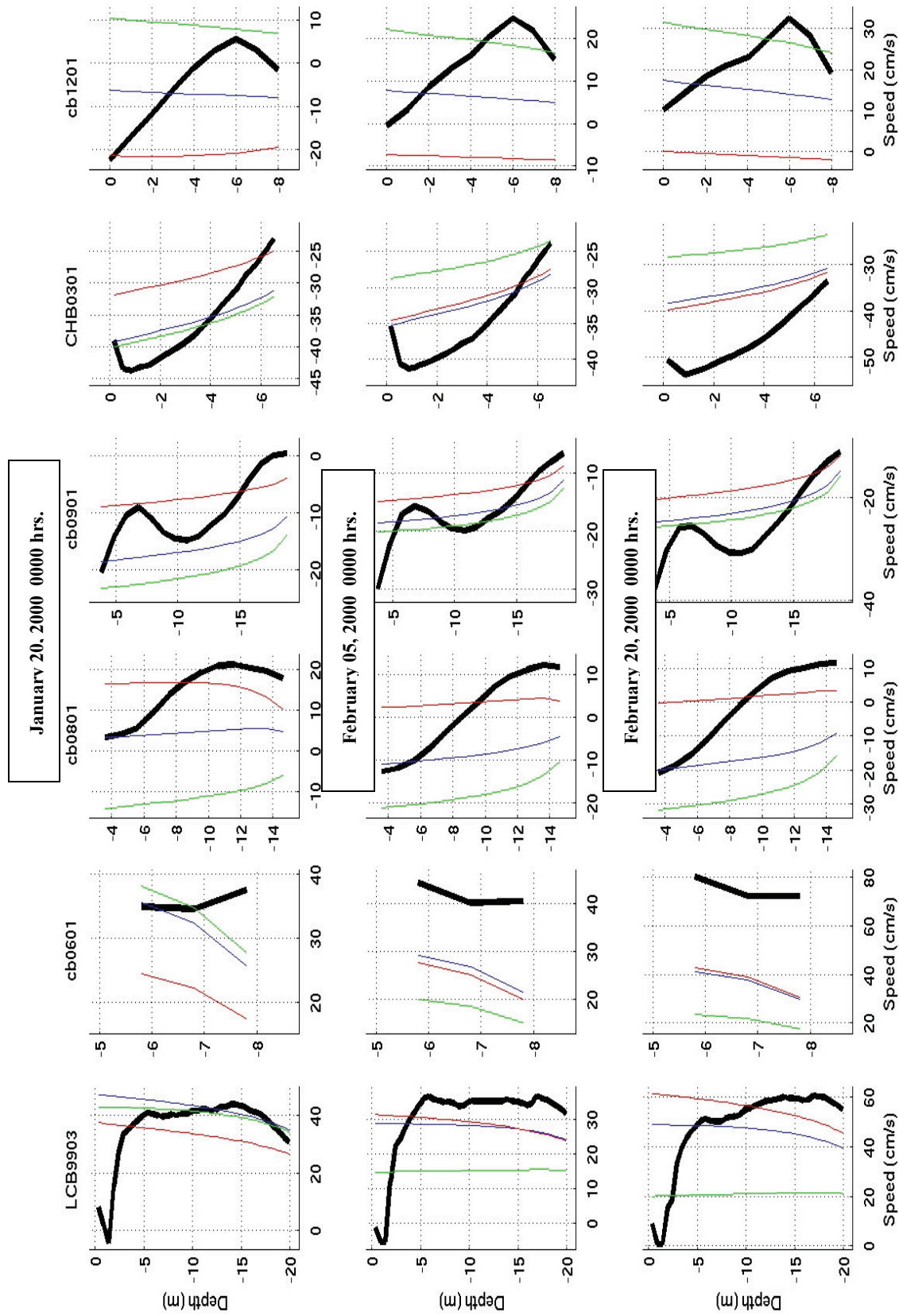


Figure 15. Vertical structure of major-direction currents for the constant density CBOFS2 simulation (black – NOS/CO-OPS/CMIST prediction, blue – CBOFS2, red – CBOFS2 with 1 hr. phase lag, green – CBOFS2 with 1 hr. phase lag).

4. SYNOPTIC HINDCAST SIMULATION

The synoptic hindcast simulation to validate the full suite of CBOFS2 output fields (water levels, currents, temperature and salinity) was run from June 01, 2003 – September 01, 2005. This time period was selected because: (i) it is sufficiently long (27 months) to show seasonal variations; (ii) it has both very dry (low river discharge) and wet (high river discharge) periods as seen from the total river discharge plot in Figure 16; and (iii) it includes an extreme meteorological event (that is, Hurricane Isabel) as shown in Figure 17. These diverse conditions will not only serve to validate the physics of the model, but will also test the numerical stability associated with the CBOFS2.

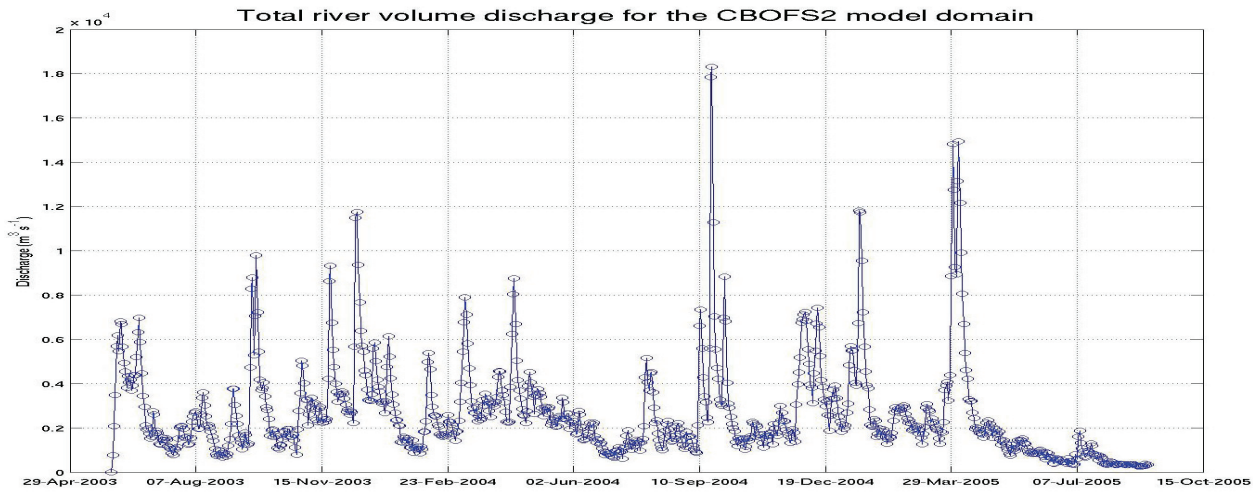


Figure 16. Total river volume discharge for the CBOFS2 model domain spanning 2003-2005.

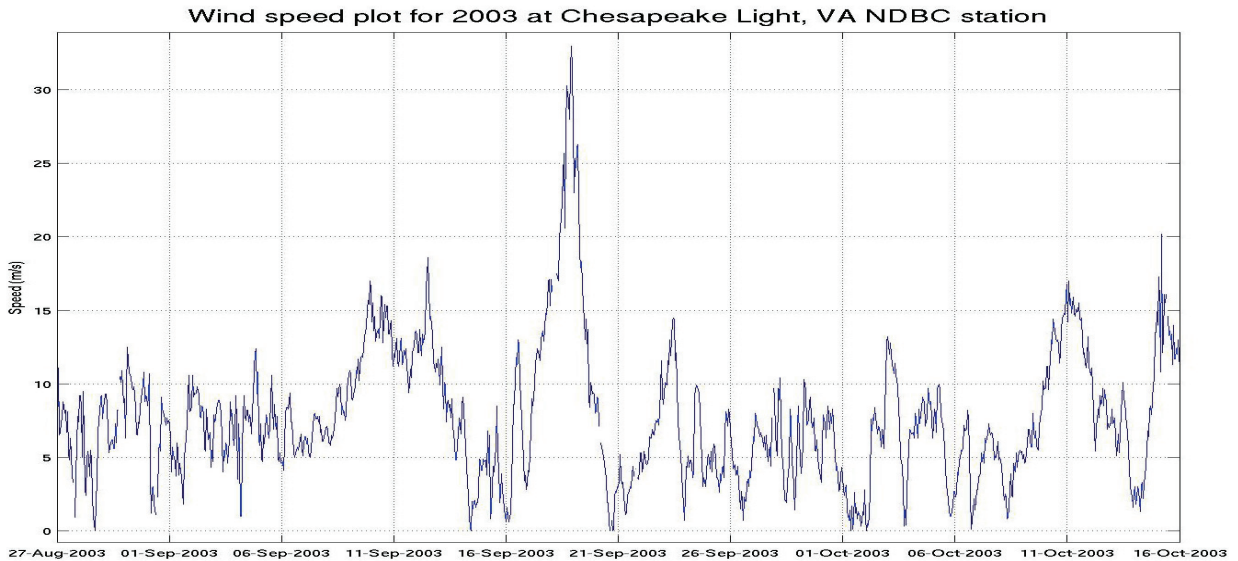


Figure 17. Wind speed plot for August-October, 2003 at Chesapeake Light, VA NOAA/National Data Buoy Center (NDBC) station showing hurricane Isabel.

4.1. Initial Conditions and Model Forcings

The model was spun-up from rest and the initial temperature (T) and salinity (S) fields were generated by (a) interpolating the World Ocean Atlas 2001 (WOA 2001, Conkright, et al., 2002) monthly climatological T and S values on to the CBOFS2 grid in the horizontal and the vertical for the mid-lower part of the Bay (below the Patuxent River), (b) interpolating the Chesapeake Bay Program (CBP, 2009) T and S values for the upper part of the Bay (above the Patuxent) and then (c) melding (a) and (b) in a smooth and continuous way through bilinear interpolation. The reason for using Bay Program T, S values for the upper segment of the Bay was that in this region, unlike in the mid-lower Bay, significant differences were seen between the Bay Program and WOA 2001 T, S values (which had good coverage in the lower Bay).

For the river forcing, the volume discharges were obtained from the US Geological Survey (USGS) historical data (USGS, 2009) and the river T, S values were obtained from the Bay Program stations closest to the corresponding USGS gauge locations.

The meteorological forcing fluxes (wind stresses and net heat flux) in CBOFS2 were computed within ROMS using its bulk flux formulation and the input fields of the wind speed components, air temperature, air pressure, air relative humidity, net shortwave radiation and downward longwave radiation were primarily taken from the 32 km resolution North American Regional Re-analysis products (NARR, 2009). These 3-hourly NARR fields for winds, air temperature, air pressure and relative humidity (via the dew point) were enhanced by spatio-temporally blending them with hourly observed historical data within the Bay and on the shelf from the following NOAA/NDBC stations (NDBC, 2009): TPLM2 (Thomas Point, MD), CHLV2 (Chesapeake Light, VA), 44014 (east of Virginia Beach, VA), 44009 (Delaware Bay southeast of Cape May, NJ) and DUCN7 (Duck Pier, NC). These stations together with the NARR grid points used for the generation of the meteorological fields are plotted in Figure 18. In order to increase the influence of the NDBC stations in the creation of these fields (via spatial interpolation), some NARR data points in the vicinity of the former were removed from the process as also depicted in Figure 18. Furthermore, in the creation of the wind, air temperature, dew point/relative humidity and net shortwave radiation fields, only water points on the NARR grid were employed as pronounced differences in them were seen between on-land points and in-sea points.

In addition, upon comparison with observations at NDBC station 44009, it was found that the optimal level of net shortwave radiation to use was 80% of the value provided by NARR and therefore a global scaling factor of 0.8 was applied to the radiation flux employed in CBOFS2. Similar comparisons for air temperature and dew point with this NDBC station yielded minor global adjustment factors/offsets which were applied to the fields before being used within CBOFS2.

For the open ocean boundary conditions along the southeastern boundary, the T and S values were taken from the WOA 2001 monthly climatology. The non-tidal water levels were those extracted from the NOS/CO-OPS Ocean City, MD and Duck, NC stations. These values were then distributed along the boundary nodes via linear interpolation using the arc distances from the two end points as also described in Section 3. The tidal component of the forcing was

generated in exactly the same manner as for the constant density simulation and thereafter the two contributions were combined at each of the boundary grid points. For the C & D canal open boundary, the T, S values were derived from the USGS station 01482800 which lies within Delaware Bay, the full (tidal plus non-tidal) water levels were prescribed using the observations at the NOS/CO-OPS Reedy Point, DE station and the barotropic currents were obtained from a prediction using the analyzed tidal harmonic constituents from NOS station 154 as also explained in Section 3.

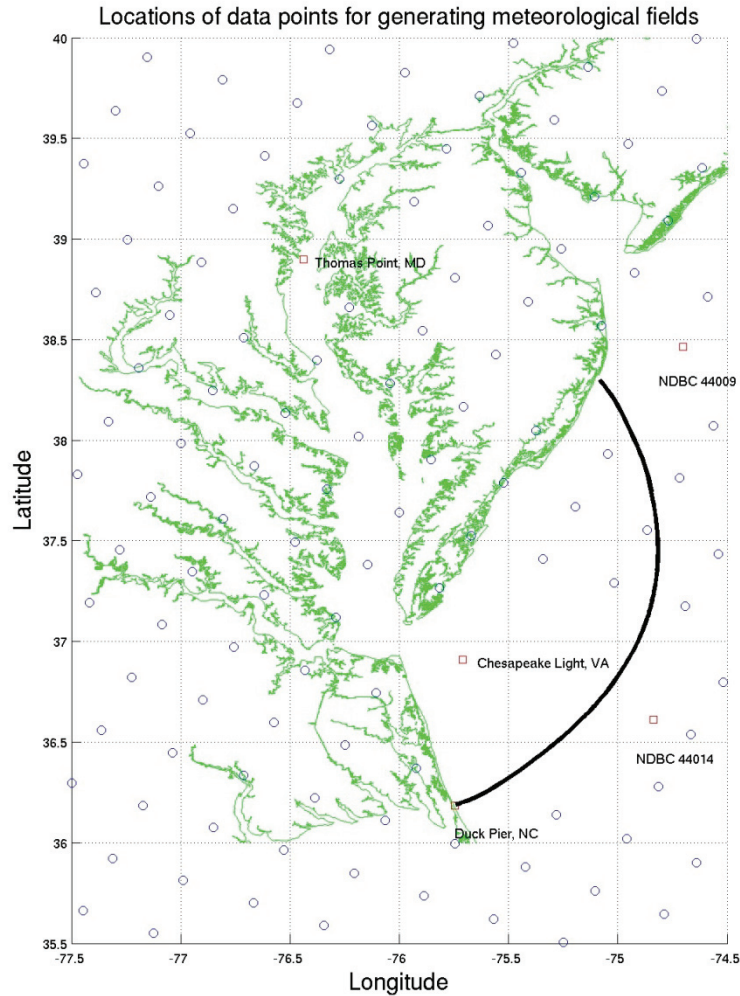


Figure 18. NARR (blue circles) and NDBC (red squares) data points used in the creation of the wind, air temperature, relative humidity/dew point and net shortwave radiation fields; the thick black line is the southeastern open boundary of the CBOFS2 computational domain.

The model was run with a 15 second baroclinic time step and a 0.75 second barotropic time step; this time step was half of that used for the constant density simulation. This reduction in its value was necessary to maintain the numerical stability of CBOFS2 (due to the fine grid employed to resolve the C & D canal when density effects were included). The model was run with MPI parallelization using 96 processors and in 15-day segments, each of which took

approximately 150 minutes to complete thereby yielding a highly efficient computational effort ratio of 1:144. The ROMS model configuration for this case was identical to that for the constant density simulation with exception that (i) for the vertical eddy-viscosity model choice, the GLS $k-\omega$ model was employed as it generated the best overall vertical T and S stratification; (ii) several additional model forcings (for example, river forcing, etc.) were included; and (iii) as described previously, a realistic T-S field was employed in the model initialization. In the application of the model forcings, the river volume discharges, winds in the meteorological forcing and the non-tidal water levels in the open boundary forcing were ramped up linearly in time during the first five days past model initialization.

CBOFS2 ran successfully for the entire 27-month period without experiencing any numerical instabilities thereby illustrating that this modeling set-up is capable of withstanding a diverse range of environmental conditions observed in the Bay. During the computations, the maximum u-component, v-component, w-component of the Courant-Freidrichs-Lewy (CFL) numbers as well as the maximum of their sum were monitored to examine their numerical stability. Due to the (i) use of the upstream-biased advection schemes in the horizontal in ROMS and hence the lack of a need for the use of explicit horizontal viscosity to control spatial numerical oscillations and the (ii) use of an implicit vertical viscosity formulation in ROMS (solved locally via a tri-diagonal solver), the CFL number alone is an adequate measure of the numerical stability associated with the overall model algorithm. Plotted in Figure 19 are the time-series for each of the CFL number components and it shows that (a) the total maximum CFL number is well below unity for the vast majority of the time and when it exceeds this limit, it does so for very brief intervals in time and in highly localized regions in the model grid (hence, not rendering CBOFS2 numerically unstable and causing model blow-ups), (b) the largest contribution to the total CFL number comes from the w-component and (c) the u-component and v-component are significantly smaller than the w-component. It has also been found that the largest CFL numbers usually occur within the C & D canal where the mesh is quite fine.

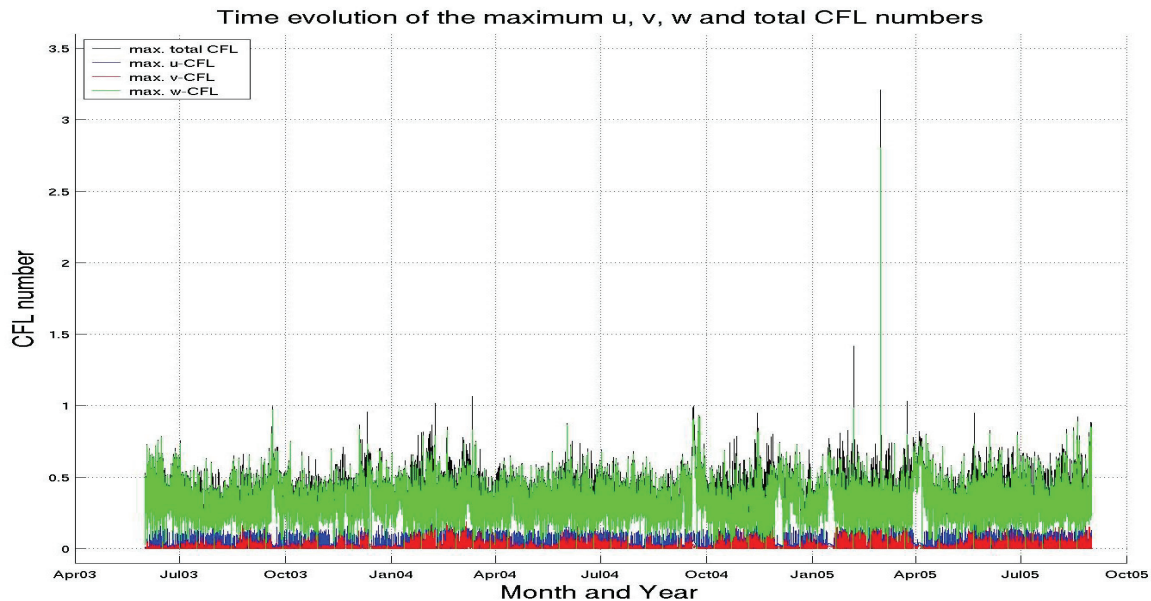


Figure 19. CFL number time-history for the synoptic hindcast simulation.

4.2. Water Level Comparisons

The water levels were compared with observed values at the NOS gauges shown in Figure 20.

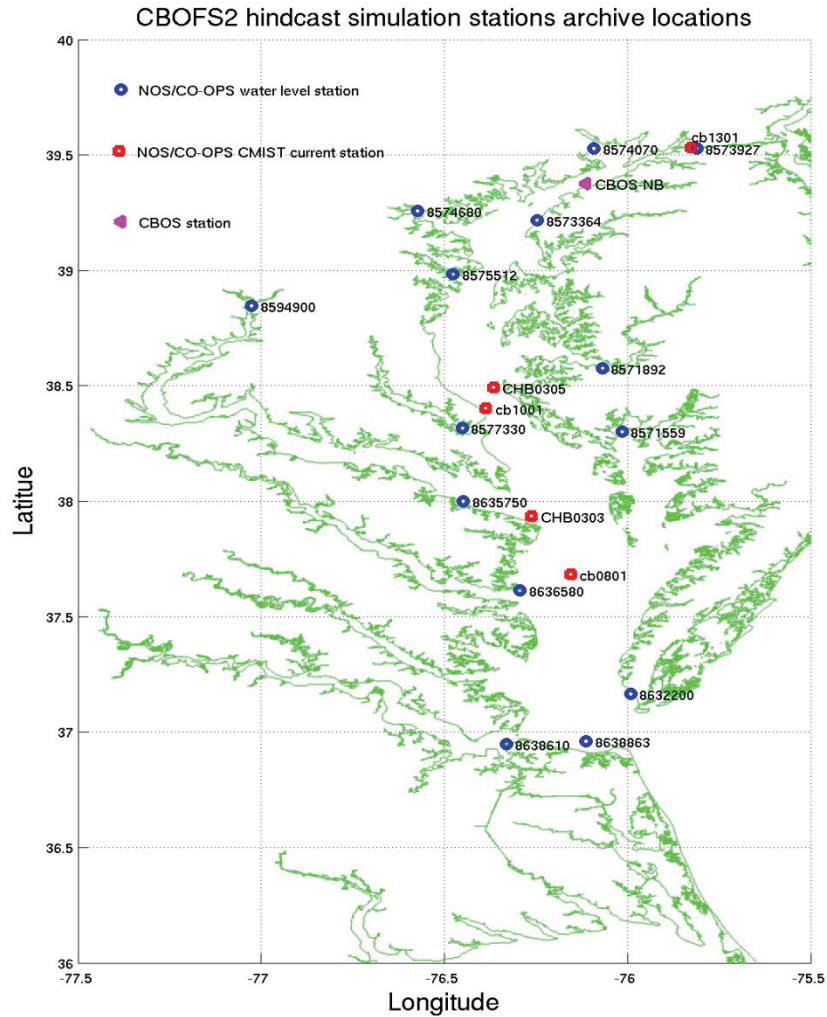


Figure 20. Water level and currents stations archive locations for the synoptic hindcast CBOFS2 simulation for comparison with observations.

The raw RMS water level errors plotted in Figure 21 have been evaluated using observations from the NOS/CO-OPS database (NOAA Tides & Currents, 2009b). They show that the errors are greater in magnitude than those for the constant density case (at coincident locations) and the largest ones are in the upper bay and up the Potomac River tributary at Washington DC.

As before, employing the translational curve method, these RMS errors were split into their amplitude and phase components and they are plotted in Figure 23. The RMSE curves themselves are plotted in Figure 22 and they satisfy the error splitting validity requirements of being smooth in space and having a single, unique global minimum.

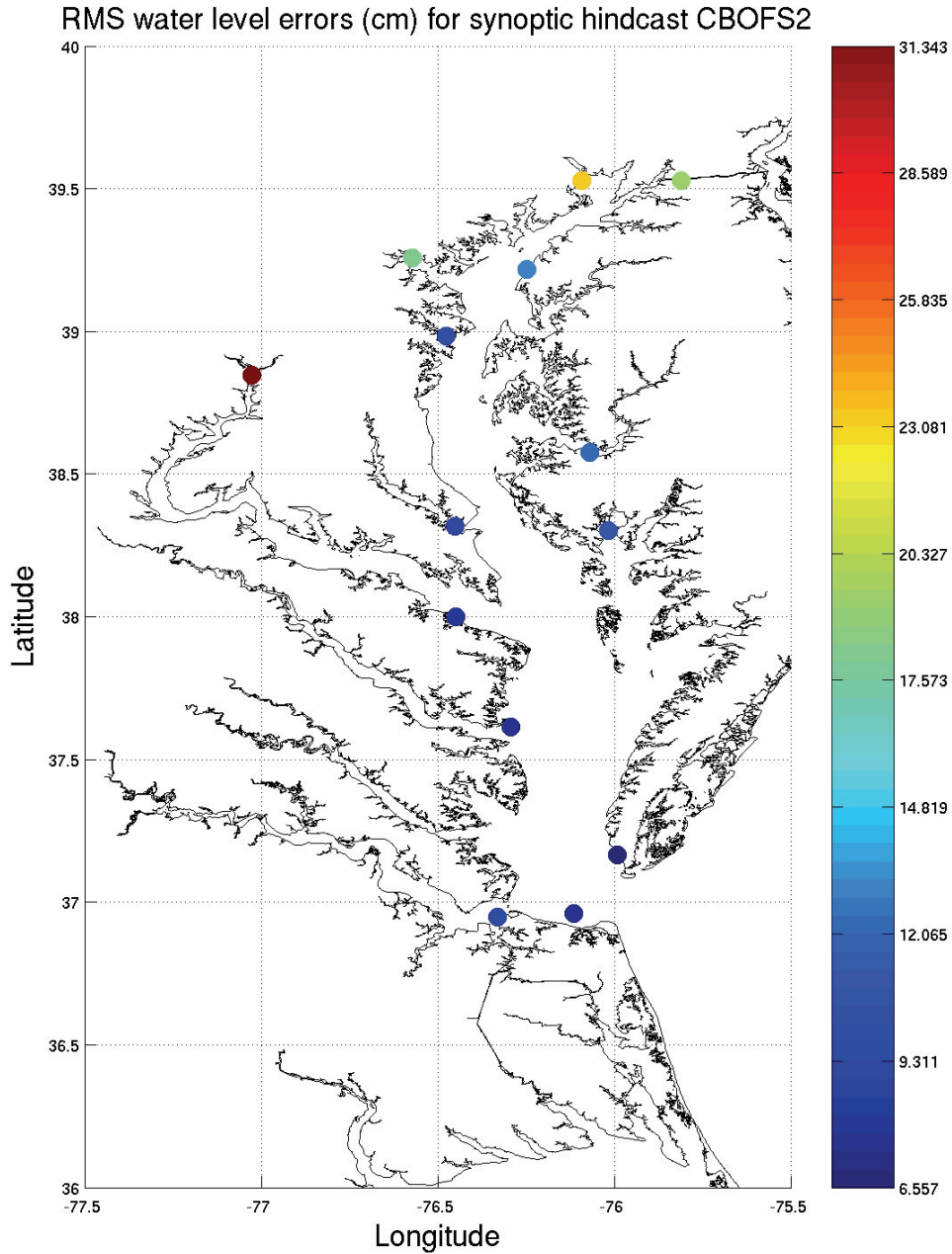


Figure 21. RMS water level errors (in cm) for the synoptic hindcast CBOFS2 simulation.

The distribution of the amplitude and phase errors in space show that they grow when moving towards the northern extent of the Bay and the smallest errors are in the vicinity of the Bay mouth. In addition, the phase error grows in magnitude when moving up the Potomac River tributary towards Washington DC. Similar inferences were made regarding the water level errors in the constant density simulation.

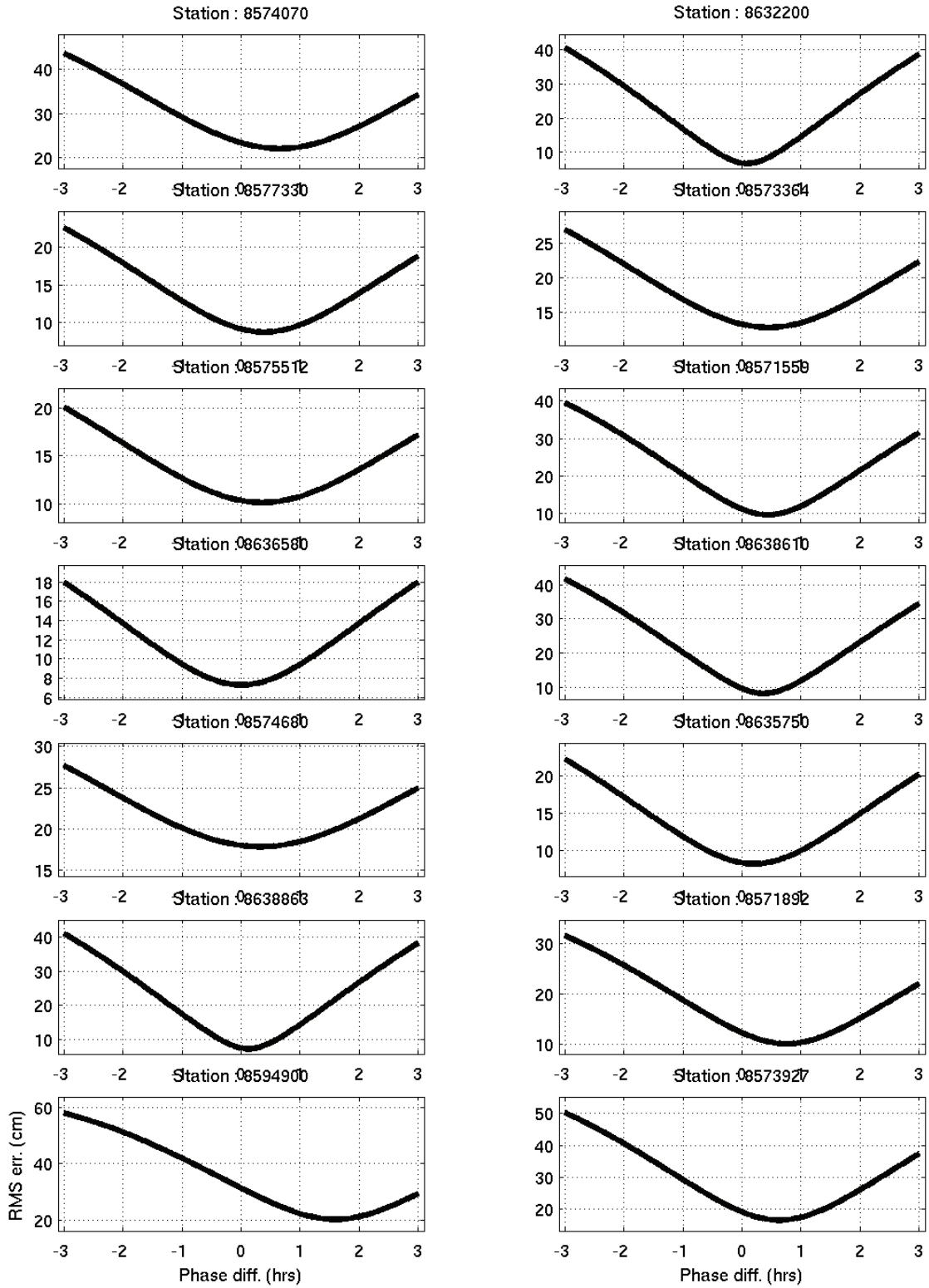


Figure 22. CBOFS2 synoptic hindcast RMSE translation curves for the comparison stations.

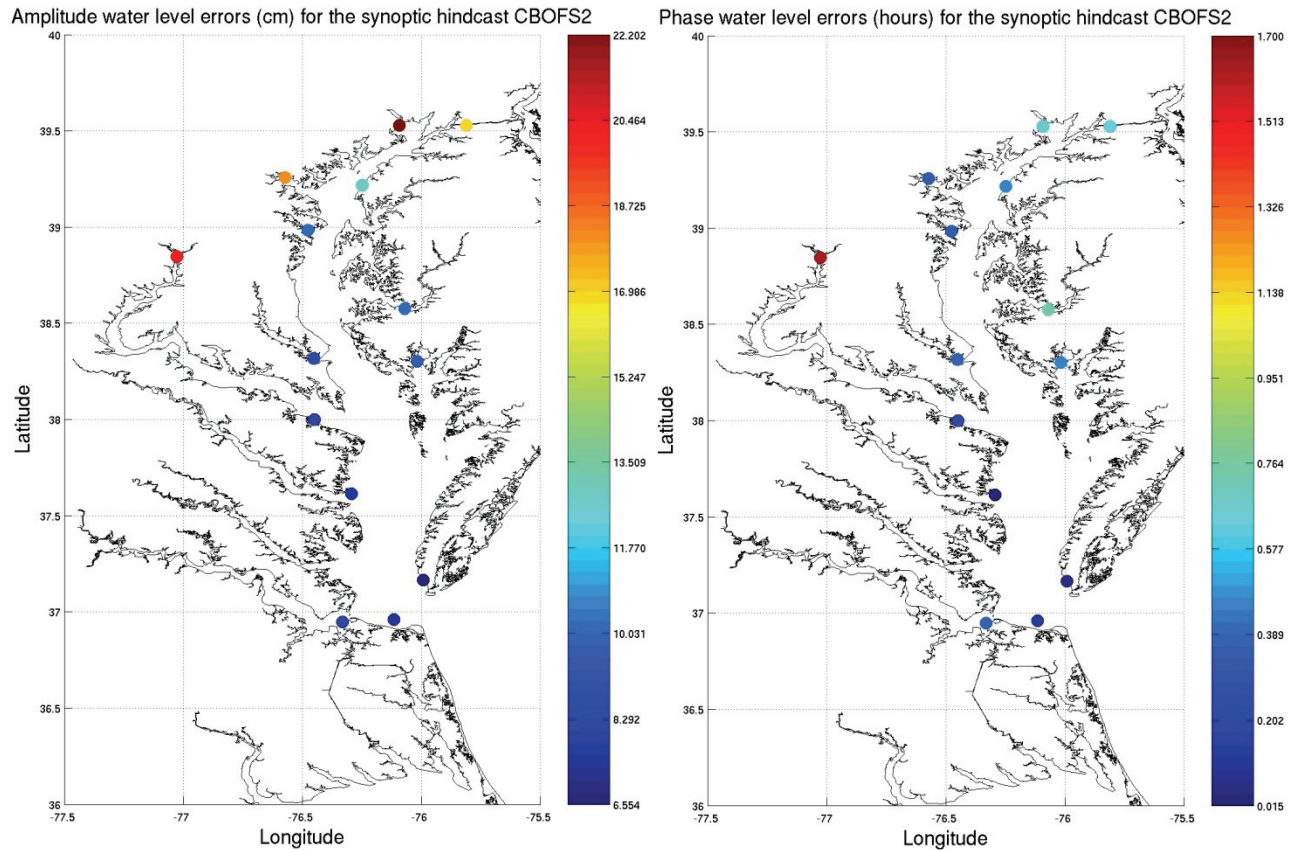


Figure 23. The amplitude error (cm) and phase error (hours) components of the RMS errors associated with the water levels for the synoptic hindcast CBOFS2 simulation.

The errors associated with the CBOFS2 water levels are summarized in Table 1. The raw RMS water level errors indicate both an improvement and a degradation relative the corresponding errors for the constant density simulation. For the stations where the RMS errors violate the NOS criterion (stations 8574070, 8574680, 8594900 and 8573927), generally, the synoptic hindcast errors exceed those of the constant density simulation. In particular, the amplitude components of the errors still remain above 15 cm whereas for the constant density tidal simulation, practically all of the stations generated errors less than 15 cm. The phase components of the errors however show a marked improvement over their constant density counterparts (although still failing to meet the stringent 15 minute/0.25 hour NOS skill assessment criterion). These CBOFS2 phase errors are always positive and hence produce a phase lead relative to observations. In terms of the Central Frequency, CF for the RMSE, only about five stations satisfy the $CF(15\text{cm}) > 90\%$ criterion and for the high and low water amplitudes, they are five and ten stations respectively. Therefore, the synoptic hindcast CBOFS2 water level predictions have a bias such that the low water amplitudes are predicted better than the high water amplitudes and such a bias was not seen in the constant density case (where the proportion of high and low water amplitudes satisfying $CF(15\text{cm}) > 90\%$ was the same). As expected, it is the stations with the smallest errors that are most likely to have $CF(15\text{cm}) > 90\%$.

Table 1. Water level error summary for the synoptic hindcast CBOFS2: Tidal range (cm), RMS error (cm) and its Central Frequency (CF), high water amplitude error (AHW_err, cm) and its CF, low water amplitude error (ALW_err, cm) and its CF (all from the CSDL skill-assessment software package), amplitude component of the RMSE (cm) and the phase component of the RMSE (hours).

Station	Range	RMSE	CF	AHW_err	CF	ALW_err	CF	Amp_err	Phs_err
8574070	57.9	23.2	37.2	25.9	7.0	18.5	39.9	22.0	0.65
8632200	79.2	6.8	96.5	7.3	96.1	5.5	98.4	6.7	0.07
8577330	35.7	9.1	91.2	10.4	88.4	6.7	96.1	8.7	0.38
8573364	36.9	13.1	76.2	16.1	60.6	8.2	93.4	12.7	0.45
8575512	29.6	10.3	87.4	10.7	85.5	8.5	92.7	10.1	0.35
8571559	62.5	11.0	85.9	13.2	79.0	7.8	93.9	9.7	0.45
8636580	34.7	7.5	95.0	6.7	95.9	7.2	95.3	7.3	0.02
8638610	74.1	9.5	88.3	12.0	81.5	6.1	97.8	8.1	0.37
8574680	34.7	17.9	54.5	21.0	30.7	12.5	79.1	17.8	0.33
8635750	37.8	8.0	93.7	9.3	91.5	6.3	96.6	8.1	0.20
8638863	77.7	7.5	95.3	9.6	91.4	7.1	96.3	7.3	0.13
8571892	49.4	12.2	80.5	11.3	85.7	8.3	93.0	10.0	0.75
8594900	85.0	31.1	48.5	20.2	34.3	18.1	47.6	20.2	1.60
8573927	87.2	19.1	55.7	14.7	67.8	16.8	53.9	16.6	0.63

4.3. Currents Comparisons

The accuracy of the CBOFS2 currents was evaluated at the NOS/CO-OPS/CMIST stations shown in Figure 20. The Chesapeake Bay Observing System (CBOS) station had time-series data but it was of poor quality and different data segments were inconsistent with each other. These CMIST stations were selected because they contained observed data in the 2003-2005 period of acceptable quality. The currents comparisons are summarized in Tables 2 and 3 and plotted in Figure 23.

Table 2 shows that the current speed RMS errors satisfy the NOS skill criterion ($CF(26 \text{ cm/s}) > 90\%$) at all of the stations and except at station cb1301 (Chesapeake City, MD along the C & D canal), where it is an improvement over its constant density counterpart. The same could be said for the current direction RMS errors given in Table 3 in that all of the stations satisfy the NOS skill criterion ($CF(22.5^\circ) > 90\%$). The current speed amplitudes and directions at flood and ebb too satisfy the NOS criteria for a majority of the stations and that maximum ebb amplitude errors are in general greater than those for the maximum flood amplitude. The RMS speed and direction errors are plotted in Figure 24 and for the former, the largest error is at station cb1301 and these errors do not show any particular spatial distribution pattern or behavior.

Figure 25 shows the RMSE translational curves for the major-current component and again, they are smooth in space and they each contain only a single, unique and well defined global minimum thus allowing the RMS errors to be split into their amplitude and phase components in a reliable manner. The amplitude and phase error components are plotted in Figure 26 and are listed in Table 4.

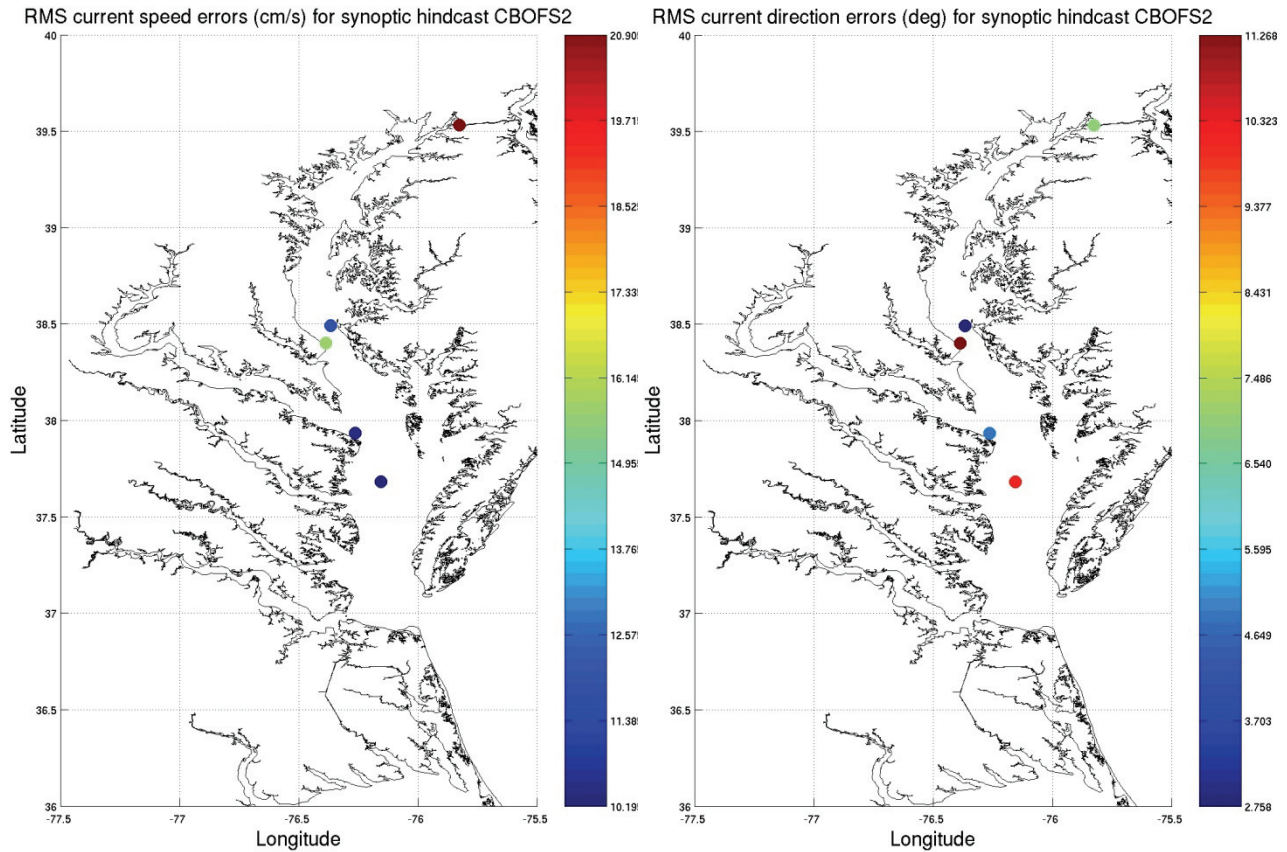


Figure 24. RMS current speed (left, cm/s) and current direction (right, degrees) errors at a depth of 5m for the CBOFS2 synoptic hindcast simulation at the NOS/CMIST observational stations (from the CSDL skill-assessment software package).

Table 2. Current speed error summary for CBOFS2 synoptic hindcast simulation: RMS of current speed error (cm/s) and its Central Frequency (CF), maximum flood current amplitude error (AFC_err, cm) and its CF, maximum ebb current amplitude error (AEC_err, cm) and its CF (all from the CSDL skill-assessment software package).

Station	RMSE	CF	AFC_err	CF	AEC_err	CF
cb0801	10.3	98.3	10.8	100.0	8.3	100.0
CHB0303	10.4	98.6	11.8	100.0	12.4	95.6
cb1001	15.6	90.6	12.7	97.1	14.0	94.3
CHB0305	12.0	97.3	11.0	100.0	18.9	84.8
cb1301	20.8	78.6	13.0	95.3	27.8	54.5

Table 3. Current direction error summary for CBOFS2 synoptic hindcast simulation: RMS of current direction error (degrees) and its Central Frequency (CF), maximum flood current direction error (DFC_err, degrees) and its CF, maximum ebb current direction error (DEC_err, degrees) and its CF (all from the CSDL skill-assessment software package).

Station	RMSE	CF	DFC_err	CF	DEC_err	CF
cb0801	10.0	94.0	12.8	93.1	19.8	77.8
CHB0303	4.9	99.6	10.9	93.3	9.7	97.1
cb1001	11.2	96.9	8.7	100.0	10.4	95.6
CHB0305	2.8	99.7	16.6	81.5	18.2	84.8
cb1301	6.9	99.9	0.6	100.0	0.5	100.0

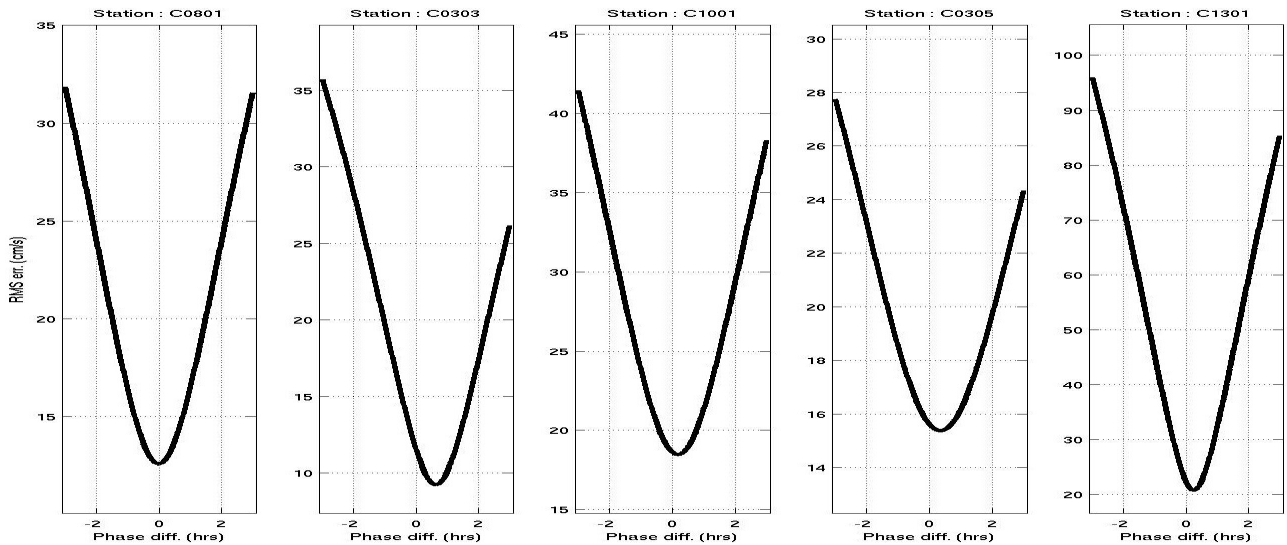


Figure 25. CBOFS2 synoptic hindcast RMSE translation curves for the major-current component at the comparison stations.

Table 4 shows that the major current component errors (both its RMSE and amplitude component) satisfy the NOS acceptable limit of being less than 26 cm/s. For cb0801, the amplitude error is larger than its constant density counterpart but the phase component is much smaller and the error at this station is purely based on the amplitude. At station cb1301, both the amplitude and phase errors are an appreciable improvement over their constant density counterparts. With the exception of station CHB0303, the phase errors are almost always in compliance with the NOS acceptable limit of being less than 15 minutes/0.25 hours and unlike for the constant density case, here the phase errors are primarily positive implying that CBOFS2 exhibits a phase lead relative to the observations.

A plot of the major current amplitude and phase errors are given in Figure 26. The amplitude error plot contains a weak and non-monotonic trend showing an increase in error when moving up the Bay but the phase errors do not show a perceivable pattern in their spatial distribution.

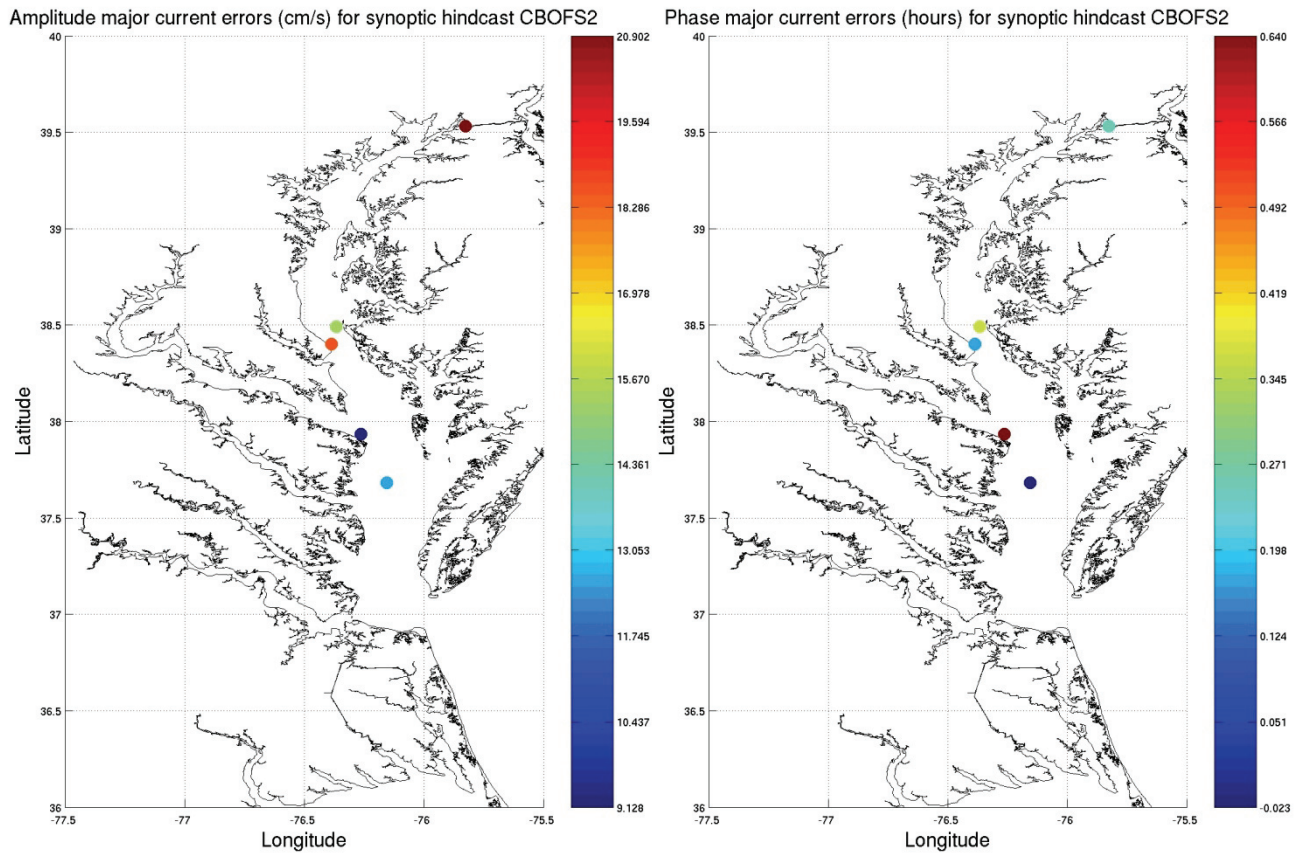


Figure 26. The amplitude (left, cm/s) and phase error (right, hours) components of the RMS errors associated with the major current in the synoptic hindcast CBOFS2 simulation.

Table 4. Major current error summary for the synoptic hindcast simulation: raw RMS error (cm/s), the amplitude component of the RMSE (cm/s) and the phase component of the RMSE (hours).

Station	RMSE	Amp_err	Phs_err
cb0801	12.6	12.6	-0.02
CHB0303	11.5	9.2	0.63
cb1001	18.6	18.5	0.17
CHB0305	15.6	15.4	0.35
cb1301	22.3	20.8	0.25

Figure 27 shows the major direction current vertical profiles at four different time snapshots (and ± 1 hour relative to them) for some of the currents comparisons stations. Stations cb1301 and cb1001 were excluded as its data is based on Side Scan Sonar measurements. It is seen that unlike for the constant density case, there is significantly more stratification associated with the CBOFS2 predictions and that they are generally in agreement with observations. This could be due to the inclusion of T and S in the computations and the use of the GLS $k-\omega$ vertical eddy-viscosity turbulence closure scheme. Observations still however show a greater degree of

vertical stratification than the model predictions. The least agreement with observations is seen to be for station CHB0305. In most cases, it is the non-displaced (in time) CBOFS2 predictions that are in closest agreement with the observations (as also was the case in the constant density simulation).

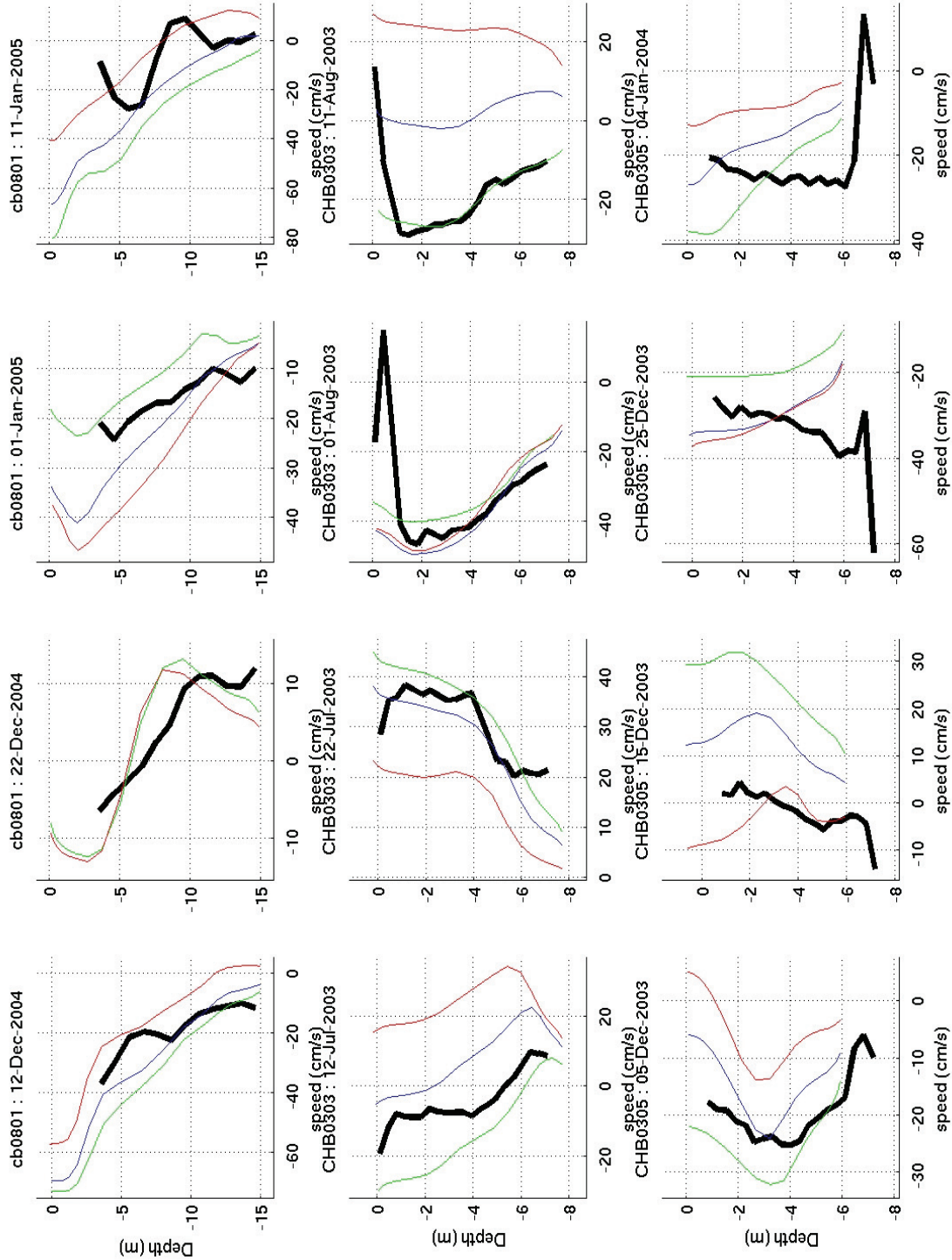


Figure 27. Vertical structure of the major-direction currents for the synoptic hindcast CBOFS2 simulation (black – NOS/CO-OPS/CMIST obs., blue – CBOFS2, red – CBOFS2 with 1 hr. phase lead, green – CBOFS2 with 1 hr. phase lag).

4.4. Temperature and Salinity Comparisons

The CBOFS2 temperature and salinity predictions were evaluated against Bay Program observations at the locations shown in Figure 28. At each of these stations, the Bay Program database provides temperature and salinity (in addition to other biogeochemical variables such as Dissolved Oxygen, Phosphorous, Nitrogen, etc.) both in time and in depth; the temporal resolution of the observations is roughly bi-weekly and they are well resolved in the vertical. The comparison of the CBOFS2 T, S values with those from the Bay Program were carried out for the period January 01, 2004 – September 01, 2005 where the first seven months of the simulation was discarded to allow for the model adjustment/spin-up.

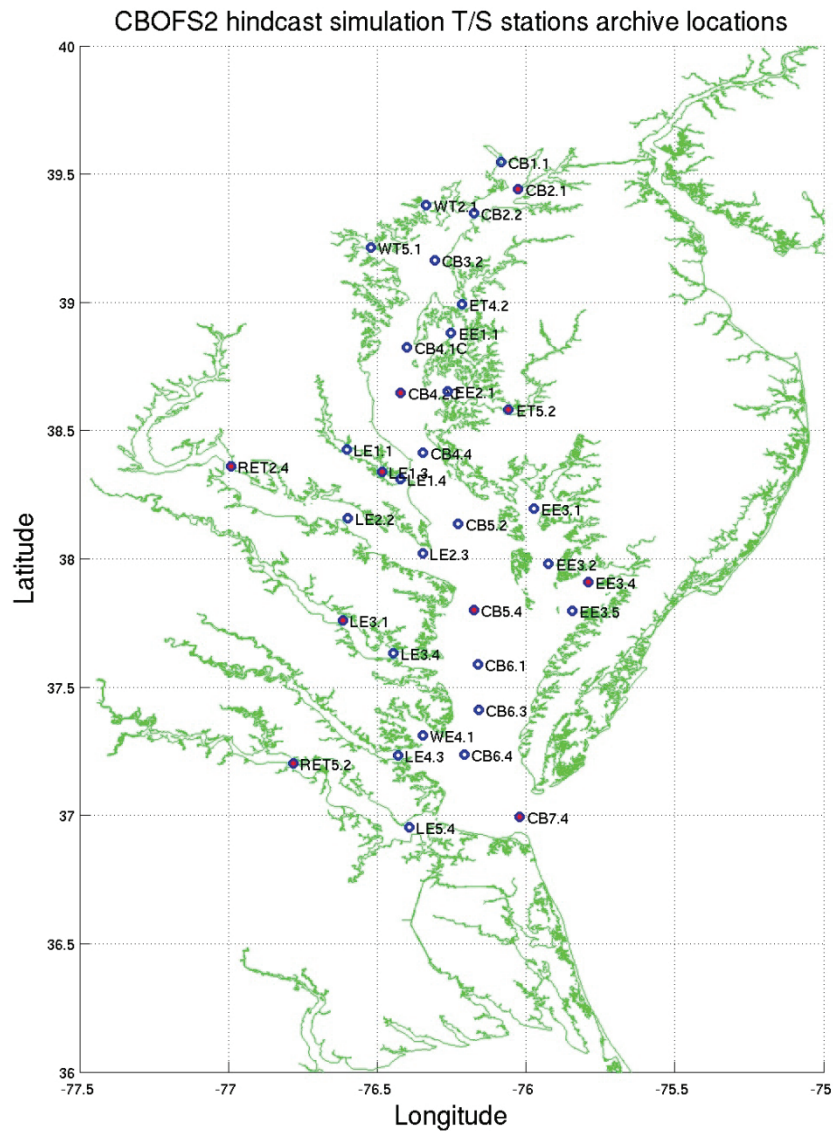


Figure 28. Temperature and salinity stations archive locations for the CBOFS2 synoptic hindcast simulation. Locations in red are stations at which local and global error analyses were performed (Figures C1-C10 in Appendix C).

At each of the stations in Figure 28, the errors/differences in T and S between CBOFS2 and the Bay Program values were evaluated as a function of both space and time (encompassing the same spatiotemporal extent as the T/S fields themselves); the CBOFS2 fields were interpolated in space and time on to the Bay Program locations using Matlab. Comparisons were made at common depths only. For measurement depths greater than model depths, no comparisons were made. Hence, these error fields show how the CBOFS2 T and S values evolve (relative to observations) spatio-temporally and can thus be considered to be the “local errors” and they also yield information about the vertical structure/stratification of the errors and are useful in distinguishing systemic errors or inconsistencies associated with modeling set-ups. Error fields at ten stations from Figure 28 (shown as red filled circles) are plotted in Appendix C (Figures C1-C10). The plots are arranged so that the top most panel gives the observed T values followed by the CBOFS2 T values followed by the difference in T between CBOFS2 and observations; this sequence is then repeated in the next three panels for S. Generation of these error fields at ± 1.0 hours to account for tidal phase errors did not alter them in any significant way. The following information can be extracted from these ten figures: (1) they clearly show the seasonal variations particularly in T and also in S as for example seen in panels one and four in Figure C1, (2) the T and S difference plots show both positive and negative values in both time and depth and are devoid of systemic trends implying that the CBOFS2 implementation is valid, (3) not only the stratifications associated with the T and S fields themselves (for example, strong stratification for S in panel four of Figure C3 (panel six) and minimal stratification for T in panel one of Figure C4) but those of T and S differences are also clearly seen from these plots – for example, in the third panel of Figure C2 it is seen that between December 2004 and February 2005, the differences in T in the vertical are somewhat constant (that is, a constant shift in CBOFS2 T values relative to observations) whereas around July 2005 in Figure C3, strong stratification in the S differences are seen where near the surface CBOFS2 is much saltier than observations whereas near the bottom, CBOFS2 is much fresher than observations, (4) sporadic and intermittent differences in T and S are also captured as shown in panel six of Figure C4 and (5) they show the depth differences between the CBOFS2 bathymetry and the Bay Program observed bathymetry as for example seen in Figure C8 and the spatio-temporal density differences in the number of observations made by the Bay Program as for example seen between Figures C8 (higher density) and C9 (lower density/more sparse).

Plotted in Figure C11 (Appendix C) are the Probability Density Functions (PDF) of the T and S errors associated with the above mentioned ten Bay Program stations (Figure 28). The errors for T are restricted to be in the interval $[-2\text{ }^{\circ}\text{C}, +2\text{ }^{\circ}\text{C}]$ and those for S in $[-4\text{ PSU}, +4\text{ PSU}]$ and the bin widths for the PDF are respectively $0.5\text{ }^{\circ}\text{C}$ and 0.5 PSU . As no discrimination is made between the temporal and spatial (vertical) error variations, these histograms therefore display the global T and S error structure as opposed to the local structure seen from Figures C1-C10 of Appendix C. These PDFs show that: (1) there are stations (for example, T differences of CB7.4, CB4.2C T) where the error spread is evenly within the full range $[-2\text{ }^{\circ}\text{C}, +2\text{ }^{\circ}\text{C}]$ and also stations (for example, S differences of ET5.2, LE1.3, RET5.2) where their spread is highly skewed in either a positive or negative direction; (2) there are stations where the error spread is broad (for example, RET 2.4) and also those where the spread is highly localized (for example, S differences for RET5.2 and CB2.1); (3) while the T errors normally occupy both positive and negative values, there are S errors which are purely negative (for example, RET5.2) or positive (for example, LE1.3 and ET5.2); (4) in general the T errors are negative implying CBOFS2 is

excessively cool and S errors are positive implying CBOFS2 is excessively salty; and, (5) along the stem/axis of the Bay, T differences have a broad spread about 0 °C with a negative bias and the S differences have a positive bias implying excessive saltiness on the part of CBOFS2 predictions but along the tributaries, while the T differences still have the same bias, S differences could have either a negative or a positive bias.

The local spatio-temporal errors (i) at or near the ocean surface; (ii) at 15-feet (of importance to NOS for navigational mariners); and (iii) at or near the ocean bottom were extracted and their RMS and mean values were evaluated. The RMS values provide a measure of the average deviation of the CBOFS2 predictions relative to the Bay Program data and the mean errors (ME) show their bias which is important in discriminating whether the CBOFS2 T and S are either warmer/cooler or saltier/fresher respectively than the observations. The CBOFS2 T, S errors are summarized in Tables C1 and C2 respectively (in Appendix C) and to identify patterns or trends they are also plotted in Figure 29. These errors at the surface, 15-foot depth and bottom for T and S are plotted in space in Figures 30 and 31 which are useful for discerning error distributions and trends in space within the CBOFS2 computational domain.

For temperature, Table C1 and Figures 29 and 30 show that: (a) the RMSE T values are between 0 and 3 °C although the majority of them are between 0 and 2 °C; (b) the ME T values are between -1 and 1.5 °C although the majority of them are between -1 and 1 °C; (c) the errors at the surface and at 15-feet (4.6m) are similar in magnitude and sign; (d) the largest errors are at the ocean bottom (or near it); (e) at the surface and at 15-feet, CBOFS2 is cooler than the observations but at the bottom CBOFS2 is warmer relative to the observed values; and (f) there is not a strong pattern to the horizontal distribution of errors in space (at any of the three depths) but the largest values tend to lie at or near the Bay axis.

For salinity, Table C2 and Figures 29 and 31 show that: (a) the RMSE S values are between 0 and 5.5 PSU, although the majority of them are between 0 and 4 PSU; (b) the ME T values are between -5 and 4 PSU, although the majority of them are between -2 PSU and 3 PSU; (c) the errors at the surface and at 15-feet are similar in magnitude and sign with the exception of stations #1 - #9 (that is, those along the Bay axis), where errors at 15-feet exceed those at the surface; (d) the largest errors, as for temperature, are at the ocean bottom (or near it); (e) at the surface and at 15-feet, CBOFS2 is saltier than the observations but at the bottom, CBOFS2 is somewhat fresher relative to the observed values; and, (f) a strong pattern to the horizontal distribution of errors in space is not seen but for the surface and 15-foot errors, the largest values tend to be along the axis of the Bay.

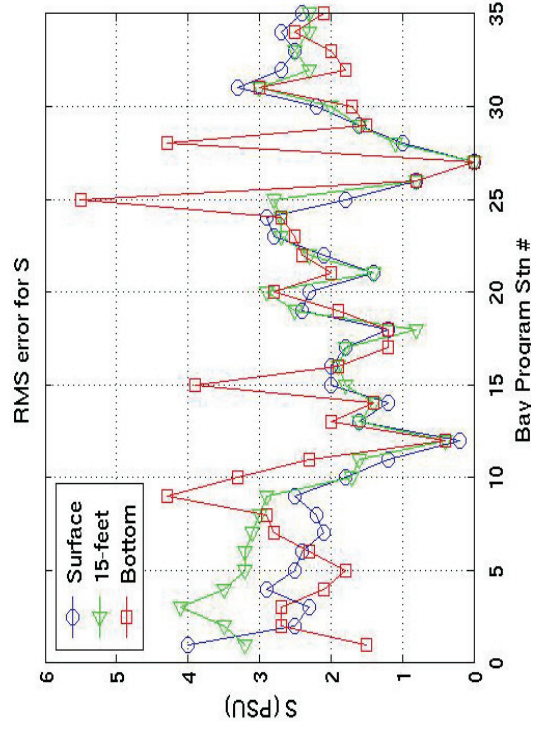
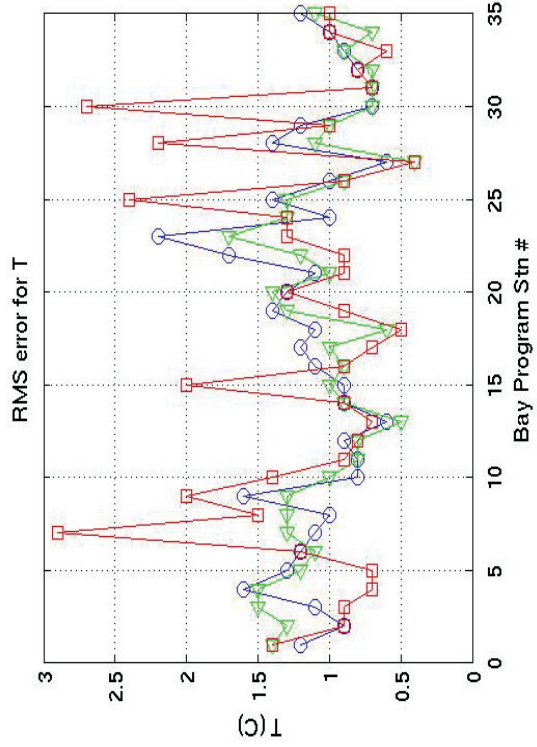
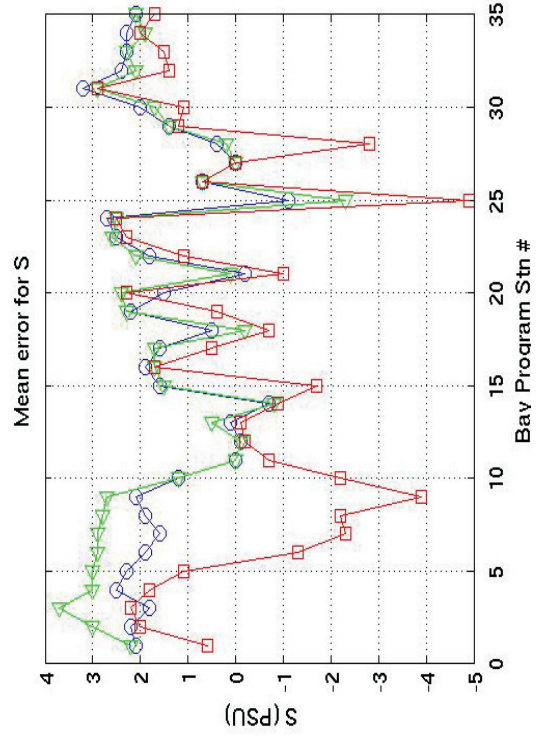
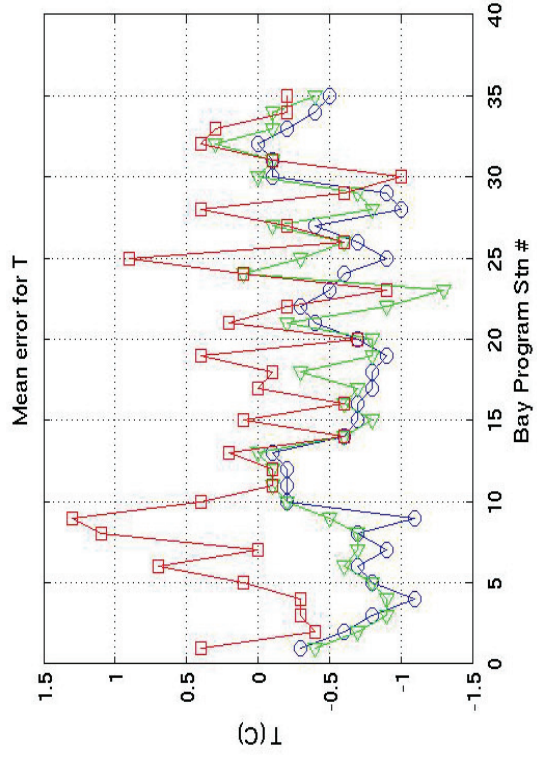


Figure 29. Plot of the RMS and mean errors for T and S as listed in Tables C1 and C1 in Appendix C.

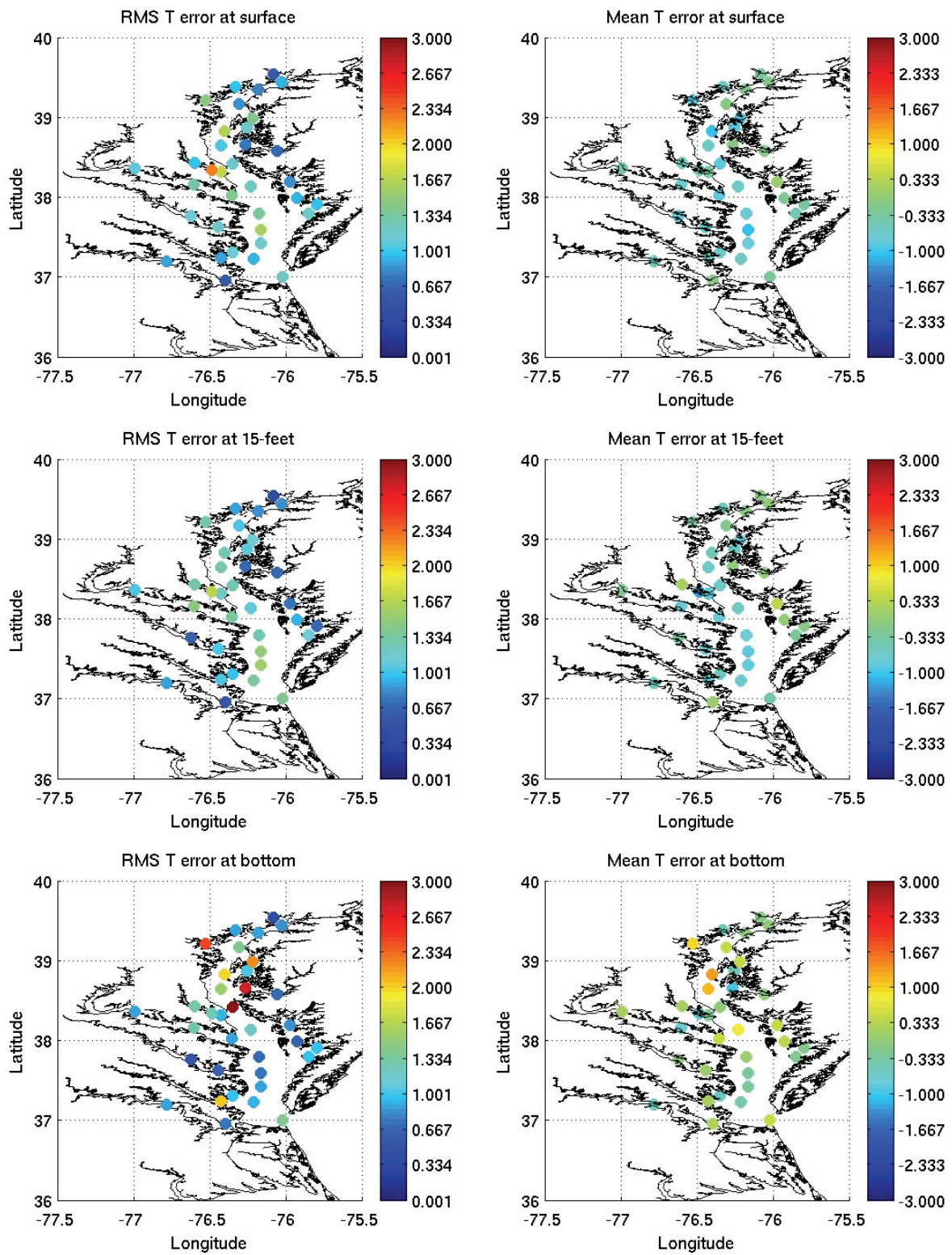


Figure 30. Plot of the RMS and mean errors for T at the surface, at 15-feet and at the bottom.

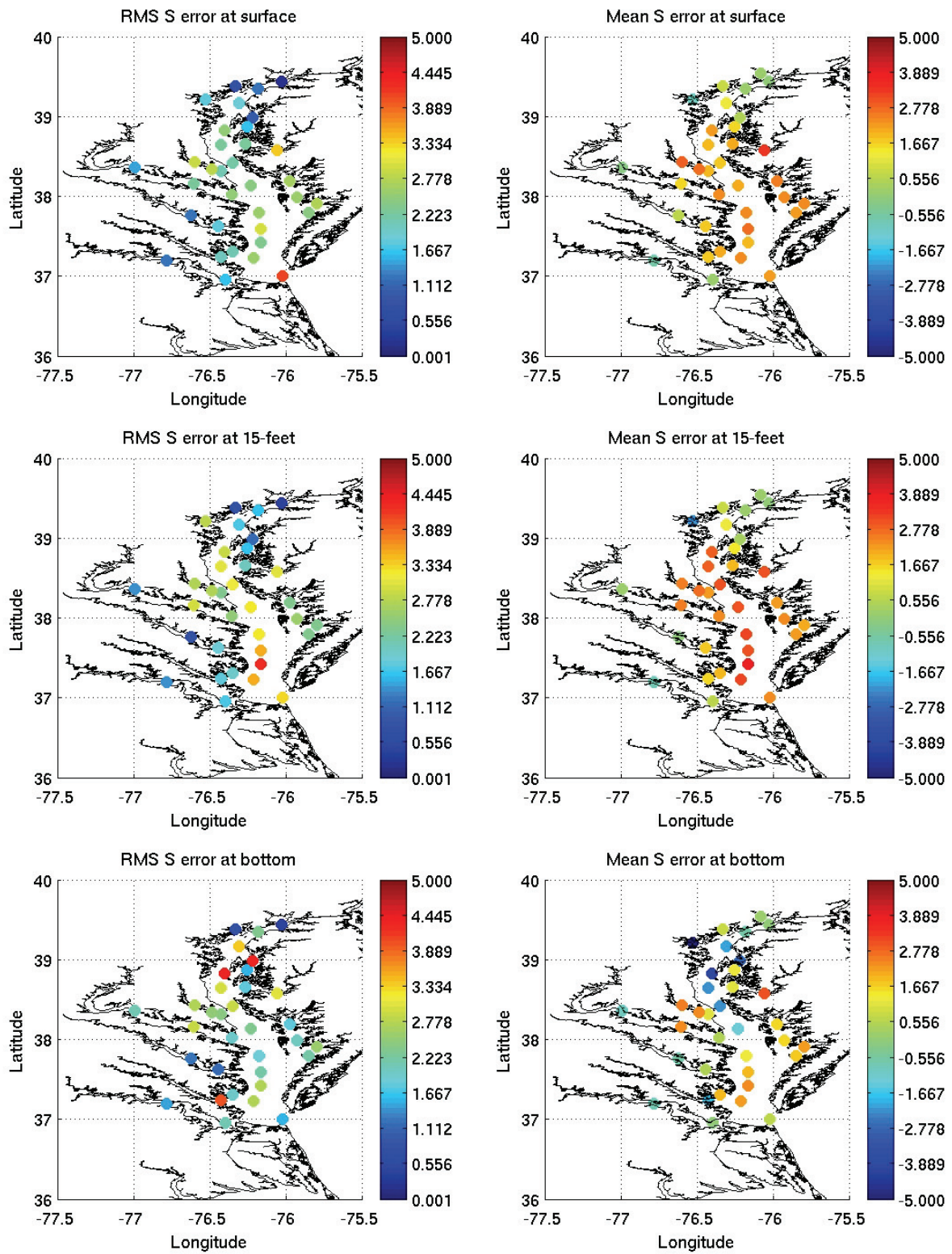


Figure 31. Plot of the RMS and mean errors for S at the surface, at 15-feet and at the bottom.

5. SEMI-OPERATIONAL NOWCAST/FORECAST SIMULATION

In order to test its viability and accuracy as an OFS, CBOFS2 was run in a nowcast/forecast mode and the resulting water levels, currents, temperature and salinity were skill-assessed against observations.

The model initialization fields were from a previous simulation segment brought in via the ROMS perfect restart algorithm. For the nowcast, the river forcing (discharges and temperature with river salinity assumed zero) was from USGS gauge data, open boundary non-tidal water levels were from the Extra-Tropical Storm Surge (ETSS) model products, the open boundary temperature and salinity variables were from Navy Coastal Ocean Model (NCOM) and the meteorological forcing viable (to be taken as inputs to the ROMS Bulk Flux formulation) were from NOAA/NWS/NCEP's Real Time Mesoscale Analysis (RTMA) model products. For the forecast, the river forcing was a persistence from the nowcast values, open boundary non-tidal water levels were from ETSS, open boundary temperature and salinity from were NCOM and the meteorological forcing variables were from the 12km spatial resolution NOAA/NWS/NCEP's North American Mesoscale (NAM) model. Otherwise, the ROMS model configuration was identical to that for the synoptic hindcast simulation.

The evaluation period was three months from April 20, 2010 to July 20, 2010. The water level observations were extracted from NWLON stations, the currents from NOS/CO-OPS/CMIST array of stations and the temperature and salinity were from the PORTS stations. Described below are the details pertaining to the skill assessment of each of these four physical parameters.

5.1. Water Level Comparisons

The water levels were skill-assessed at each of the locations shown in Figure 32 and the derived RMSE and CF(15cm) skill metrics (from the CSDL skill-assessment software package) are summarized in Tables D1 and D2 respectively of Appendix D. The stations listed in the tables span from the south to the north of Chesapeake Bay.

Table D1 shows that with the exception of station 8594900 (Washington, DC) and station 8573927 (Chesapeake City, MD) all of the others satisfy the NOS skill criterion of being below 15 cm for 90% of the time. As in the synoptic hindcast simulation, there is a large error at Washington, DC due to poor phase accuracy. The RMSE values at Washington, DC and Chesapeake City are similar in values to their synoptic hindcast counterparts. It is seen that the nowcast and the 00h, 06h, 12h, 18h and 24h forecast RMSE values are similar in magnitude to each other with the latter frequently showing an improvement over the former.

The Central Frequencies in Table D2 also reflect the inferences made regarding Table D1. The lowest CF values are at Washington, DC and Chesapeake City, MD as expected and this metric maintains its value (at each comparison station) when moving from a nowcast to a forecast and all the way up to a 24-hour forecast. As with the synoptic hindcast simulations, stations with the lowest RMSE values tend to possess the highest CF values.

In summary, the water level RMSE and CF metrics for this semi-operational set-up are as good as and if not better (at stations 8577330, 8636580, 8574680, 8635750) than their hindcast counterparts. Furthermore, these CBOFS2 water level forecasts are reliable up to 24 hours.

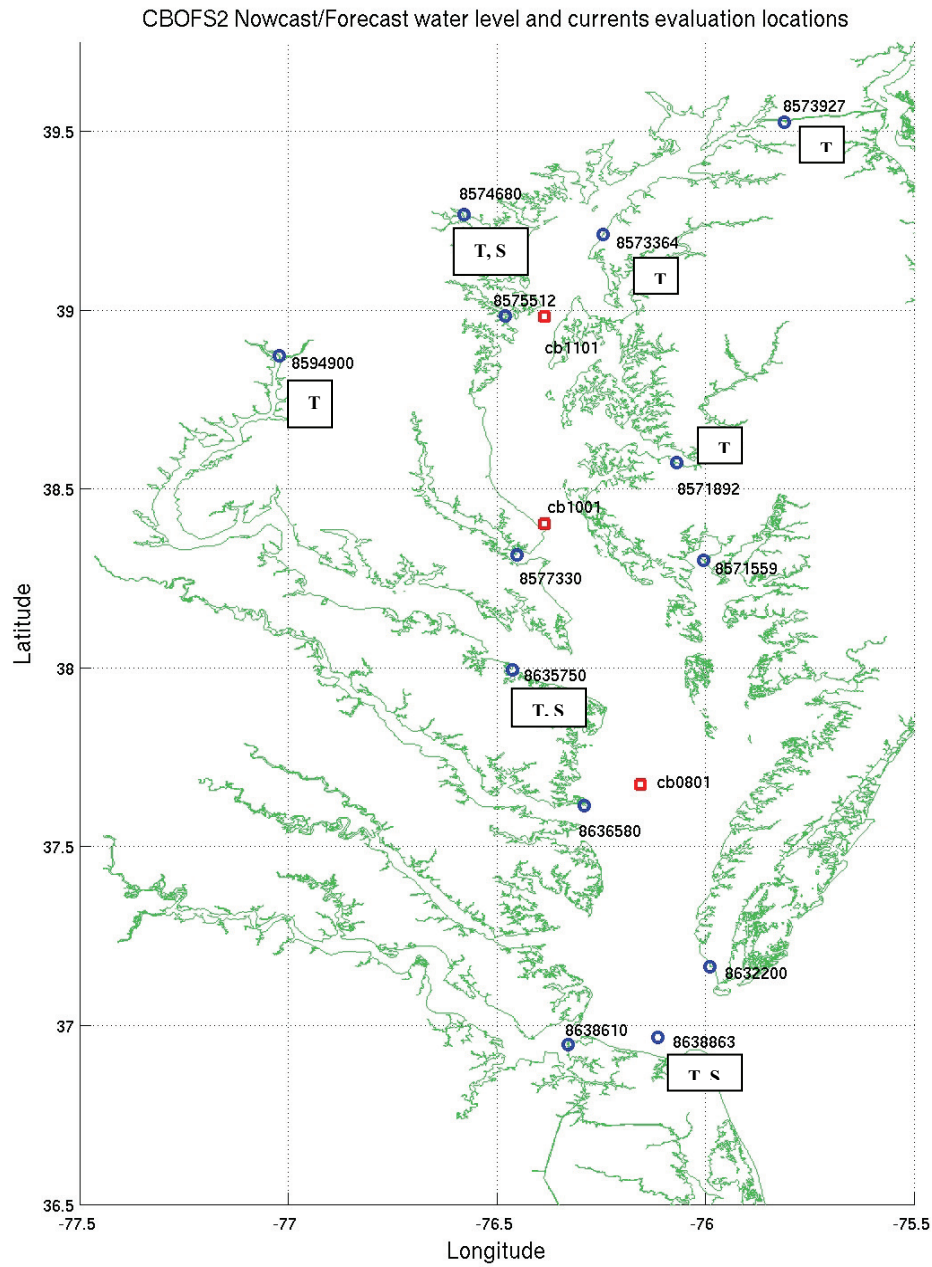


Figure 32. Locations of the stations where water level (blue circles) and currents (red squares) skill assessments were performed. The temperature and salinity comparison stations are demarcated with a box next them.

5.2. Currents Comparisons

The corresponding currents comparisons (for speed and direction) at the stations locations plotted also in Figure 32 are given in Tables D3-D6 (Appendix D). They show that the RMSE of the speeds and their CF values are comparable with the corresponding stations for the hindcast simulations. Moreover, they maintain their values during the 24-hour forecast period and any deterioration of accuracy relative to that of the nowcast is not significant. This is also true for the RMSE and CF values associated with the currents directions but here, as the forecast progresses in time, a lowering of accuracy relative to the nowcast, although not drastic, is seen. The metrics for currents directions too are consistent with their counterparts in the synoptic hindcast simulations. Both the speed and direction RMSE errors at station cb1101 are seen to be somewhat greater than those for stations cb1001 and cb0801 and hence also a corresponding degradation of the CF values.

5.3. Temperature Comparisons

Temperature comparisons were performed at the locations also shown in Figure 32 and at a depth of 1m to avoid the effects of the model surface bulk flux boundary conditions. The RMSE and CF values given in Tables D7 and D8 (Appendix D) show that: (i) the RMSE errors are less than 2°C, (ii) CF > 90% almost always, (iii) the accuracy associated with (i) and (ii) cover all the stations examined (as opposed to drastic accuracy differences between different stations/regions within the computational domain) and (iv) the accuracy in terms of the RMSE and CF hold well beyond the hindcast and into the 24-hour forecast. As the synoptic hindcast simulations were validated against bi-weekly Chesapeake Bay Program (CBP) temperature vertical profiles which were not time-series, a direct comparison of the accuracy of these nowcast/forecast predictions against the hindcast predictions cannot be made.

5.4. Salinity Comparisons

The salinity RMSE and CF values compared at the locations plotted in Figure 32 at a 1m depth (to be consistent with the comparisons for temperature) given in Tables D9 and D10 (Appendix D) show that: (i) their RMSE errors are less than 2 PSU with the exception of station 8638863 (CBBT), (ii) CF > 90% again with the exception of the same station and (iii) the accuracy in terms of the RMSE and CF hold well beyond the hindcast and into the 24-hour forecast. As the synoptic hindcast simulations were validated against bi-weekly Chesapeake Bay Program (CBP) salinity vertical profiles which were not time-series, here too a direct comparison of the accuracy of these nowcast/forecast predictions against the hindcast predictions cannot be made. The reason for the relatively large RMSE and relatively low CF for CBBT is not known and a plot of the observed and modeled salinity time-series at a 1m depth are given in Figure 33. To provide a second observational data source, the bi-weekly measured, low-resolution S values from CBP station CB8.1 are included in the plot for reference. This CBP station is located geographically close to the CBBT station and the plotted data is also at a 1m depth.

Figure 33 shows that both the model predicted salinity and the observations have reasonable values. The CBP observations are clearly devoid of the high (temporal) resolution information contained within the PORTS observations. Both the CBOFS2 predictions and the CBP

observations show a more tempered behavior relative to the PORTS observations and the two sets of observations show large disagreements after (approximately) Julian Day 175; due to the lack of sufficient temporal resolution in the CBP observations, the disagreement during Julian Days 140-150 cannot be verified. In terms of the trends in the S values, the model predictions appear to follow the CPB observations where: (i) the former is almost always saltier than the latter and, (ii) the model-observation disagreement is usually within a range of about [-1,3] PSU. In the synoptic hindcast simulation too, the model was seen to be saltier than observations for the shallower depths.

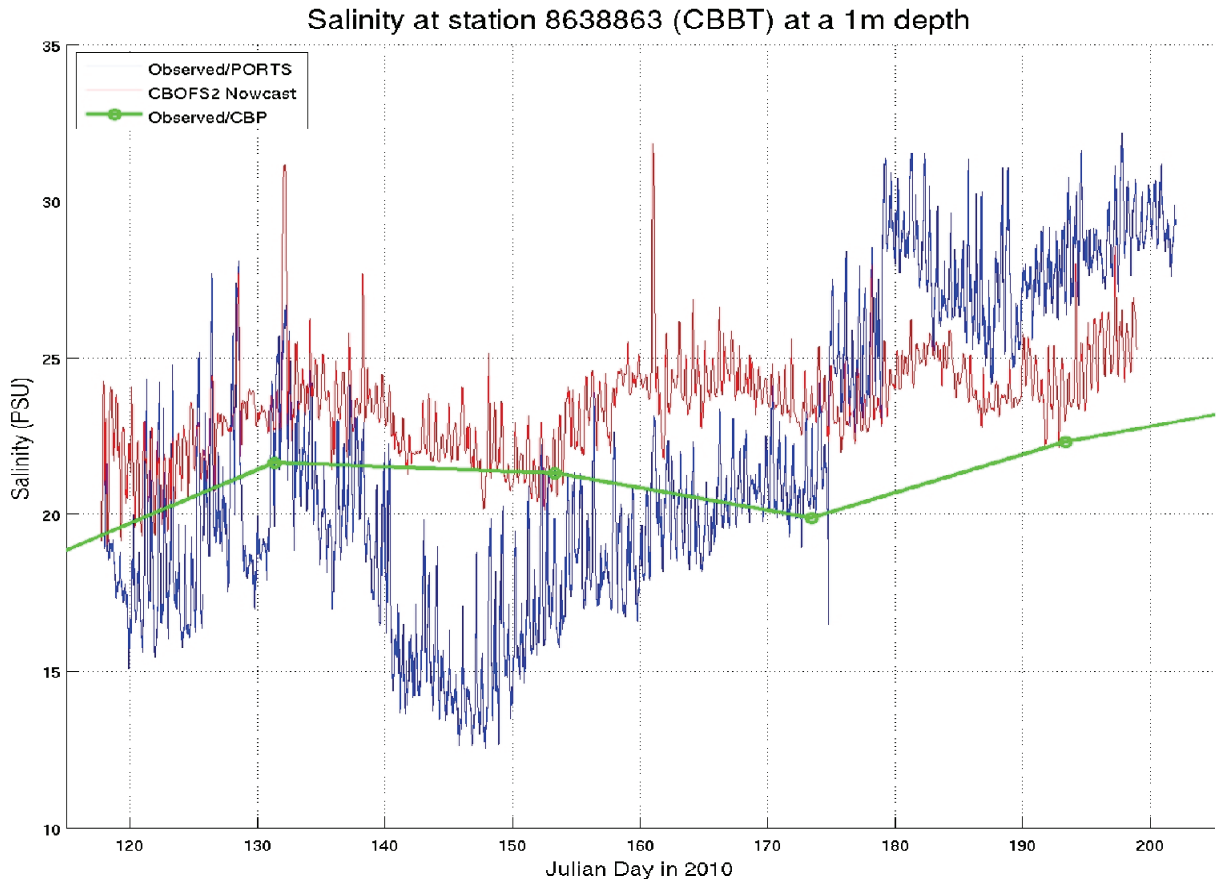


Figure 33. Salinity time-series at station 8638863 (CBBT).

6. SUMMARY AND CONCLUSIONS

The NOS operational Chesapeake Bay model, (CBOFS), is only capable of generating water levels and depth-integrated currents due to its two-dimensional, barotropic nature. Therefore, an upgrade to this modeling framework was proposed and as a consequence the fully three-dimensional CBOFS2 set-up based on the Rutgers University's ROMS model was developed. It covers the whole of the Chesapeake Bay up to and including Reedy Point, DE along the C & D canal and also includes Ocean City, MD and Duck, NC along its southeastern boundary which extends as far as the 100m isobath on the shelf.

The evaluation of this new modeling set-up was carried out in three stages. First, a constant density three-dimensional baroclinic simulation was performed to ensure the accuracy of the tides – water levels and currents. Thereafter, a synoptic hindcast simulation (using observed and climatological initialization and forcing fields) spanning June 01, 2003 to September 01, 2005 was performed to validate the water levels, currents, temperature and salinity. Finally, the synoptic hindcast CBOFS2 set-up was employed to perform a 3-month as a semi-operational nowcast/forecast simulation and its outputs were again skill-assessed.

A summary of the results are as follows:

- (1) All three configurations of CBOFS2 ran successfully without encountering any numerical instabilities. Hence, this modeling set-up is capable of withstanding a diverse range of environmental conditions within the Bay (that is, the high and low river discharges and potential extreme meteorological events that may pass through the Bay). The Courant-Friedrichs-Lewy (CFL) numerical stability parameter was monitored during the synoptic hindcast simulations and for the most part, it was below unity and its overall value was dominated by the contribution from the vertical velocity (w) component.
- (2) Under a MPI parallelization it was found that CBOFS2 was computationally highly efficient yielding a computational effort ratio of 1:144 with the use of 96 processors.
- (3) The water level comparisons showed that the constant density simulation produced smaller amplitude errors but the synoptic hindcast simulation generated smaller phase errors relative to each other. The amplitude errors were less than 22 cm and phase errors at many locations were less than 0.5 hours. In general, both the amplitude and phase errors increase in magnitude when moving up the Bay and for the latter, this is also true when moving up tributaries.
- (4) The currents comparisons show better agreement with predictions and observed data than the water levels. The comparisons for the synoptic hindcast simulation were also an improvement over those for the constant density simulation and the NOS skill criteria for both speed and direction were always met. This is also true for the amplitude of the major-direction current component and for its phase, in most cases, the phase error was less than 0.5 hours.

- (5) The RMS error splitting (into an amplitude and phase component) method described in this report was found to be very robust and reliable for both water levels and currents and for both the constant density and synoptic hindcast simulations. In all cases, the two required conditions of there being smooth RMSE curves (in space) and each of them having a unique, global minimum were met which also implied that the CBOFS2 time-series and the observations were both composed of the same set of (at least dominant) tidal harmonic constituents.
- (6) The temperature and salinity comparisons showed that at a majority of the locations, their RMS errors relative to the Chesapeake Bay Program data were less than 2°C and 4 PSU respectively and their mean errors were in the ranges of [-1°C, 1°C] and [-2 PSU, 3 PSU] respectively. The errors at the surface and at a 15-foot depth were similar and the largest errors were in the vicinity of the ocean bottom, indicating errors in stratification. Closer to the ocean surface, CBOFS2 was cooler and saltier than the Bay Program observations and closer to the ocean bottom, it was warmer and fresher than the observations. Thus, CBOFS2 generates less stratification than reality. This could be an attribute of the vertical eddy-viscosity model (GLS $k-\omega$ model) employed in CBOFS2; however, upon testing the full suite of turbulence models available within ROMS, this particular closure model generated the most accurate overall T and S stratification (relative to observations). The horizontal T/S spatial error distributions do not show pronounced trends although for the shallower depths they are mainly along the axis of the Bay.
- (7) The semi-operational nowcast/forecast CBOFS2 simulation showed that the predicted water levels, currents, temperature and salinity were as accurate as those from the hindcast simulation or better. Furthermore, the accuracy of the predictions were valid for up to and including a 24-hour forecast period.

This report therefore has carefully and thoroughly quantified the model solution errors associated with CBOFS2. Its predictive accuracy for water level, currents, temperature and salinity warrant it being accepted as a NOS Operational Forecast System (OFS) upgrade to the presently available CBOFS.

Future efforts could be directed towards: (i) reduction of the water level phase errors encountered when moving up tributaries; (ii) reduction of the water level amplitude and phase errors encountered when moving up the Bay; (iii) improving the salinity predictions near the ocean bottom to further reduce salinity errors; (iv) further reduction of both the temperature and salinity errors in the vertical; (v) further research into the reduced open boundary conditions for fully three-dimensional flow; and, (vi) employing model high-resolution nests for the tributaries in Chesapeake Bay and in particular for the Potomac and James rivers in order to better resolve the physical processes within them. For (i) and (ii) perhaps the use of a spatially variable bottom friction coefficient is conducive and the examination of the effects of the extent and the shape of the southern open ocean boundary may also be worthwhile; as for (iii) and (iv) other GLS turbulence model constant sets and models themselves may be worth experimenting with. In addition to the above, the lateral open ocean boundaries of CBOFS2 could also be coupled to a basin-scale model which will provide the full suite of open boundary forcing variables and thereby account for the shelf dynamics and its influence on the Bay better.

ACKNOWLEDGMENTS

The authors wish to thank Dr. Zizang Yang of CSDL for generating the CBOFS2 grid using the DELFT3D grid generator, Dr. Jiangtao Xu for the many illuminating discussions on the physics of the Chesapeake Bay and her modeling experience and help with the Chesapeake Bay Program database, Mr. Patrick Burke, Mr. Christopher Paternostro, Mr. Armin Pruessner, Ms. Maria Little for help with the latest NOS harmonic analysis software, the use of the CMIST website and access to CMIST and water level data, and Dr. Aijun Zhang for help with the use of the CSDL skill-assessment software package.

REFERENCES

- Berliand, M. E. and Berliand, T. G., 1952. Determining the net longwave radiation of the earth with consideration of the effects of cloudiness (in Russian), *Izv. Akad. Nauk SSSR, Ser. Geofiz* 1.
- Browne, D. R. and Fisher C. W., 1988. Tide and tidal currents in the Chesapeake Bay, *NOAA Technical Report*, NOS OMA 3, p. 34.
- CBP, Chesapeake Bay Program Data Hub, 2009. <http://www.chesapeakebay.net/dataandtools.aspx?menuitem=14872>
- Chapman, D. C., 1985. Numerical treatment of cross-shelf open boundaries in a barotropic coastal ocean model, *Oceanography*, Vol. 15, pp. 1060-1075.
- CMIST, Currents Measurements Interface for the Study of Tides (CMIST), 2009. <https://cmist.noaa.gov/cmist/ssl/login.do>
- Conkright, M. E., Locarnini, R. A., Garcia, H. E., O'Brian, T. D., Boyer, T. P., Stephens, C., and Anotonov, J. I., 2002. World Ocean Atlas 2001: Objective Analyses, Data Statistics, and Figures, CD-ROM Documentation, *National Oceanographic Data Center*, Silver Spring, MD, pp. 17.
- Delft 3D grid generator (Delft3D), 2009, <http://delftsoftware.wldelft.nl/>
- EC2001, 2009, report from <http://www.unc.edu/ims/ccats/tides/tides.htm>
- Fairall, C.W., E.F. Bradley, D.P. Rogers, J.B. Edson and G.S. Young, 1996a: Bulk parameterization of air-sea fluxes for tropical ocean-global atmosphere Coupled-Ocean Atmosphere Response Experiment, *Journal of Geophysical Research*, Vol. 101, pp. 3747-3764.
- Fairall, C.W., E.F. Bradley, J.S. Godfrey, G.A. Wick, J.B. Edson, and G.S. Young, 1996b: Cool-skin and warm-layer effects on sea surface temperature, *Journal of Geophysical Research*, Vol. 101, pp. 1295-1308.
- Feyen, J., 2008, Personal communication.
- Flather, R. A., 1976. A tidal model of the northwest European continental shelf, *Memoires de la Societe Royale de Sciences de Liege*, Vol. 6, pp. 141-164.
- Gross, T., Bosley, K., and Hess, K., 2000. The Chesapeake Bay Operational Forecast System (CBOFS): Technical Documentation, *NOAA/NOS Technical Report*, OCS/CO-OPS 1.

- Liu, W. T., Katsaros, K. B. and, Businger, J. A., 1979. Bulk parameterization of the air-sea exchange of heat and water vapor including the molecular constraints at the interface, *Journal of Atmospheric Sciences*, Vol. 36, pp. 1722-1735.
- Luettich, R.A., Westerink J. J., and Scheffner N. W., 1992. ADCIRC: an advanced three-dimensional circulation model for shelves coasts and estuaries, report 1: theory and methodology of ADCIRC-2DDI and ADCIRC-3DL, *Dredging Research Program Technical Report DRP-92-6*, U.S. Army Engineers Waterways Experiment Station, Vicksburg, MS, 137p.
- Mellor, G. L., and Yamada, T., 1982. Development of a turbulence closure model for geophysical fluid problems, *Reviews of Geophysics and Space Physics*, Vol. 20, pp. 851-875.
- National Data Buoy Center (NDBC), NOAA, 2009. http://www.ndbc.noaa.gov/maps/southeast_hist.shtml
- NOAA Tides & Currents, Harmonic Constituents – Stations Selection (Tides & Currents), 2009a. http://tidesandcurrents.noaa.gov/station_retrieve.shtml?type=Harmonic+Constituents
- NOAA Tides & Currents, Historic Tide Data – Stations Selection (Tides & Currents), 2009b. http://tidesandcurrents.noaa.gov/station_retrieve.shtml?type=Historic+Tide+Data
- North American Regional Reanalysis (NARR), 2009. <http://www.emc.ncep.noaa.gov/mmb/rrean/>
- Ocean Modeling Discussion (ROMS/TOMS), 2008. <https://www.myroms.org/forum/viewtopic.php?f=14&t=1029>
- Shchepetkin, A. F. and McWilliams, J. C., 1998. Quasi-monotone advection schemes based on explicit locally adaptive dissipation, *Monthly Weather Review*, Vol. 126, pp. 1541-1580.
- Shchepetkin, A. F. and McWilliams, J. C., 2003. A method for computing horizontal pressure-gradient forcing in an oceanic model with a nonaligned vertical coordinate, *Journal of Geophysical Research*, Vol. 108, No. C3, pp 1-34.
- Shchepetkin, A. F. and McWilliams, J. C., 2004. The Regional Oceanic Modeling System: a split-explicit, free-surface, topography-following-coordinate ocean model, *Ocean Modelling*, Vol. 9 (4), pp. 347-404.
- Song, Y. T., and Haidvogel, D. B., 1994. A semi-implicit ocean circulation model using a generalized topography following coordinate system, *Journal of Computational Physics*, Vol. 115, pp. 228-244.

- Styles, R., and Glenn, S. M., 2000. Modeling stratified wave and current bottom boundary layers in the continental shelf, *Journal of Geophysical Research*, Vol. 105, pp. 24119-24139.
- T_Tide Harmonic Analysis Toolbox, 2007. http://www.eos.ubc.ca/~rich/#T_Tide
- USGS Surface-water daily data for the nation, National Water Information System: Web Interface (USGS) 2009. http://nwis.waterdata.usgs.gov/nwis/dv?referred_module=sw&search_criteria=search_site_no&submitted_form=introduction
- Warner, J. C., Sherwood, C. R., Arango, H. G., and Signell R. P., 2005. Performance of four turbulence closure methods implemented using a generic length scale method, *Ocean Modelling*, Vol. 8, pp. 81-113.
- Zervas, C., Tidal current analysis procedures and associated computer programs, NOAA Technical Memorandum NOS CO-OPS 0021, 1999.
- Zhang, A., Hess, K., Wei, E. and Myers, E., 2009. Implementation of model skill assessment software for water level and current in tidal regions, *NOAA Technical Report*, NOS CS 24.

APPENDIX A: CBOFS2 CONSTANT DENSITY WATER LEVEL HARMONIC CONSTITUENTS AND SKILL ASSESSMENTS

Table A1. Water level harmonic constituents summary for CBOFS2; amplitudes are in meters and phases are in hours.

Stn ID	M2		N2		K1		O1		P1		L2	
	Amp	Phs										
8571892	0.243	8.022	0.045	7.409	0.051	22.080	0.041	23.926	0.011	21.345	0.010	8.317
8573364	0.207	11.296	0.040	10.552	0.069	0.339	0.054	-0.021	0.016	23.297	0.009	0.088
8574680	0.192	11.113	0.038	10.411	0.067	0.412	0.054	0.065	0.016	-0.649	0.007	12.093
8575512	0.153	9.643	0.030	9.030	0.058	23.496	0.047	-0.681	0.013	22.635	0.004	10.116
8577330	0.188	6.397	0.036	5.644	0.034	20.697	0.029	22.850	0.008	19.975	0.007	7.230
8632200	0.386	1.042	0.086	0.415	0.071	13.297	0.050	15.025	0.019	12.708	0.004	1.104
8638863	0.398	0.638	0.091	0.035	0.073	12.798	0.051	14.516	0.021	12.421	0.003	-0.630
8638610	0.373	1.290	0.083	0.742	0.066	13.603	0.047	15.269	0.018	13.203	0.005	0.420
8635750	0.199	5.748	0.040	5.000	0.031	18.948	0.024	21.272	0.007	18.163	0.006	6.753
8573927	0.363	2.308	0.057	1.554	0.046	25.557	0.033	0.165	0.027	20.523	0.020	2.079
8637624	0.358	1.573	0.077	1.118	0.055	13.948	0.038	15.635	0.014	13.464	0.008	0.440
8638433	0.273	4.409	0.054	3.759	0.065	17.193	0.050	18.690	0.014	17.013	0.010	4.866
8638489	0.478	6.297	0.080	5.928	0.076	18.642	0.056	20.039	0.016	18.845	0.029	6.130
8636580	0.154	3.809	0.034	3.024	0.033	16.076	0.022	18.210	0.008	15.389	0.003	5.747
8635150	0.221	7.025	0.047	6.343	0.038	20.211	0.029	22.377	0.008	19.420	0.005	7.989
8594900	0.387	-1.101	0.067	10.503	0.052	23.403	0.037	-0.423	0.010	-1.036	0.021	-0.109
8574070	0.298	1.432	0.049	0.499	0.073	1.882	0.055	1.248	0.019	-0.047	0.019	2.015
8571559	0.350	5.945	0.068	5.362	0.047	18.430	0.034	20.404	0.011	17.642	0.012	6.228
8571214	0.227	5.324	0.046	4.550	0.038	18.144	0.029	20.304	0.009	17.274	0.007	6.431
8576363	0.155	8.191	0.029	7.560	0.047	22.665	0.040	24.435	0.011	21.887	0.006	8.541
8632974	0.207	3.233	0.046	2.489	0.043	15.544	0.030	17.514	0.011	14.747	0.004	4.965
8573903	0.302	1.677	0.048	0.809	0.064	1.589	0.048	0.703	0.020	-1.758	0.019	1.951

Table A2. Water level harmonic constituents summary from observations (NOS/CO-OPS database); amplitudes are in meters and phases are in hours.

Stn ID	M2		N2		K1		O1		P1		L2	
	Amp	Phs										
8571892	0.239	9.081	0.047	8.460	0.050	22.631	0.039	25.525	0.020	22.482	0.019	9.811
8573364	0.174	11.958	0.037	11.396	0.069	0.219	0.058	1.004	0.023	23.558	0.008	1.057
8574680	0.159	11.627	0.034	11.048	0.069	0.532	0.056	1.076	0.022	0.087	0.007	12.046
8575512	0.139	10.061	0.029	9.511	0.059	23.715	0.048	0.430	0.020	23.317	0.010	10.434
8577330	0.171	6.859	0.036	6.058	0.027	20.983	0.023	23.840	0.012	21.318	0.012	7.918
8632200	0.388	1.121	0.088	0.432	0.059	12.858	0.046	15.319	0.019	13.484	0.018	1.605
8638863	0.380	0.725	0.090	0.049	0.058	12.293	0.045	14.982	0.018	12.574	0.014	0.975
8638610	0.366	1.611	0.081	0.995	0.049	13.357	0.042	16.108	0.015	13.310	0.012	1.541
8635750	0.184	6.086	0.040	5.355	0.023	18.363	0.019	21.423	0.009	19.587	0.011	6.885
8573927	0.434	3.243	0.075	2.679	0.032	22.884	0.014	0.179	0.010	22.127	0.030	3.072
8637624	0.361	1.849	0.080	1.273	0.051	13.177	0.038	15.850	0.015	12.882	0.015	1.693
8638433	0.287	4.285	0.058	3.949	0.060	16.149	0.039	19.902	0.020	16.412	0.008	4.609
8638489	0.422	8.574	0.073	8.467	0.076	19.673	0.059	23.445	0.025	19.935	0.012	8.673
8636580	0.175	3.561	0.038	2.954	0.030	15.072	0.023	17.636	0.008	15.402	0.005	3.928
8635150	0.246	7.380	0.050	6.814	0.030	19.566	0.026	22.341	0.011	21.125	0.013	7.864
8594900	0.407	0.704	0.075	12.535	0.046	23.735	0.035	1.621	0.013	0.294	0.027	1.134
8574070	0.282	2.481	0.052	1.565	0.084	1.842	0.059	2.309	0.019	1.304	0.021	3.620
8571559	0.310	6.607	0.066	6.167	0.042	18.762	0.033	21.430	0.014	19.721	0.011	6.736
8571214	0.203	5.469	0.039	4.800	0.036	17.539	0.024	20.822	0.000	5.000	0.012	5.830
8576363	0.139	8.585	0.029	7.792	0.045	23.044	0.036	25.247	0.017	22.501	0.010	9.907
8632974	0.216	3.316	0.052	2.598	0.033	15.731	0.031	17.465	0.000	5.000	0.009	4.692
8573903	0.274	2.526	0.059	1.600	0.076	1.243	0.049	1.614	0.027	1.116	0.022	3.041

Table A3. Water level error summary: Tidal range (cm), RMS error (cm) and its Central Frequency (CF), high water amplitude error (AHW_err, cm) and its CF, low water amplitude error (ALW_err, cm) and its CF (all from the CSDL skill-assessment software package), amplitude component of the RMSE (cm) and the phase component of the RMSE (hours).

Station	Range	RMSE	CF	AHW_err	CF	ALW_err	CF	Amp_err	Phs_err
8571892	49.4	15.4	64.4	12.0	96.6	13.4	79.1	12.1	1.03
8573364	36.9	18.3	43.3	21.3	2.3	13.5	77.9	17.6	0.67
8574680	34.7	15.3	56.7	18.2	9.2	10.6	94.2	14.8	0.53
8575512	29.6	14.2	66.0	15.2	37.9	11.5	93.0	14.0	0.45
8638863	77.7	8.3	97.8	9.2	100.0	5.9	100.0	8.3	0.07
8638610	74.1	9.2	90.6	8.1	100.0	7.1	100.0	8.2	0.30
8635750	37.8	12.0	84.8	13.7	73.3	9.6	100.0	11.8	0.32
8573927	87.2	20.2	53.7	10.7	89.7	16.9	40.2	15.1	0.90
8637624	72.5	10.4	88.2	9.9	100.0	12.3	82.8	9.8	0.25
8638433	56.1	10.5	91.4	8.3	100.0	7.3	100.0	10.4	-0.12
8638489	85.3	38.6	18.1	21.5	2.3	7.6	100.0	12.2	2.22
8636580	35.4	12.2	87.3	8.5	100.0	13.4	79.3	12.1	-0.25
8635150	49.7	11.4	84.0	8.1	100.0	14.4	62.1	10.9	0.35
8594900	85.0	29.5	41.0	8.0	100.0	13.1	75.6	11.7	1.80
8574070	57.9	15.8	62.3	13.8	70.1	9.9	88.5	11.3	0.98
8571559	62.5	9.3	91.8	10.0	100.0	2.9	100.0	4.8	0.62
8577330	35.7	12.5	78.6	13.9	68.6	10.2	100.0	12.1	0.43
8632200	79.2	9.0	97.5	8.2	100.0	8.9	100.0	8.9	0.07

APPENDIX B: CBOFS2 CONSTANT DENSITY CURRENTS HARMONIC CONSTITUENTS AND SKILL ASSESSMENTS

Table B1. True eastward current harmonic constituents summary for CBOFS2; amplitudes are in m/s and phases are in hours.

True Eastward Current (U)

Stn ID	M2		N2		K1		O1		P1		L2	
	Amp	Phs										
LCB9903	0.471	7.000	0.124	6.600	0.111	0.400	0.079	1.700	0.037	0.500	0.018	6.400
cb0601	0.334	6.600	0.077	6.200	0.048	21.900	0.032	24.500	0.016	22.100	0.011	6.000
cb0801	0.056	10.400	0.013	10.200	0.016	5.000	0.012	6.100	0.005	5.100	0.002	9.800
cb0901	0.133	11.200	0.032	10.700	0.021	2.500	0.014	3.100	0.007	2.500	0.005	10.300
CHB0301	0.146	0.200	0.031	12.100	0.039	4.100	0.026	4.700	0.013	4.100	0.004	11.700
cb1201	0.030	9.800	0.005	9.300	0.005	17.100	0.003	18.100	0.002	17.200	0.001	9.000
cb1301	0.917	11.800	0.157	11.300	0.081	5.000	0.150	3.800	0.027	4.900	0.022	10.900
NOS 68	0.046	8.684	0.009	5.707	0.005	11.761	0.006	5.071	0.002	11.826	0.001	11.548
NOS 63	0.022	0.262	0.004	9.849	0.004	15.065	0.004	8.298	0.001	15.148	0.001	3.221
NOS 27	0.118	10.292	0.023	7.303	0.007	11.282	0.007	5.228	0.002	11.344	0.003	0.982
NOS 174	0.091	0.248	0.018	9.645	0.008	15.644	0.010	9.266	0.003	15.730	0.003	3.390
NOS 123	0.033	2.143	0.006	11.667	0.004	12.160	0.004	3.729	0.001	12.227	0.001	5.161
NOS 130	0.041	9.498	0.008	6.477	0.008	6.801	0.009	25.059	0.003	6.839	0.001	0.217

Table B2. True northward current harmonic constituents summary for CBOFS2; amplitudes are in m/s and phases are in hours.

True Northward Current (V)

Stn ID	M2		N2		K1		O1		P1		L2	
	Amp	Phs	Amp	Phs	Amp	Phs	Amp	Phs	Amp	Phs	Amp	Phs
LCB9903	0.243	0.800	0.062	0.400	0.054	12.600	0.035	14.300	0.018	12.700	0.009	0.400
cb0601	0.148	1.000	0.034	0.500	0.022	10.000	0.015	11.200	0.007	10.100	0.005	0.500
cb0801	0.271	3.300	0.061	2.900	0.059	15.400	0.043	17.400	0.020	15.500	0.009	2.800
cb0901	0.136	5.000	0.033	4.500	0.022	14.900	0.016	16.900	0.007	15.000	0.005	4.300
CHB0301	0.220	6.100	0.047	5.600	0.060	15.900	0.039	17.500	0.020	16.100	0.007	5.400
cb1201	0.267	9.700	0.051	9.100	0.051	18.900	0.034	20.700	0.017	19.000	0.007	8.800
cb1301	0.116	5.600	0.019	5.000	0.011	17.200	0.019	16.800	0.004	17.200	0.003	4.900
NOS 68	0.337	9.557	0.065	6.688	0.041	12.213	0.044	5.738	0.013	12.280	0.009	0.125
NOS 63	0.431	9.443	0.084	6.540	0.045	11.881	0.048	5.250	0.015	11.946	0.012	0.044
NOS 27	0.032	10.689	0.006	7.609	0.002	12.047	0.002	5.379	0.001	12.113	0.001	1.463
NOS 174	0.030	0.235	0.006	9.670	0.003	14.833	0.003	8.083	0.001	14.914	0.001	3.343
NOS 123	0.097	9.050	0.019	6.013	0.016	5.711	0.017	24.155	0.005	5.742	0.003	11.978
NOS 130	0.037	3.843	0.007	0.693	0.005	16.774	0.004	9.381	0.002	16.866	0.001	6.878

Table B3. True eastward current harmonic constituents summary from observations (NOS/CO-OPS/CMIST database and NOS survey); amplitudes are in m/s and phases are in hours.

True Eastward Current (U)

Stn ID	M2		N2		K1		O1		P1		L2	
	Amp	Phs										
LCB9903	0.459	6.100	0.102	5.400	0.078	1.700	0.033	22.600	0.026	1.400	0.015	5.200
cb0601	0.678	5.800	0.150	4.800	0.134	22.100	0.087	23.400	0.044	22.200	0.021	4.600
cb0801	0.087	8.300	0.022	9.600	0.010	23.400	0.004	19.700	0.003	23.100	0.003	9.200
cb0901	0.155	10.900	0.035	10.200	0.030	3.600	0.022	5.700	0.010	3.800	0.005	9.800
CHB0301	0.133	11.700	0.026	10.700	0.036	5.400	0.034	1.200	0.012	5.100	0.004	10.300
cb1201	0.053	6.900	0.019	5.600	0.021	14.900	0.008	12.300	0.007	14.700	0.003	5.400
cb1301	0.541	11.300	0.084	11.000	0.094	6.000	0.050	3.200	0.031	5.800	0.012	10.600
NOS 68	0.040	10.575	0.008	9.740	0.020	5.425	0.002	10.055	0.007	5.455	0.001	11.375
NOS 63	0.061	5.096	0.012	5.418	0.017	20.557	0.023	21.143	0.006	20.670	0.002	4.785
NOS 27	0.324	4.513	0.063	4.212	0.016	14.175	0.017	16.022	0.005	14.252	0.009	4.802
NOS 174	0.086	6.424	0.017	6.030	0.020	18.622	0.012	21.244	0.007	18.725	0.002	6.807
NOS 123	0.008	3.236	0.002	1.308	0.008	3.517	0.005	7.437	0.003	3.536	0.000	5.090
NOS 130	0.039	1.325	0.008	0.352	0.026	6.948	0.022	9.632	0.009	6.986	0.001	2.266

Table B4. True northward current harmonic constituents summary from observations (NOS/CO-OPS/CMIST database and NOS survey); amplitudes are in m/s and phases are in hours.

True Northward Current (V)

Stn ID	M2		N2		K1		O1		P1		L2	
	Amp	Phs										
LCB9903	0.240	12.000	0.048	12.000	0.027	13.800	0.009	8.300	0.009	13.500	0.007	11.500
cb0601	0.111	11.700	0.050	10.200	0.017	9.200	0.004	4.100	0.006	8.900	0.007	9.800
cb0801	0.277	3.200	0.047	1.800	0.047	16.600	0.030	17.200	0.016	16.600	0.007	1.700
cb0901	0.150	4.700	0.029	3.000	0.018	15.800	0.025	18.100	0.006	16.000	0.004	2.900
CHB0301	0.172	5.300	0.032	4.200	0.053	17.100	0.047	13.200	0.018	16.800	0.005	4.100
cb1201	0.231	9.900	0.052	8.400	0.064	18.200	0.076	21.500	0.021	18.500	0.007	8.100
cb1301	0.079	5.100	0.012	4.600	0.014	17.900	0.007	16.300	0.005	17.800	0.002	4.500
NOS 68	0.304	2.080	0.059	1.002	0.020	13.490	0.029	16.331	0.007	13.564	0.009	3.122
NOS 63	0.280	12.114	0.054	12.250	0.027	22.093	0.030	1.399	0.009	22.214	0.008	11.985
NOS 27	0.095	4.423	0.018	4.522	0.005	14.733	0.007	12.429	0.001	14.814	0.003	4.331
NOS 174	0.010	6.659	0.002	5.721	0.004	1.403	0.005	21.602	0.001	1.411	0.000	7.566
NOS 123	0.170	2.760	0.033	2.036	0.060	4.694	0.040	7.064	0.020	4.720	0.005	3.461
NOS 130	0.044	7.494	0.008	6.691	0.023	19.493	0.009	21.918	0.007	19.600	0.001	8.270

Table B5. Current speed error summary: RMS of current speed error (cm/s) and its Central Frequency (CF), maximum flood current amplitude error (AFC_err, cm) and its CF, maximum ebb current amplitude error (AEC_err, cm) and its CF (all from the CSDL skill-assessment software package).

Station	RMSE	CF	AFC_err	CF	AEC_err	CF
LCB9903	12.6	96.5	11.1	100.0	11.1	100.0
cb0601	30.5	50.6	40.0	9.3	35.7	20.9
cb0801	5.9	100.0	4.4	100.0	6.0	100.0
cb0901	4.4	100.0	3.5	100.0	6.4	100.0
CHB0301	9.2	100.0	10.2	100.0	3.7	100.0
cb1201	6.4	100.0	5.4	100.0	6.0	100.0
cb1301	31.1	43.8	34.8	14.3	39.7	0.0

Table B6. Current direction error summary: RMS of current direction error (degrees) and its Central Frequency (CF), maximum flood current direction error (DFC_err, degrees) and its CF, maximum ebb current direction error (DEC_err, degrees) and its CF (all from the CSDL skill-assessment software package).

Station	RMSE	CF	DFC_err	CF	DEC_err	CF
LCB9903	3.8	100.0	6.3	100.0	2.9	100.0
cb0601	11.1	92.4	12.1	100.0	10.3	100.0
cb0801	3.7	100.0	8.2	98.8	8.8	100.0
cb0901	0.1	100.0	5.8	98.8	5.4	100.0
CBB0301	1.6	100.0	5.5	100.0	4.5	100.0
cb1201	3.8	100.0	13.4	91.9	5.0	100.0
cb1301	8.3	99.8	1.1	100.0	0.5	100.0

Table B7. Major current error summary: raw RMS error (cm/s), the amplitude component of the RMSE (cm/s) and the phase component of the RMSE (hours).

Station	RMSE	Amp_err	Phs_err
LCB9903	13.9	11.2	-0.38
cb0601	32.8	28.6	-0.80
cb0801	6.2	5.0	-0.33
cb0901	4.7	4.0	-0.30
CHB0301	10.5	6.7	-0.87
cb1201	6.3	6.0	0.18
cb1301	32.9	30.2	-0.53

APPENDIX C: CBOFS2 SYNOPTIC HINDCAST TEMPERATURE AND SALINITY SKILL ASSESSMENTS

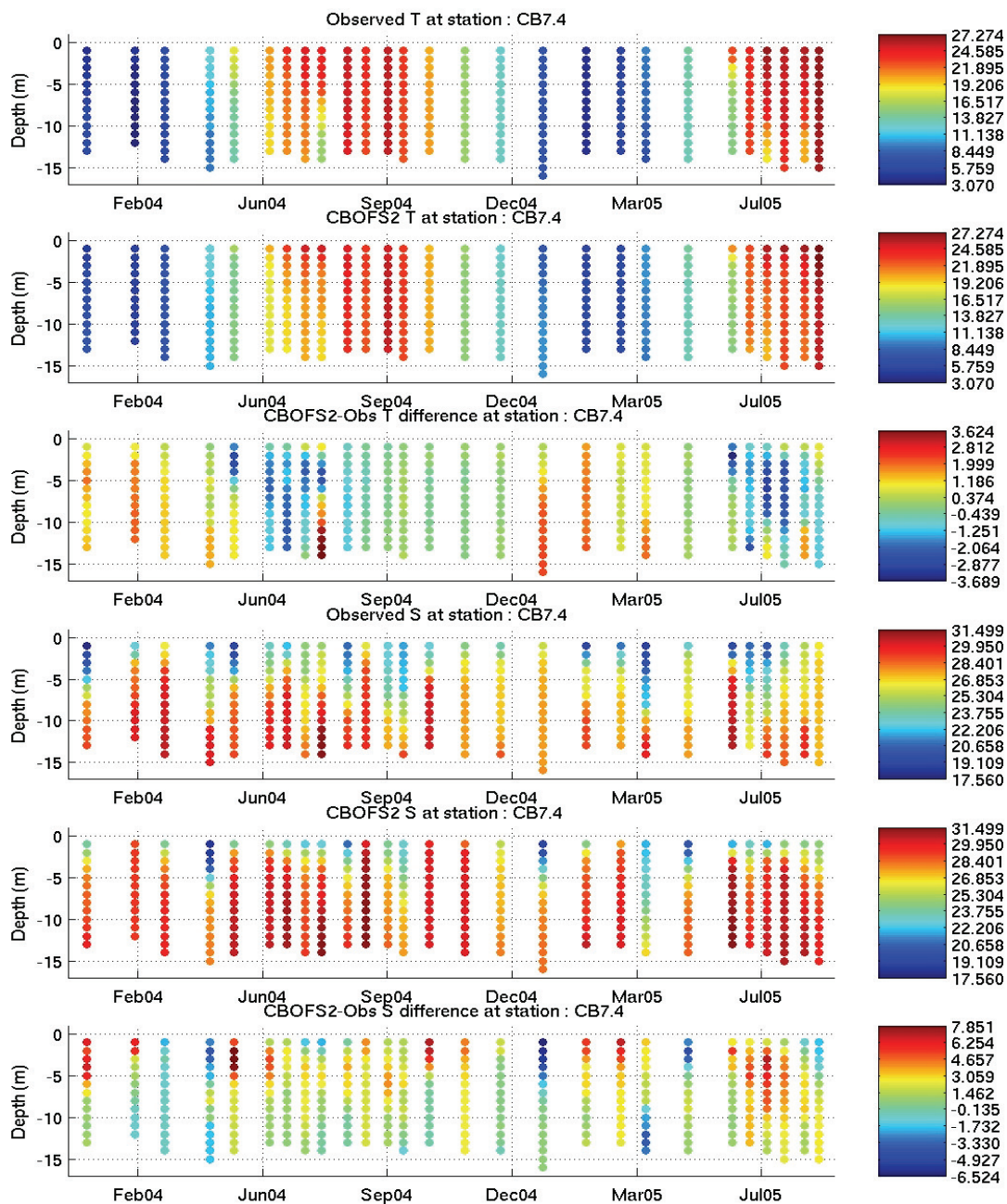


Figure C1. Observed Bay Program T/S, CBOFS2 predicted T/S and their differences at station CB7.4.

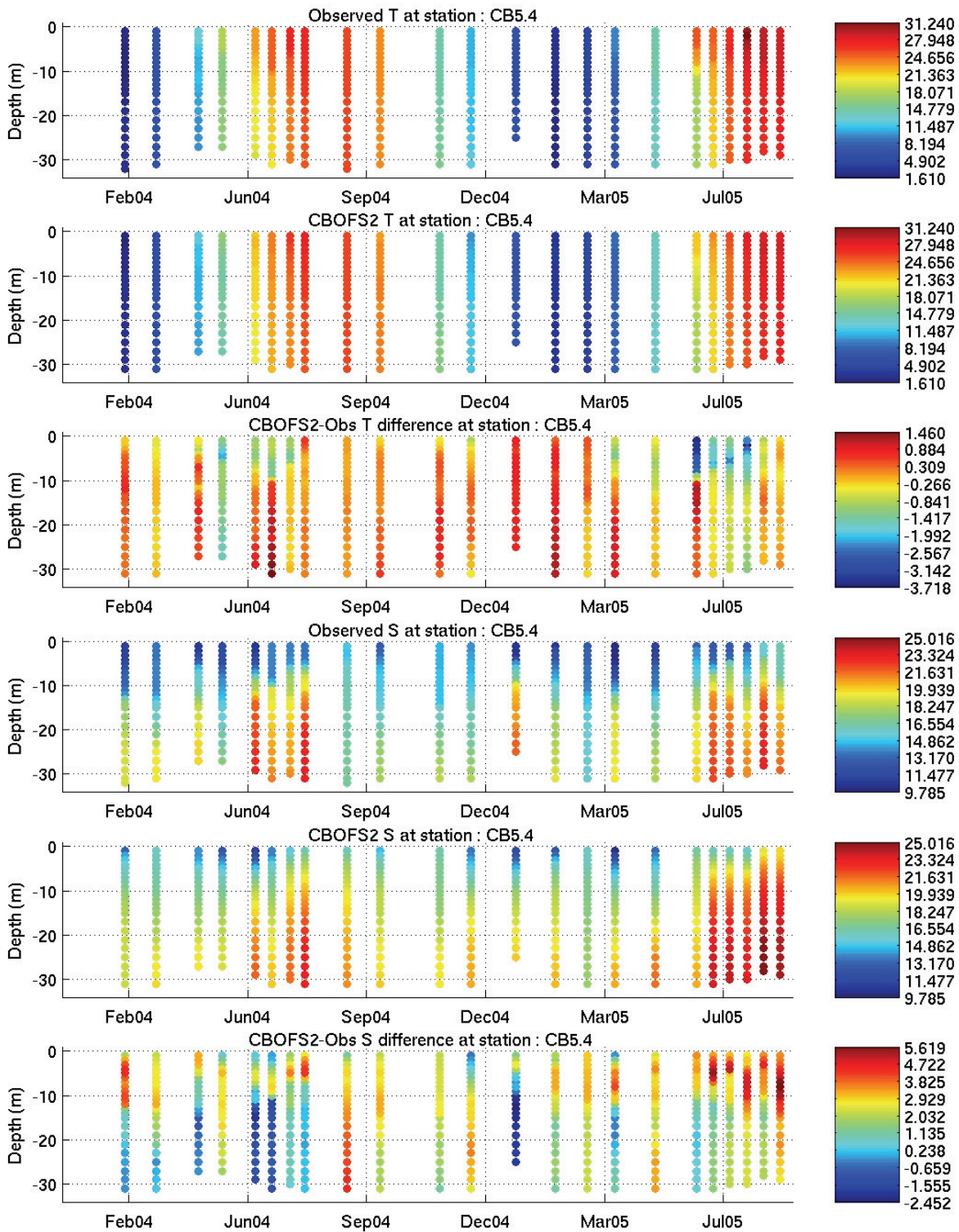


Figure C2. Observed Bay Program T/S, CBOFS2 predicted T/S and their differences at station CB5.4.

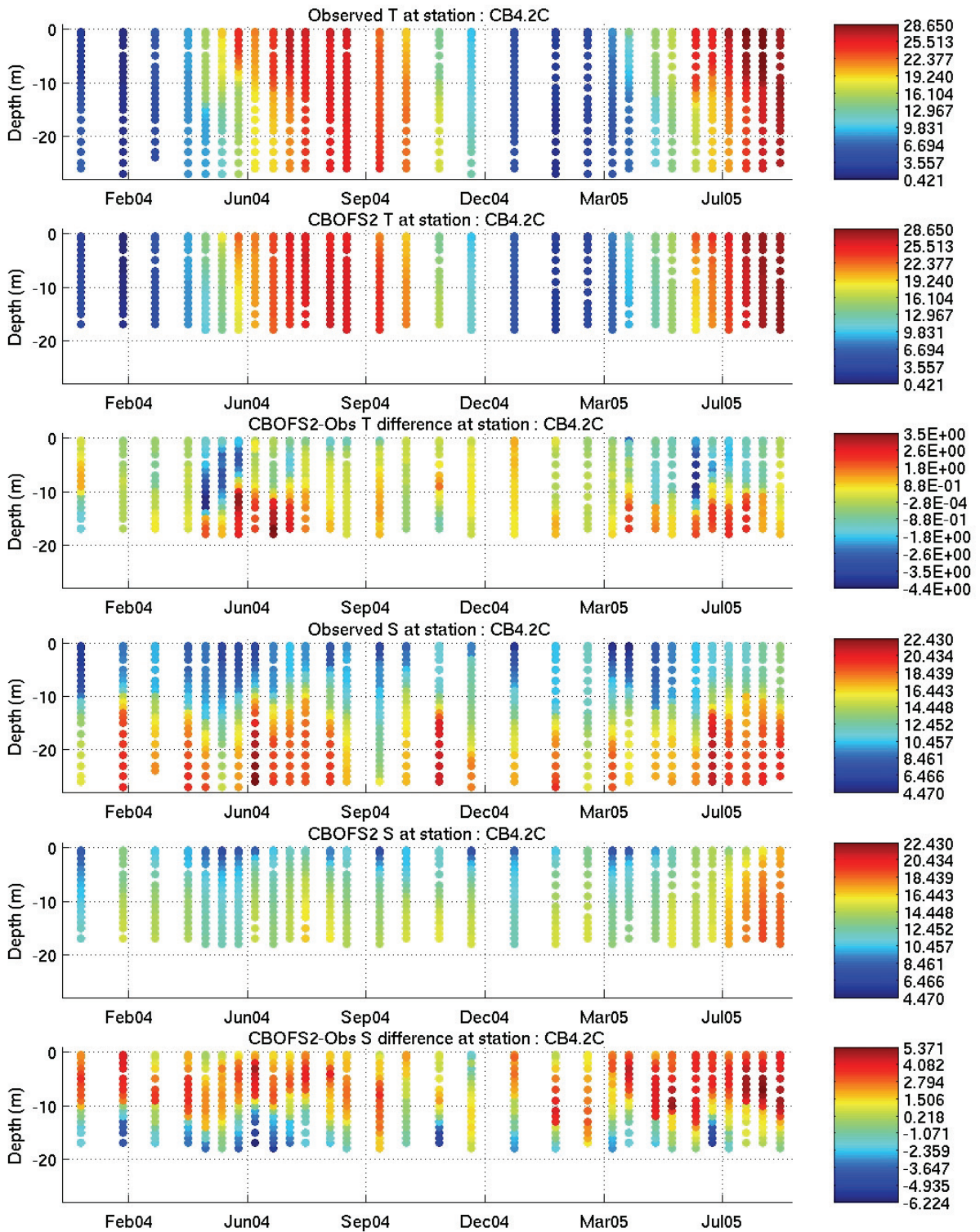


Figure C3. Observed Bay Program T/S, CBOFS2 predicted T/S and their differences at station CB4.2C.

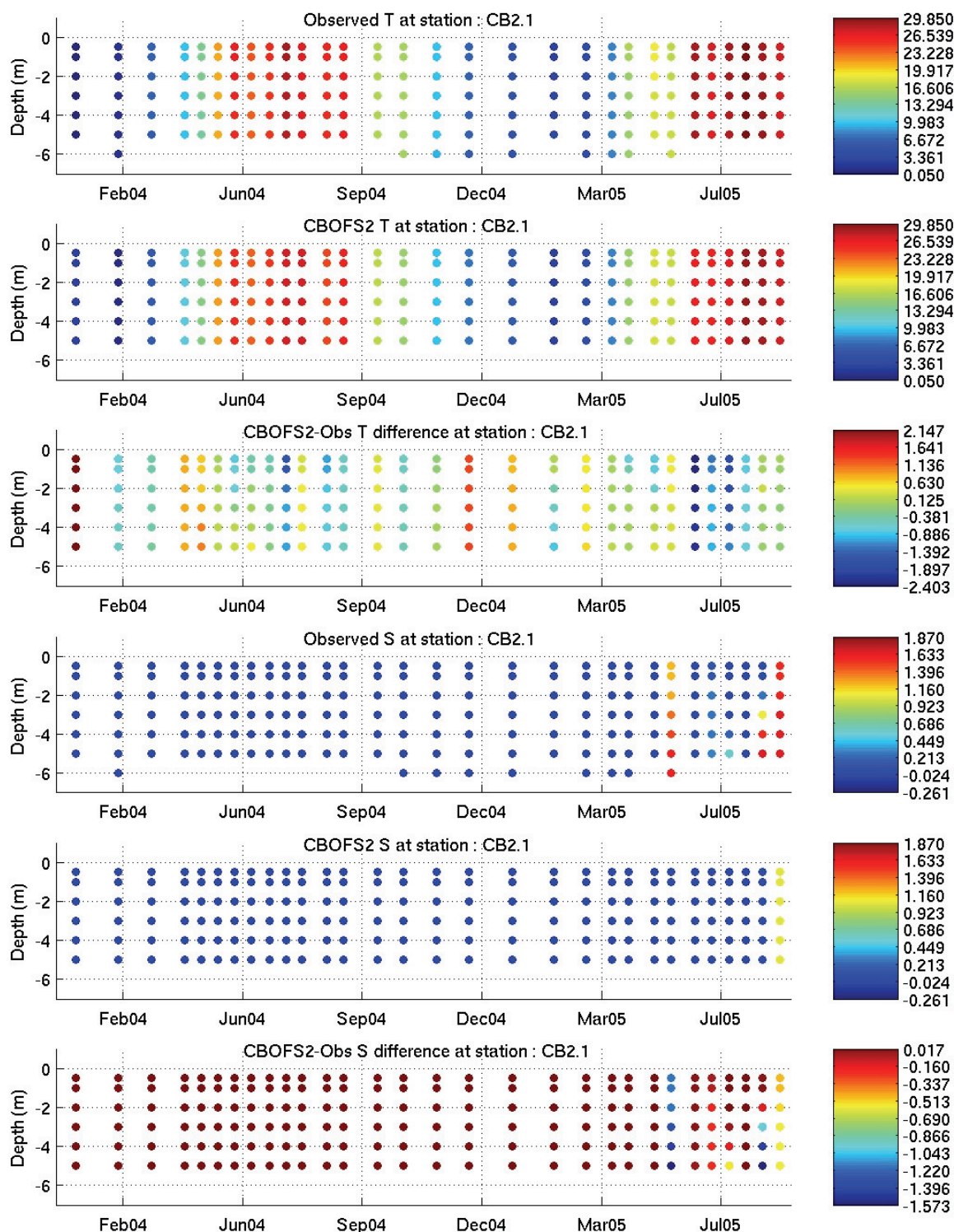


Figure C4. Observed Bay Program T/S, CBOFS2 predicted T/S and their differences at station CB2.1.

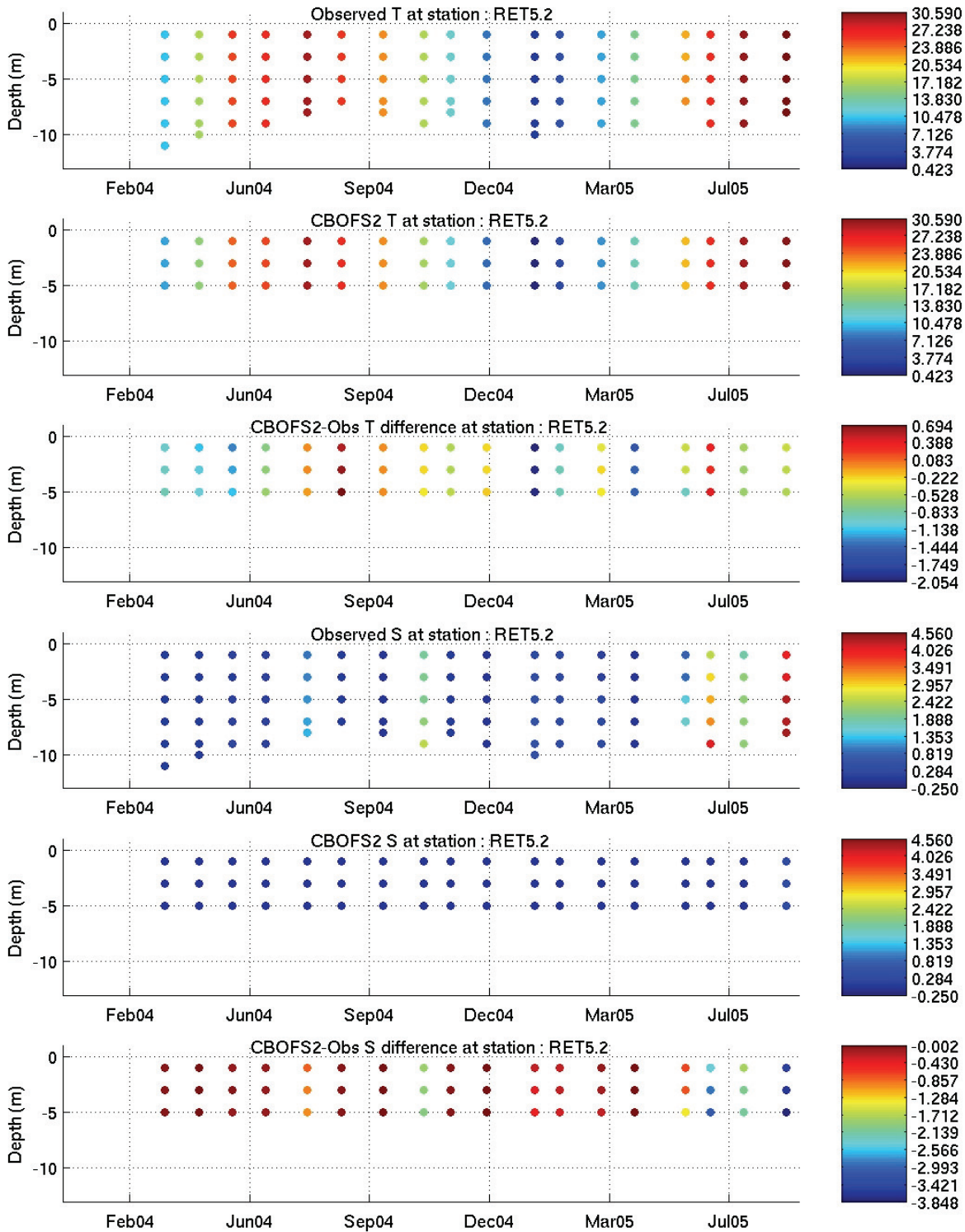


Figure C5. Observed Bay Program T/S, CBOFS2 predicted T/S and their differences at station RET5.2.

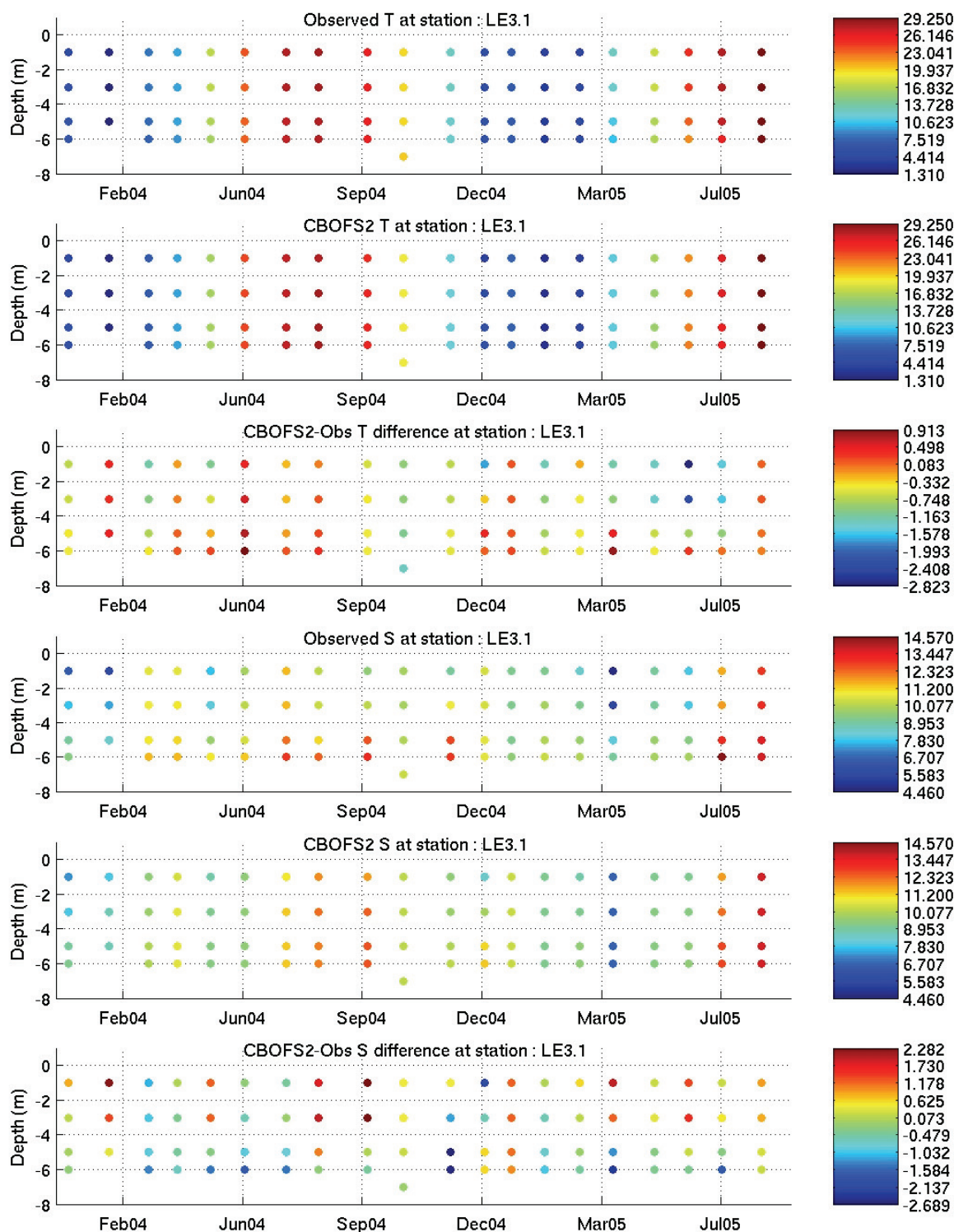


Figure C6. Observed Bay Program T/S, CBOFS2 predicted T/S and their differences at station LE3.1.

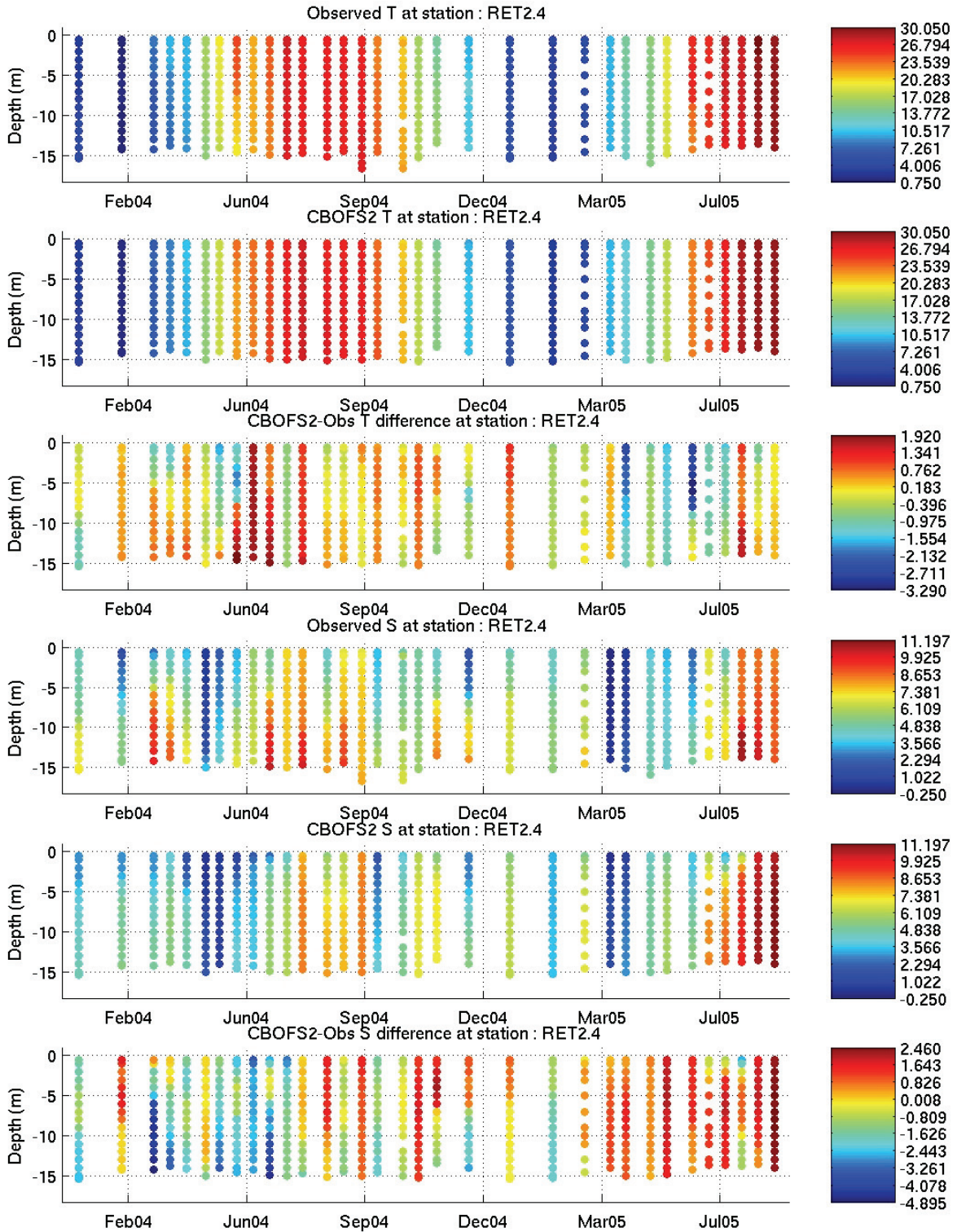


Figure C7. Observed Bay Program T/S, CBOFS2 predicted T/S and their differences at station RET2.4.

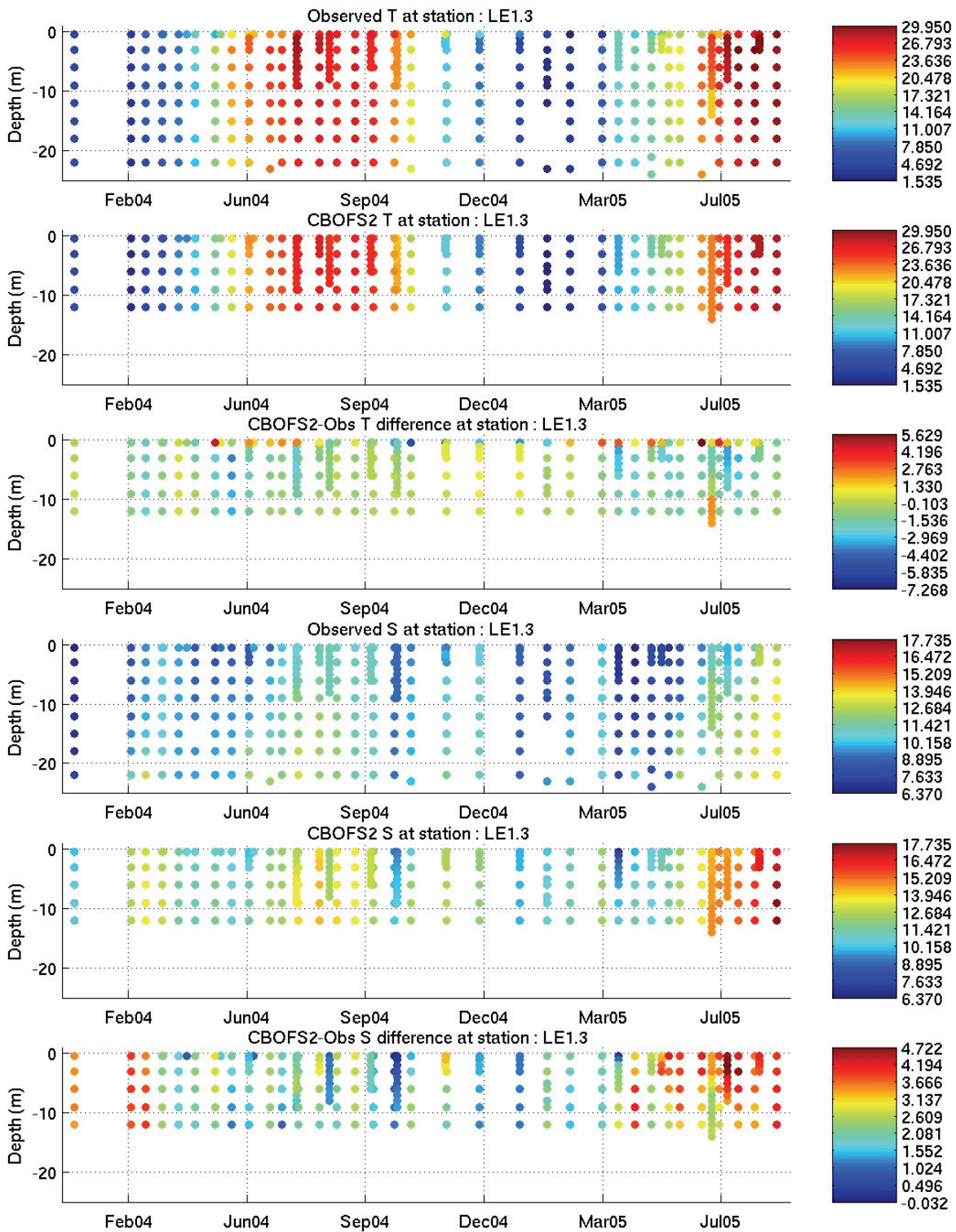


Figure C8. Observed Bay Program T/S, CBOFS2 predicted T/S and their differences at station LE1.3.

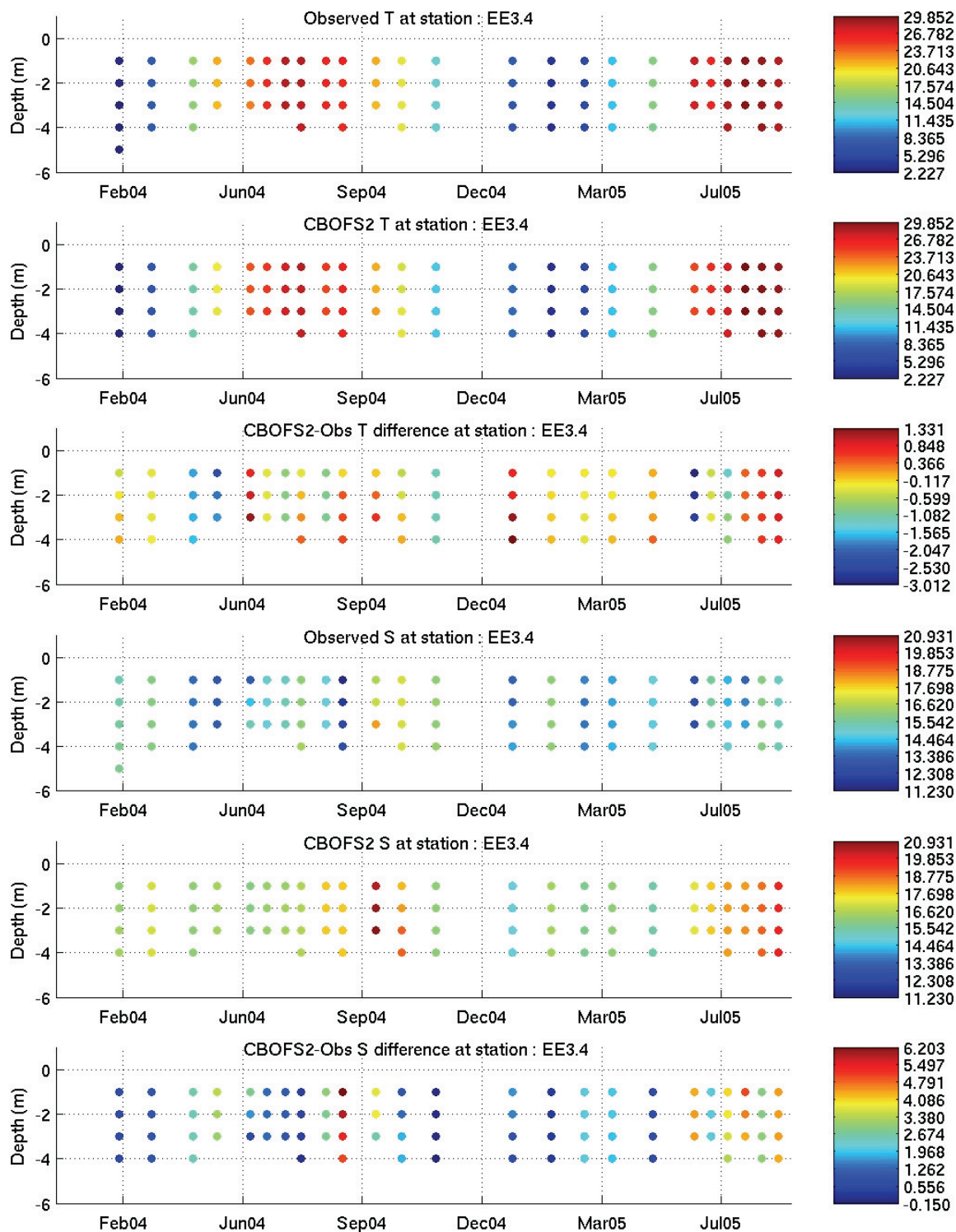


Figure C9. Observed Bay Program T/S, CBOFS2 predicted T/S and their differences at station EE3.4.

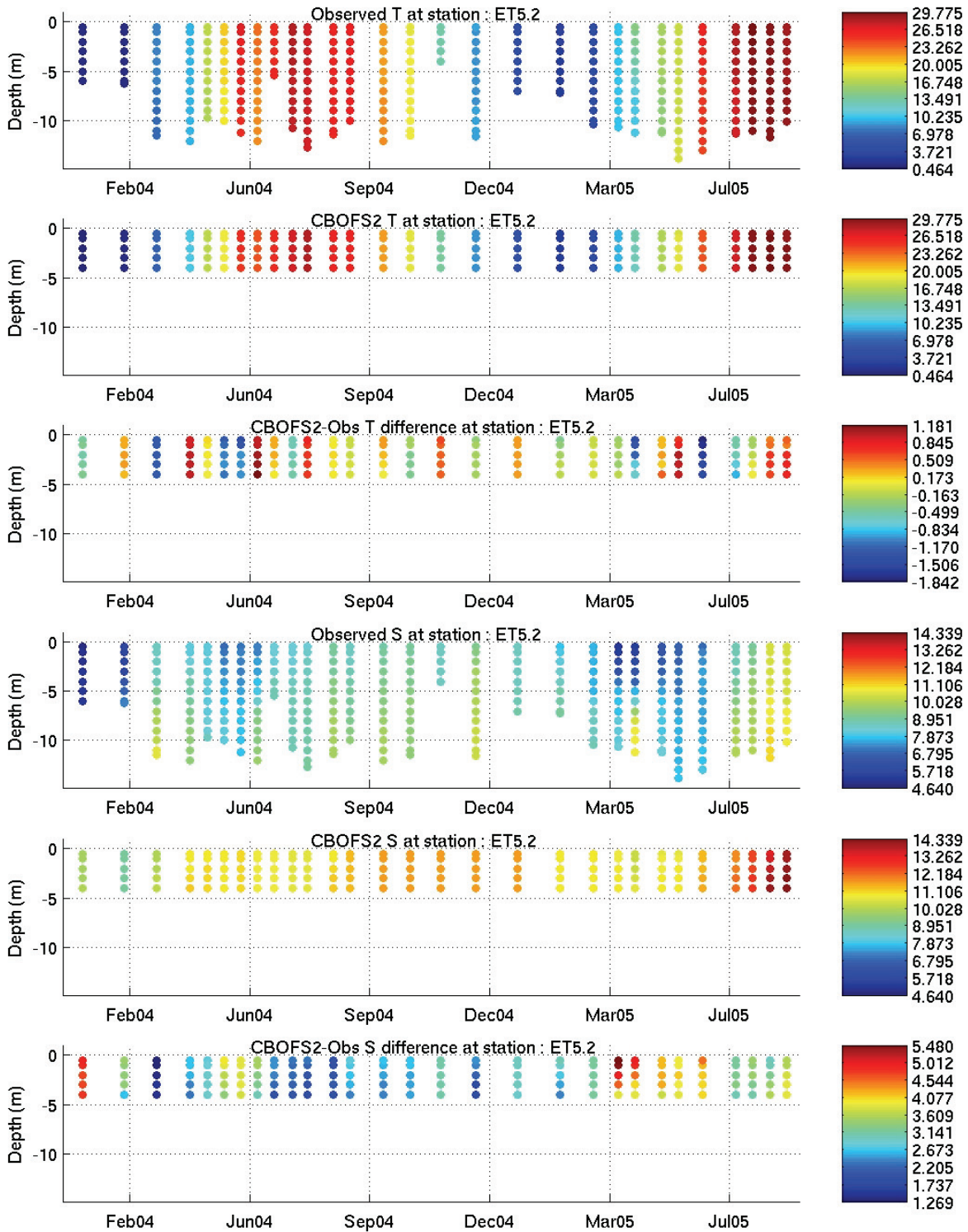


Figure C10. Observed Bay Program T/S, CBOFS2 predicted T/S and their differences at station ET5.2.

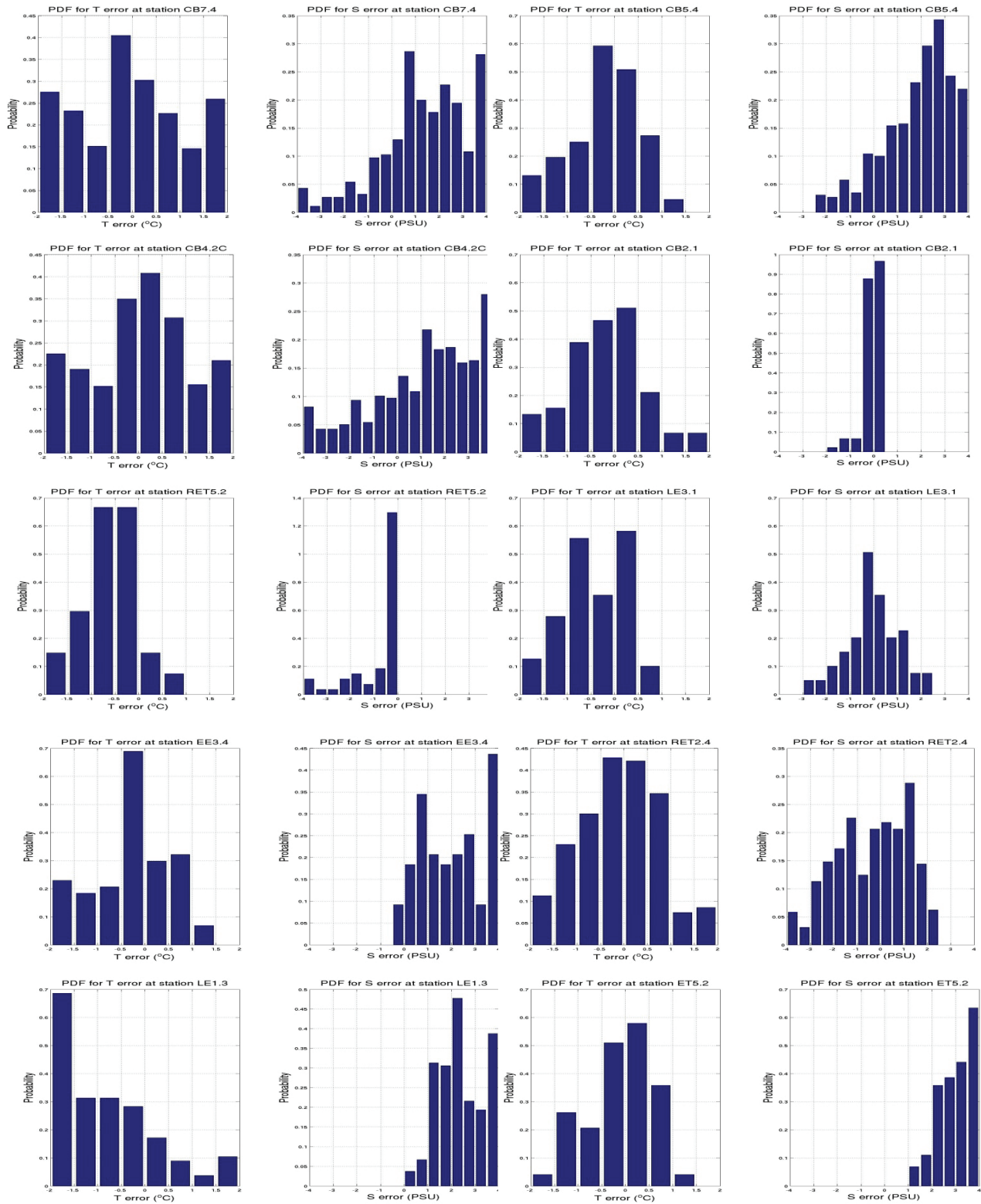


Figure C11. Histograms of local errors (in time and depth) for T and S corresponding to Figures C1-C10. The T and S histogram bin widths are 0.5 °C and 0.5 PSU respectively.

Table C1. The RMS and mean errors (calculated in time) for temperature at the surface, at 15-feet below the surface and at the bottom.

#	Station	Surface		15-feet		Bottom	
		RMSE	Mean E	RMSE	Mean E	RMSE	Mean E
1	CB7.4	1.2	-0.3	1.4	-0.4	1.4	0.4
2	CB6.4	0.9	-0.6	1.3	-0.7	0.9	-0.4
3	CB6.3	1.1	-0.8	1.5	-0.9	0.9	-0.3
4	CB6.1	1.6	-1.1	1.5	-0.9	0.7	-0.3
5	CB5.4	1.3	-0.8	1.2	-0.8	0.7	0.1
6	CB5.2	1.2	-0.7	1.1	-0.6	1.2	0.7
7	CB4.4	1.1	-0.9	1.3	-0.7	2.9	-0.0
8	CB4.2C	1.0	-0.7	1.3	-0.7	1.5	1.1
9	CB4.1C	1.6	-1.1	1.3	-0.5	2.0	1.3
10	CB3.2	0.8	-0.2	1.0	-0.2	1.4	0.4
11	CB2.2	0.8	-0.2	0.8	-0.1	0.9	-0.1
12	CB2.1	0.9	-0.2	0.8	-0.1	0.8	-0.1
13	LE5.4	0.6	-0.1	0.5	0.0	0.7	0.2
14	RET5.2	0.9	-0.6	0.9	-0.6	0.9	-0.6
15	LE4.3	0.9	-0.7	1.0	-0.8	2.0	0.1
16	WE4.1	1.1	-0.7	0.9	-0.6	0.9	-0.6
17	LE3.4	1.2	-0.8	1.0	-0.7	0.7	0.0
18	LE3.1	1.1	-0.8	0.6	-0.3	0.5	-0.1
19	LE2.3	1.4	-0.9	1.3	-0.8	0.9	0.4
20	LE2.2	1.3	-0.7	1.4	-0.8	1.3	-0.7
21	RET2.4	1.1	-0.4	1.0	-0.2	0.9	0.2
22	LE1.4	1.7	-0.3	1.2	-0.9	0.9	-0.2
23	LE1.3	2.2	-0.5	1.7	-1.3	1.3	-0.9
24	LE1.1	1.0	-0.6	1.3	0.1	1.3	0.1
25	WT5.1	1.4	-0.9	1.3	-0.3	2.4	0.9
26	WT2.1	1.0	-0.7	0.9	-0.6	0.9	-0.6
27	CB1.1	0.6	-0.4	0.4	-0.1	0.4	-0.2
28	ET4.2	1.4	-1.0	1.1	-0.8	2.2	0.4
29	EE1.1	1.2	-0.9	1.0	-0.7	1.0	-0.6
30	EE2.1	0.7	-0.1	0.7	-0.0	2.7	-1.0
31	ET5.2	0.7	-0.1	0.7	-0.1	0.7	-0.1
32	EE3.1	0.8	0.0	0.7	0.3	0.8	0.4
33	EE3.2	0.9	-0.2	0.9	-0.1	0.6	0.3
34	EE3.4	1.0	-0.4	0.7	-0.1	1.0	-0.2
35	EE3.5	1.2	-0.5	1.1	-0.4	1.0	-0.2

Table C2. The RMS and mean errors (calculated in time) for salinity at the surface, at 15-feet below the surface and at the bottom.

#	Station	Surface		15-feet		Bottom	
		RMSE	Mean E	RMSE	Mean E	RMSE	Mean E
1	CB7.4	4.0	2.1	3.2	2.2	1.5	0.6
2	CB6.4	2.5	2.2	3.5	3.0	2.7	2.0
3	CB6.3	2.3	1.8	4.1	3.7	2.7	2.2
4	CB6.1	2.9	2.5	3.5	3.0	2.1	1.8
5	CB5.4	2.5	2.3	3.2	3.0	1.8	1.1
6	CB5.2	2.4	1.9	3.2	2.9	2.3	-1.3
7	CB4.4	2.1	1.6	3.1	2.9	2.8	-2.3
8	CB4.2C	2.2	1.9	3.0	2.8	2.9	-2.2
9	CB4.1C	2.5	2.1	2.9	2.7	4.3	-3.9
10	CB3.2	1.8	1.2	1.7	1.2	3.3	-2.2
11	CB2.2	1.2	0.0	1.6	0.0	2.3	-0.7
12	CB2.1	0.2	-0.1	0.4	-0.1	0.4	-0.2
13	LE5.4	1.6	0.1	1.6	0.5	2.0	-0.1
14	RET5.2	1.2	-0.7	1.4	-0.8	1.4	-0.9
15	LE4.3	2.0	1.6	1.8	1.5	3.9	-1.7
16	WE4.1	2.0	1.9	1.9	1.7	1.9	1.7
17	LE3.4	1.8	1.6	1.8	1.7	1.2	0.5
18	LE3.1	1.2	0.5	0.8	-0.2	1.2	-0.7
19	LE2.3	2.4	2.2	2.5	2.3	1.9	0.4
20	LE2.2	2.3	1.5	2.9	2.4	2.8	2.3
21	RET2.4	1.4	-0.2	1.4	0.1	2.0	-1.0
22	LE1.4	2.1	1.8	2.3	2.1	2.4	1.1
23	LE1.3	2.8	2.5	2.7	2.6	2.5	2.3
24	LE1.1	2.9	2.7	2.7	2.5	2.7	2.5
25	WT5.1	1.8	-1.1	2.8	-2.3	5.5	-4.9
26	WT2.1	0.8	0.7	0.8	0.7	0.8	0.7
27	CB1.1	0.0	0.0	0.0	0.0	0.0	0.0
28	ET4.2	1.0	0.4	1.1	0.2	4.3	-2.8
29	EE1.1	1.6	1.4	1.6	1.4	1.5	1.2
30	EE2.1	2.2	2.0	2.0	1.7	1.7	1.1
31	ET5.2	3.3	3.2	3.0	2.9	3.0	2.9
32	EE3.1	2.7	2.4	2.3	2.1	1.8	1.4
33	EE3.2	2.5	2.3	2.5	2.3	2.0	1.5
34	EE3.4	2.7	2.3	2.3	1.9	2.5	2.0
35	EE3.5	2.4	2.1	2.3	2.1	2.1	1.7

APPENDIX D: CBOFS2 SEMI-OPERATIONAL NOWCAST/FORECAST SKILL ASSESSMENTS

Table D1. RMSE (m) values for the water levels for the semi-operational nowcast/forecast CBOFS2 (from the CSDL skill assessment software package).

Stn ID	Nowcast	Fcst-00h	Fcst-06h	Fcst-12h	Fcst-18h	Fcst-24h
8638610	0.100	0.092	0.099	0.090	0.086	0.088
8638863	0.074	0.086	0.075	0.071	0.067	0.070
8632200	0.074	0.075	0.072	0.071	0.067	0.070
8636580	0.049	0.048	0.048	0.054	0.053	0.058
8635750	0.058	0.057	0.059	0.060	0.059	0.059
8577330	0.075	0.074	0.075	0.075	0.072	0.073
8571559	0.107	0.103	0.103	0.099	0.095	0.091
8571892	0.119	0.119	0.121	0.122	0.110	0.112
8594900	0.311	0.305	0.299	0.300	0.278	0.280
8575512	0.086	0.087	0.087	0.087	0.084	0.086
8573364	0.123	0.121	0.121	0.120	0.120	0.118
8574680	0.108	0.109	0.108	0.108	0.108	0.106
8573927	0.170	0.168	0.160	0.166	0.168	0.154

Table D2. CF(15cm) values for the water levels for the semi-operational nowcast/forecast CBOFS2 (from the CSDL skill assessment software package).

Stn ID	Nowcast	Fcst-00h	Fcst-06h	Fcst-12h	Fcst-18h	Fcst-24h
8638610	85.8	89.5	87.2	89.8	90.1	90.1
8638863	95.8	91.8	95.1	96.7	96.7	97.7
8632200	95.6	96.1	95.1	96.7	98.0	96.4
8636580	99.4	99.7	99.7	99.0	98.4	98.4
8635750	98.8	99.0	98.7	98.7	98.7	97.7
8577330	96.5	96.7	96.7	98.0	97.0	96.1
8571559	83.6	85.2	86.5	86.5	89.1	90.8
8571892	76.8	77.3	76.3	77.0	81.6	81.6
8594900	41.8	45.4	46.7	44.7	48.4	47.0
8575512	91.9	92.1	91.8	92.4	92.8	92.1
8573364	75.1	74.0	75.7	76.0	76.0	76.3
8574680	82.9	82.9	83.2	81.9	81.6	82.6
8573927	58.9	56.6	61.5	58.9	60.2	64.5

Table D3. RMSE (m/s) values for the current speed at 15 feet for the semi-operational nowcast/forecast CBOFS2 (from the CSDL skill assessment software package).

Stn ID	Nowcast	Fcst-00h	Fcst-06h	Fcst-12h	Fcst-18h	Fcst-24h
cb0801	0.107	0.087	0.086	0.088	0.094	0.087
cb1001	0.150	0.139	0.145	0.152	0.156	0.150
cb1101	0.208	0.228	0.230	0.232	0.227	0.228

Table D4. CF(26cm/s) values for the current speed at 15 feet for the semi-operational nowcast/forecast CBOFS2 (from the CSDL skill assessment software package).

Stn ID	Nowcast	Fcst-00h	Fcst-06h	Fcst-12h	Fcst-18h	Fcst-24h
cb0801	98.3	100.0	100.0	100.0	100.0	100.0
cb1001	90.8	89.3	90.0	88.2	93.9	94.1
cb1101	76.3	67.8	62.7	65.5	68.5	67.3

Table D5. RMSE (degrees) values for the current direction at 15 feet for the semi-operational nowcast/forecast CBOFS2 (from the CSDL skill assessment software package).

Stn ID	Nowcast	Fcst-00h	Fcst-06h	Fcst-12h	Fcst-18h	Fcst-24h
cb0801	14.267	21.934	23.253	23.061	22.837	23.442
cb1001	9.619	17.380	18.128	18.424	17.423	18.066
cb1101	13.578	18.554	25.432	26.423	19.247	19.123

Table D6. CF(22.5°) values for the current direction at 15 feet for the semi-operational nowcast/forecast CBOFS2 (from the CSDL skill assessment software package).

Stn ID	Nowcast	Fcst-00h	Fcst-06h	Fcst-12h	Fcst-18h	Fcst-24h
cb0801	90.1	84.3	82.4	78.4	79.6	71.2
cb1001	94.8	82.1	80.0	73.5	84.8	82.4
cb1101	86.3	76.3	71.2	72.4	66.7	76.4

Table D7. RMSE ($^{\circ}\text{C}$) values for temperature at a 1m depth for the semi-operational nowcast/forecast CBOFS2 (from the CSDL skill assessment software package).

Stn ID	Nowcast	Fcst-00h	Fcst-06h	Fcst-12h	Fcst-18h	Fcst-24h
8638863	1.797	1.862	1.877	1.836	1.837	1.861
8635750	1.347	1.350	1.340	1.296	1.283	1.267
8571892	0.933	0.898	0.895	0.888	0.873	0.865
8594900	1.616	1.680	1.678	1.678	1.678	1.673
8573364	1.016	1.035	1.023	1.028	1.016	0.985
8574680	1.860	1.849	1.847	1.825	1.817	1.797
8573927	0.834	0.894	0.899	0.890	0.881	0.812

Table D8. CF(3°C) values for temperature at a 1m depth for the semi-operational nowcast/forecast CBOFS2 (from the CSDL skill assessment software package).

Stn ID	Nowcast	Fcst-00h	Fcst-06h	Fcst-12h	Fcst-18h	Fcst-24h
8638863	91.7	91.9	91.2	92.6	92.2	90.9
8635750	97.2	97.6	98.0	96.6	97.6	97.6
8571892	99.4	99.3	99.3	100.0	100.0	99.7
8594900	89.8	88.9	88.9	89.2	88.5	88.5
8573364	97.8	97.6	98.0	98.0	97.6	98.3
8574680	90.1	89.5	89.5	89.5	89.5	88.9
8573927	99.7	99.3	99.3	99.3	99.3	99.7

Table D9. RMSE (PSU) values for salinity at a 1m depth for the semi-operational nowcast/forecast CBOFS2 (from the CSDL skill assessment software package).

Stn ID	Nowcast	Fcst-00h	Fcst-06h	Fcst-12h	Fcst-18h	Fcst-24h
8638863	4.799	5.406	5.584	5.590	5.577	5.611
8635750	1.827	1.803	1.802	1.794	1.793	1.792
8574680	1.910	1.961	1.950	1.938	1.931	1.931

Table D10. CF(3.5 PSU) values for salinity at a 1m depth for the semi-operational nowcast/forecast CBOFS2 (from the CSDL skill assessment software package).

Stn ID	Nowcast	Fcst-00h	Fcst-06h	Fcst-12h	Fcst-18h	Fcst-24h
8638863	43.5	43.6	42.2	42.2	42.2	42.2
8635750	97.2	97.3	97.3	97.0	97.0	97.0
8574680	97.1	97.0	97.3	97.6	97.6	97.6